Static Voltage Stability Analysis for Islanded Microgrids

Author:
Liang, Xinyu

Publication Date:
2023

DOI:

License:

Static Voltage Stability Analysis for Islanded Microgrids

by

Xinyu Liang

A thesis in fulfilment of the requirements for the degree of

Master of Philosophy

School of Electrical Engineering and Telecommunications

Faculty of Engineering

University of New South Wales

September 2022

1. Originality, Copyright And Authenticity Statements

Thesis Title and Abstract	Declarations	Inclusion of Publications Statement	Corrected Thesis and Responses

ORIGINALITY STATEMENT

☑ I hereby declare that this submission is my own work and to the best of my knowledge it contains no materials previously published or written by another person, or substantial proportions of material which have been accepted for the award of any other degree or diploma at UNSW or any other educational institution, except where due acknowledgement is made in the thesis. Any contribution made to the research by others, with whom I have worked at UNSW or elsewhere, is explicitly acknowledged in the thesis. I also declare that the intellectual content of this thesis is the product of my own work, except to the extent that assistance from others in the project's design and conception or in style, presentation and linguistic expression is acknowledged.

COPYRIGHT STATEMENT

☑ I hereby grant the University of New South Wales or its agents a non-exclusive licence to archive and to make available (including to members of the public) my thesis or dissertation in whole or part in the University libraries in all forms of media, now or here after known. I acknowledge that I retain all intellectual property rights which subsist in my thesis or dissertation, such as copyright and patent rights, subject to applicable law. I also retain the right to use all or part of my thesis or dissertation in future works (such as articles or books).

For any substantial portions of copyright material used in this thesis, written permission for use has been obtained, or the copyright material is removed from the final public version of the thesis.

AUTHENTICITY STATEMENT

☑ I certify that the Library deposit digital copy is a direct equivalent of the final officially approved version of my thesis.

2. Inclusion of Publications Statement

Thesis Title and Abstract	Declarations	Inclusion of Publications Statement	Corrected Thesis and Responses

UNSW is supportive of candidates publishing their research results during their candidature as detailed in the UNSW Thesis Examination Procedure.

Publications can be used in the candidate's thesis in lieu of a Chapter provided:

- The candidate contributed **greater than 50%** of the content in the publication and are the "primary author", i.e. they were responsible primarily for the planning, execution and preparation of the work for publication.
- The candidate has obtained approval to include the publication in their thesis in lieu of a Chapter from their Supervisor and Postgraduate Coordinator.
- The publication is not subject to any obligations or contractual agreements with a third party that would constrain its inclusion in the thesis.

☑ The candidate has declared that **their thesis has publications - either published or submitted for publication - incorporated into it in lieu of a Chapter/s. Details of these publications are provided below.**.

Publication Details #1

Full Title:	Analytical Methods of Voltage Stability in Renewable Dominated Power Systems: A Review
Authors:	Xinyu Liang, Hua Chai, Jayashri Ravishankar
Journal or Book Name:	MDPI Electricity 2022
Volume/Page Numbers:	3(1)/75-107
Date Accepted/Published:	Accepted: 7 February 2022 / Published: 19 February 2022
Status:	published
The Candidate's Contribution to the Work:	Conceptualization, methodology, validation, formal analysis, investigation, and writing—original draft preparation.
Location of the work in the thesis and/or how the work is incorporated in the thesis:	Located in Chapter 2 which is the literature review in the thesis.

Candidate's Declaration

> ✓ **I confirm that where I have used a publication in lieu of a chapter, the listed publication(s) above meet(s) the requirements to be included in the thesis. I also declare that I have complied with the Thesis Examination Procedure.**

Acknowledgement

I owe my sincere gratitude to my supervisor A/Prof Jayashri Ravishankar for guiding and supporting me to complete the research and develop this thesis. I am extremely grateful for her patience throughout the journey of my research, her professionalism exhibiting a great example of academic research, and meticulous care and support that motivated me during my hard times.

A special thanks to Zhenyu Liu, for providing technical support required for the research. I am also grateful to Hua Chai for guiding me through all the processes.

Finally, my special thanks to my parents who supported me mentally and financially. They are my solid backing. Without them I could not have gone this far.

Xinyu Liang

Sydney

September 2022

Abstract

The ongoing development of renewable energy and microgrid technologies has gradually transformed the conventional energy infrastructure into a modernized system with more distributed generation and localized energy storage options. Compared with power grids utilizing synchronous generation, inverter-based networks cannot physically provide large amounts of inertia. Therefore, more advanced, and extensive studies regarding stability considerations are required for such systems. Appropriate analytical methods are needed for the voltage stability analysis of renewable-dominated power systems, which incorporate many inverters and distributed energy sources. Microgrid voltage stability is being challenged as the power output of renewable energy generation is not as stable as the traditional generation used in the main grid. Therefore, the choice of voltage stability analysis techniques plays an important role in the stable operation of the microgrid. This thesis comprehensively studies static voltage stability analyses of islanded microgrids with high levels of renewable energy penetration. Firstly, a series of generalized evaluation schemes and improvement methods relating to the voltage stability of power systems integrated with various distributed energy resources are discussed. This study presents guidelines for voltage stability analysis and instability mitigation methods for modern renewable-rich power systems. Then, four dominant VSI techniques for microgrids are studied and compared in this paper. An islanded microgrid system is modelled based on the IEEE-14-bus system in PSCAD. The model evaluates the stability results analyzed by different voltage stability indices (VSIs). Four simulation scenarios are applied in this thesis,

including changing the output power of distributed generations (DGs) and the connection position of the DGs. The advantages and disadvantages of each technique are discussed based on the simulation results. A ranking of bus voltage stability is obtained based on the simulation and the VSI calculation. Finally, a novel static voltage stability analysis technique is proposed.

Table of contents

Abbreviations

CCDGS	Constant-Current Distributed Generators
CDF	Cumulative Distribution Function
CMEM	Cumulant-based Maximum Entropy Method
CPDGS	Constant-Power Distributed Generators
CSMF	Control Systems Modelling Functions
DFIG-WECS	Doubly-Fed Induction Generator-based Wind Energy Conversion System
DG	Distributed Generator
ESS	Energy Storage System
FRT	Fault Ride-Through
FVSI	Fast Voltage Stability Index
HEPF	Holomorphic Embedded Power Flow
LG	Line to Ground
LIB	Limited Induced Bifurcation
LLG	Double Line to Ground
LLLG	Three-Phase Line to Ground
LMI	Linear Matrix Inequality
MCM	Monte Carlo Method
MLP	Maximum Loading Point
NT	Nataf Transform

PCC   Point of Common Coupling

PDF   Probability Density Function

PSCAD   Power Systems Computer Aided Design

PV   Photovoltaic

SEM   Standard Error of the Mean

SNB   Saddle-Node Bifurcation

SVD   Singular Value Decomposition

UHVDC   Ultrahigh-Voltage Direct-Current

VSI   Voltage Stability Index

List of Figures

List of Tables

1 Introduction

1.1 Background

The growing concerns about climate change and the need to stop relying on fossil fuels as sources of energy are promoting the development of renewable forms of energy. The microgrid concept has now come into being as one method of generating renewable energy. Unlike traditional power grids, microgrids are low- or medium-voltage DC or AC power systems containing distributed generators (DGs) and energy storage systems (ESS) [1]. Generally, DGs include solar and wind turbine systems and normally, the energy storage system consists of batteries, flywheels, and supercapacitors [2]. As synchronous generators are being gradually replaced by renewable sources, which are inverter-based, the system's voltage stability is being challenged [3]. Compared to the traditional power grid, the islanded microgrid has weaker voltage control ability. In order to avoid the risk of the system becoming unstable, it is essential to predict the voltage stability issues in microgrids.

Voltage stability is defined as the capacity of the system to maintain a stable voltage at every bus without any voltage collapse during normal operations or during a disturbance in the power system [4]. The voltage stability issue can be classified according to the nature and duration of disturbance. Generally, research into voltage stability and its analysis seeks to quantify how far the system's operating state is from the voltage collapse point and hence determine the stability margin [5]. As a small power system, an islanded microgrid

consists of only renewable energy generations, a diesel generator, energy storage system

and loads that are all connected through shorter lines. As shown in Figure 1.1 below, the

islanded microgrid does not have a stable synchronous power generation like the

traditional power grid. With this in mind, it is crucial to examine the voltage stability of

islanded microgrids.
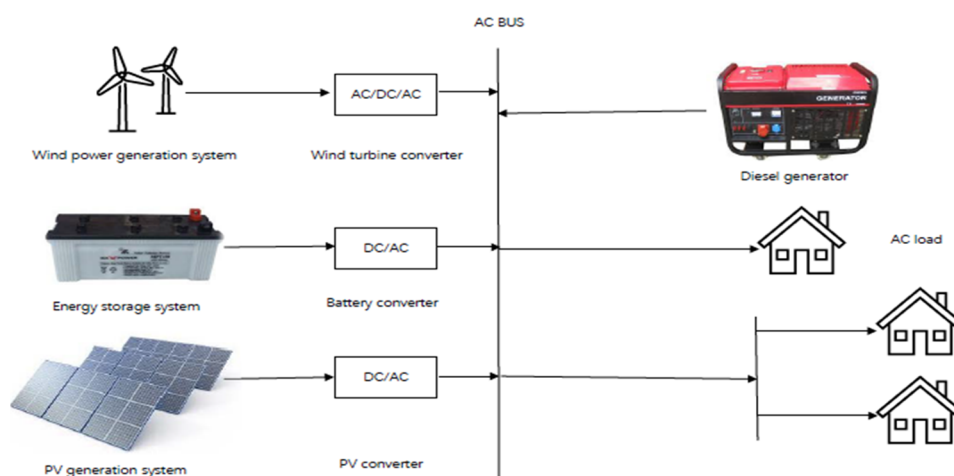
Figure 1.1 Islanded microgrid structure

Researchers in recent years have proposed several voltage stability analysis techniques

for the islanded microgrid. There are in fact two main voltage stability analysis categories:

static and dynamic analysis. The continuation load flow method using P-V and V-Q curves

is the most commonly employed static voltage stability analysis technique. The stable

operation limit can be resolved by constantly updating and calculating the load flow

equation. This is the voltage stability limit and it is the margin of stable and unstable states

of the microgrid [6]. Apart from this, modal analysis of the Jacobian matrix is an effective

way to identify the weakest bus. This method deduces the Thevenin-based voltage stability

margin [7]. Unlike the previous method, this technique does not require complex

calculations. Singular value decomposition also plays a crucial role in the static voltage stability analysis. The singular point of the Jacobian matrix of the load flow equation can represent the voltage collapse point of the microgrid, since the Jacobian matrix can be close to singularity when the load condition is close to a critical state [8].

Dynamic voltage stability analysis can explain the high-time varying components' behaviour more practically than microgrid static assessment. Time-domain simulation is the most commonly used strategy in dynamic analysis. In reference [9], a generalised load flow calculation model is proposed to simulate the microgrid, whereas a time-domain nonlinear equation is presented to simulate the distributed generator system. A dynamic analysis index based on network loss sensitivity theory designed for online tests and simulation is proposed in [10]. However, the dynamic analysis method is complex and time-consuming, so in effect it is not suitable for islanded microgrids with several DGs. Based on load flow voltage stability analysis methods, researchers have devised many voltage stability analysis indices (VSIs) with high accuracy and simplified calculation, and these indices are more suitable for microgrids.

1.2 Objectives

The main objective of this thesis is to develop a novel voltage stability analysis technique suitable for islanded microgrids and compare it to existing voltage stability analysis techniques regarding comprehensive performance issues such as calculation time and evaluation accuracy. In islanded microgrids, where the system is disconnected from the main grid and operates independently, voltage stability analysis is critical and essential for ensuring system stability. In order to analysis the stability of the islanded microgrid in terms of voltage fluctuations, static voltage stability analysis and dynamic voltage stability analysis are the two main approaches. While both methods have their advantages and limitations, this thesis mainly considers the static voltage stability analysis for the following reasons.:

The main reason is that the static method is computationally less intensive and faster. Static analysis can provide a comprehensive assessment of the system's voltage stability with relatively low computational resources. This is especially important in islanded microgrids where there may be limited computational resources. Besides, fast decision-making is necessary in case of voltage instability events. Consequently, the ability to use fewer parameters for efficient calculations is a significant advantage of static analysis methods.

Also, the main research objective in this thesis is identifying the critical buses and weakest area of the microgrid that require attention and corrective actions, such as reactive power compensation or load shedding. In islanded microgrids where the system is isolated

from the main grid, voltage instability can have severe consequences, such as blackouts or system damage. Thus, identifying critical buses for further corrective actions is crucial for maintaining the stable operation of the islanded microgrid. Static voltage stability analysis can identify the critical buses and easily satisfy this research objective.

Since islanded microgrids may have limited reactive power resources, it is important to determine the required amount of reactive power support needed to maintain voltage stability in islanded microgrid. Static voltage stability analysis can provide these information, which is necessary for designing the microgrid's reactive power compensation system and planning for its operation.

Lastly, static voltage stability analysis is useful for long-term planning and analysis for islanded microgrids. It can help planner assess the DGs capacity setting and connection location, which is important for ensuring the microgrid meets the load demand and avoids voltage collapse. Static voltage stability analysis is a better way to identify potential issues that may arise in the future and allow for proactive measures to be taken to mitigate these issues rather the dynamic analysis methods.

In conclusion, while dynamic voltage stability analysis is useful for capturing the time-varying behaviour of the system during transient events, static voltage stability analysis is essential for islanded microgrid voltage stability analysis and to meet the research objectives in this thesis. By considering static voltage stability analysis, islanded microgrid designer can maintain stable operation, prevent blackout, and ensure the basic power

supply reliability and sustainability.

In addition, in order to accurately assess the advantages and disadvantages of each method, a simulation model is needed to conduct the experiment. Another goal is building an improved IEEE 14-bus-based islanded microgrid model with a PV generator, wind turbine generator, and energy storage system in PSCAD for further simulation. In summary, the aims of this research are to:

- Design a 14-bus islanded microgrid model with different DGs in PSCAD.

- Develop a novel static voltage stability analysis technique which is suitable for islanded microgrid.

- Compare the comprehensive performance of the new method with other voltage stability analysis techniques using the PSCAD model.

1.3 Methodology

Figure 1.2 illustrates the methodology employed for this study. This work includes both the theoretical analysis of the state-of-the-art voltage stability analysis method, and practical steps including the modelling, novel technique development and simulation-based experiments for verification and comparison.
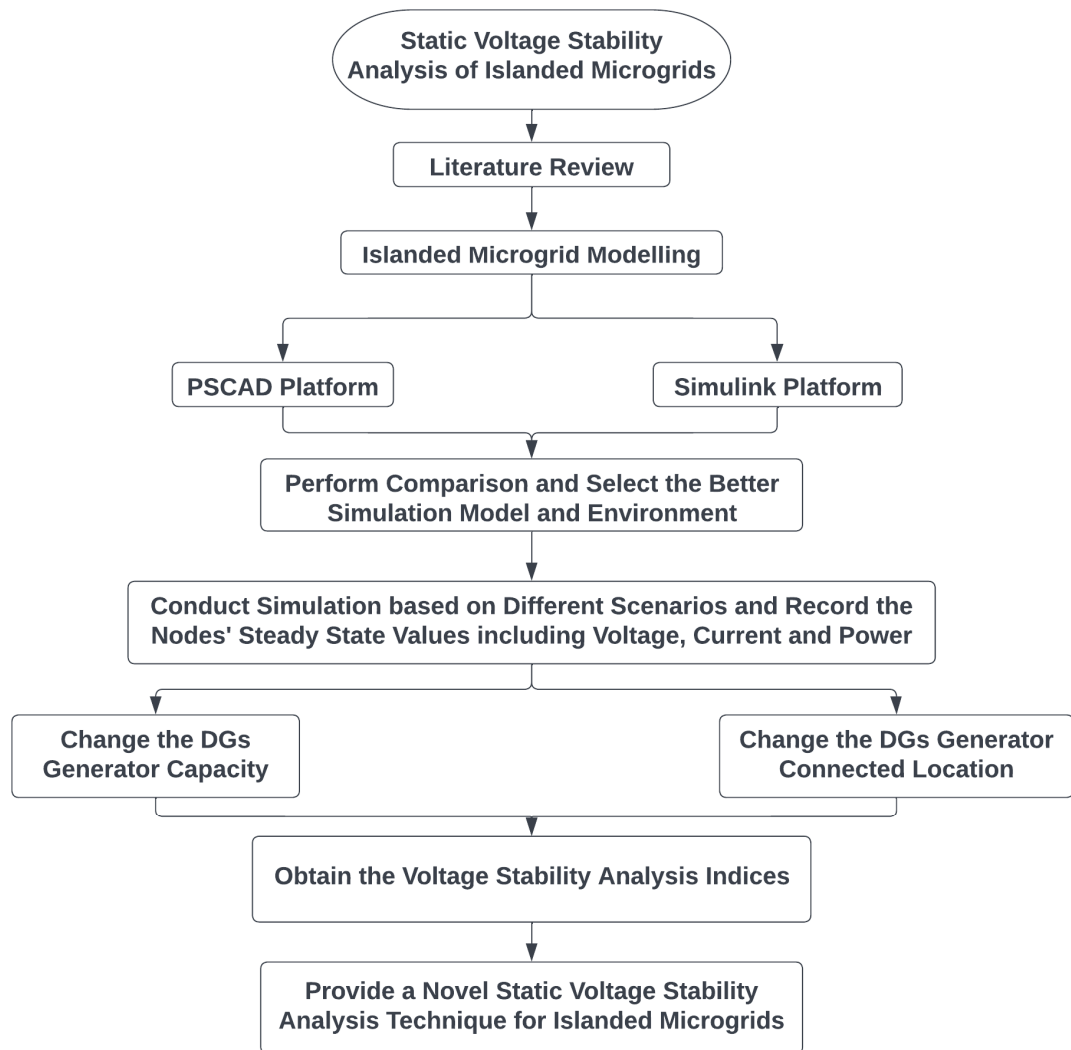
Figure 1.2 Methodology of the research

1.3.1 Analysis of Voltage Stability Analysis Methods

A comparative study of current techniques for voltage stability analysis methods is presented. Different existing static voltage stability analysis indices are selected and examined in detail. These techniques are compared for their advantages and limitations. In order to obtain a clear comparison, an islanded microgrid simulation model is established and applied. A suitable simulation and modelling software is selected via comparison of

different software packages. In practice, the power output of the distributed generators may be influenced by external conditions and the connection nodes. Several scenarios with different power output settings and connection bus settings are applied in the simulation, the objective being to obtain accurate analysis outcomes.

1.3.2 Design of Voltage Stability Index for Islanded Microgrids

Based on the simulation described in the literature and the comparison study, the gap in our knowledge and limitations of the previous voltage stability analysis techniques are found. In this research, the limitations of existing voltage stability indices are focused. A novel approach is developed by combining the advantages of different voltage stability analysis methods for improving performance. The comparison study between the other indices and the novel index is carried out using PSCAD software. Following the simulation work, the accuracy of the novel voltage stability index is investigated by comparing it with other techniques.

1.4 Thesis Structure

Chapter 1 - Introduction. This chapter provides the background on the voltage stability analysis techniques used for microgrids. It articulates the significance of this work, the research aims, methodology and contributions to the literature on this subject.

Chapter 2 – Analytical Methods of Voltage Stability in Renewable Dominated

Power Systems: A Review. This chapter delivers a comprehensive classification and summary of the current research work and provides research directions. Stated here is the critical analysis of knowledge gaps in microgrid voltage stability analysis technique.

Chapter 3 - Modelling of Islanded Microgrids. This chapter describes the software-based design process and presents simulation scenarios and results in terms of the IEEE 14-bus islanded microgrid. An improved 14 bus islanded microgrid with PV, wind turbine, and energy storage system is considered and designed using PSCAD software.

Chapter 4 - Comparison study on State-of-the-Art Static Voltage Stability Analysis Techniques. Presented here is a literature-based case study on state-of-the-art voltage stability analysis methods and the simulation-based comparison study on four voltage stability analysis techniques. Furthermore, the advantages and limitations of the techniques are discussed.

Chapter 5 – An Improved Voltage Stability Analysis Technique for Islanded Microgrids. This chapter encapsulates a study of the novel voltage stability analysis technique design based on existing voltage stability indices in the literature. The improved performance of the novel technique regarding evaluation accuracy and computation efficiency is discussed.

Chapter 6 – Conclusion and Future Research. This chapter summarises all the key conclusions of previous chapters and proposes future research directions on this topic.

References – This section contains a bibliography of all the literature referred to in the thesis. The IEEE reference style is applied.

In this thesis, Chapters 2, and parts of Chapter 3, 4, and 5 have been published in peer-reviewed journal and conference papers.

1.5 Research Contributions

The contributions from this research are:

- A comprehensive review of voltage stability analysis methods and the case study.

- Development of a 14-bus islanded microgrid model with different DGs in PSCAD.

- Comparison of existing state-of-the-art methods for calculating the voltage stability index of islanded microgrids based on the islanded microgrid model.

- Development and optimization of a novel voltage stability analysis technique which is suitable for islanded microgrid.

- Comparison of performance of the new method with other voltage stability analysis techniques using the PSCAD model.

1.6 Publications

The work in this thesis has led to the following publications.

<u>Journals</u>
1. **X. Liang**, H. Chai, and J. Ravishankar, "Analytical Methods of Voltage Stability in Renewable Dominated Power Systems: A Review," Electricity, vol. 3, no. 1, pp. 75-107, 2022. [Online]. Available: https://www.mdpi.com/2673-4826/3/1/6.
2. **X. Liang** and J. Ravishankar, " A Novel Optimized Static Voltage Stability Analysis Technique for Islanded Microgrids," Submitted to Universal Journal of Electrical Engineering (UJEE).

<u>Conferences</u>
1. **X. Liang** and J. Ravishankar, "Voltage Stability Indices for Islanded Microgrids," in 32nd Australasian Universities Power Engineering Conference (AUPEC), 2022. (Presented in 2022 AUPEC)

2 Analytical Methods of Voltage Stability in Renewable Dominated Power Systems: A Review

2.1 Background

This chapter presents the literature review of the voltage stability analysis techniques in renewable dominated power systems. The contents of this chapter have already been published as per the citation below.

X. Liang, H. Chai, and J. Ravishankar, "Analytical Methods of Voltage Stability in Renewable Dominated Power Systems: A Review," Electricity, vol. 3, no. 1, pp. 75-107, 2022. [Online]. Available: https://www.mdpi.com/2673-4826/3/1/6.

The entire chapter detailed here is verbatim reproduced from the above paper, except that the figure and table numbers are changed to match the thesis flow. This paper is an open access publication and therefore has the full copyright permission to use in this thesis. Approval has been sought from the co-authors as well.

2.2 Abstract

The ongoing development of renewable energy and microgrid technologies has gradually transformed the conventional energy infrastructure and upgraded it into a modernized system with more distributed generation and localized energy storage options.

Compared with power grids utilizing synchronous generation, inverter-based networks cannot physically provide large amounts of inertia, which means that more advanced and extensive studies regarding stability considerations are required for such systems. Therefore, appropriate analytical methods are needed for the voltage stability analysis of renewable-dominated power systems, which incorporate a large number of inverters and distributed energy sources. This paper provides a comprehensive literature review of voltage stability analyses of power systems with high levels of renewable energy penetration. A series of generalized evaluation schemes and improvement methods relating to the voltage stability of power systems integrated with various distributed energy resources are discussed. The existing voltage stability analysis methods and corresponding simulation verification models for microgrids are also reviewed in a systematic manner. The traditional and improved voltage stability analysis methods are reviewed according to the microgrid operation mode, the types of distributed generators, and the microgrid configurations. Moreover, the voltage stability indices, which play a crucial role in voltage stability assessments, are critically evaluated in terms of the applicable conditions. The associated modeling and simulation techniques are also presented and discussed. This contribution presents guidelines for voltage stability analysis and instability mitigation methods for modern renewable-rich power systems.

Keywords: voltage stability; microgrids; renewable energy integration

2.3 Introduction

Voltage stability has become a progressively significant issue in modern power distribution networks due to increasing load demands and distributed generation penetration. Compared with traditional power systems, the voltage control capability of renewable energy power generation systems is limited [11-13]. As traditional synchronous generators are gradually being replaced by inverter-based renewable energy generation systems, the stability, system frequency, and voltage of power systems are being challenged [3]. When the voltage control capability of a specific power system is lower than a certain range, the power system becomes unstable. For example, in a double-fed induction generator-based wind energy conversion system (DFIG-WECS), the voltage control capability is dependent on the wind generation penetration rate [14]. The system becomes unstable if the wind power penetration level is beyond 28.06%. Changing the thyristor-controlled series capacitor can improve the voltage control capability, meaning that the system can maintain a steady operation with a higher wind power penetration rate [14]. Therefore, the impact on the system's voltage stability of having distributed generation to the power grid should be carefully studied [14-17].

When experiencing a significant disturbance, microgrids can disconnect from the main power grid through the point of common coupling (PCC) to achieve independent operation, thereby isolating themselves from the main power grid. Therefore, there are many potential stability issues during the operation and maintenance of microgrids, specifically regarding whether the voltages of buses and feeders are stable within a reasonable range under

normal operation and during contingencies [18]. Voltage stability is broadly defined as "the

ability of the power system to maintain steady voltages at all buses of the system after being

subjected to a disturbance from a given initial operating condition" [19]. Due to the

relatively low voltage level in microgrids, uncompensated loads, and the limited damping

function of inverter-based generation, microgrids may experience various voltage

problems and collapse risks [20]. Therefore, the voltage stability analysis of microgrids is an

important research area. Research on the voltage stability of microgrids can be

systematically classified based on the interference scale. In addition, systems can be

classified according to the operation mode of the microgrids. Additional classification

methods are defined according to the duration of the dynamics and the dynamic conditions

of other parts of the system [18]. Figure 2.1 shows the classification process for voltage

stability analysis in microgrids.
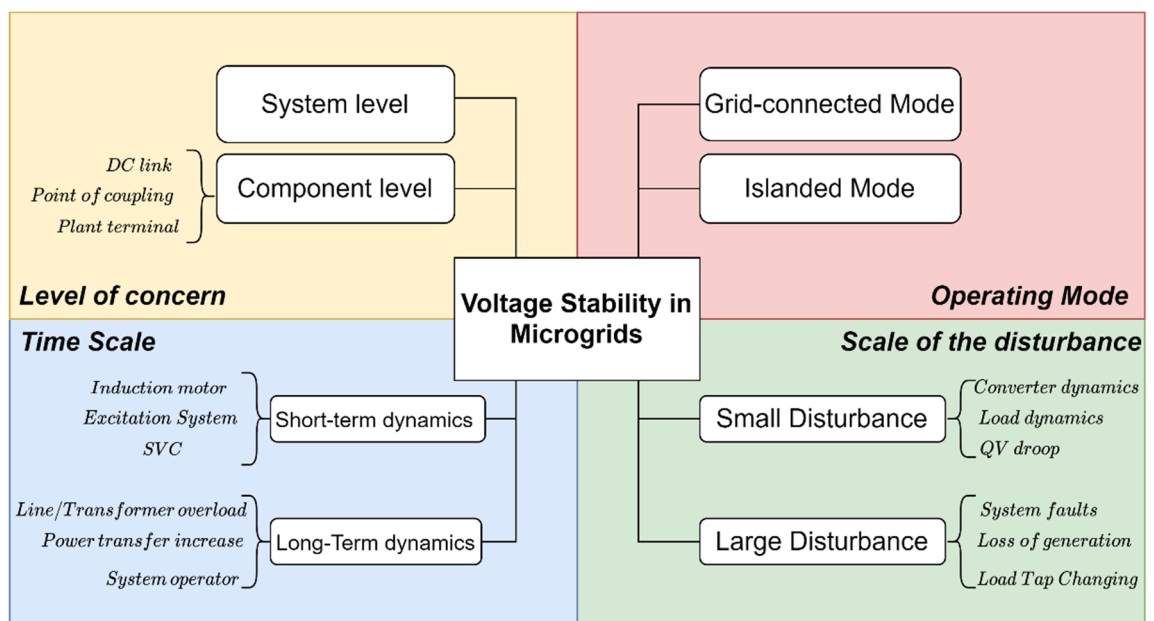
Figure 2.1 Voltage stability classification in microgrids

The classification diagram shown in Figure 2.1 starts from the operation state of the

microgrids and expresses several common factors influencing voltage stability. Among these, tap changers are the main sources of voltage stability problems in utility microgrids [18]. Voltage stability in remote microgrids is related to reactive power compensation in the network. The voltage stability problem in facility microgrids mainly comes from the type and quantity of micro power supply and under-voltage load shedding. Various disturbances can be classified in terms of the disturbance size and duration, resulting in different voltage stability issues in microgrids. Large disturbances affect the entire system's stability for long durations and can cause problems including line faults and generation loss. Voltage fluctuations due to significant disturbances reflect the ability of microgrids to regulate bus and feeder voltages, which requires the nonlinear characteristics of the power system components to be considered. Small disturbances are related to minor changes in the system, such as load changes. For voltage stability problems resulting from minor disturbances, such as load increment changes and other minor changes, a linear approximation of the power system components can be used in the analysis.

Voltage stability analyses can be divided into two main categories: analytical methods and optimization strategies. Static and dynamic analyses constitute two branches of voltage stability analysis. The uniqueness of static voltage stability analyses was shown by [21, 22] through comparative simulation experiments using the Jacobian method, voltage sensitivity method, active and reactive loss sensitivity method, and energy function method. A previous study [23] involved a DC microgrid with ZIP load connected. Such loads have the ability to adjust the proportional power and bus voltage weighting value simultaneously.

This article uses the Laplace matrix in the stability analysis of the system.

The dynamic voltage stability analysis methods have not been clearly classified, unlike the static voltage stability analysis methods. A previous study [24] researched the relationship between steady-state behavior and a dynamic model of a power system. Another study [25] presented a dynamic analysis of different PV penetration effects on a power network. In [26], the effects of thermostatically controlled loads on the dynamic voltage stability of a power system were investigated based on the small disturbance method. Several voltage stability improvement strategies have been reported in the related body of literature. The main strategies for voltage stability improvement include reactive compensation, load shedding, modified current limiters of micro-sources, and voltage regulations with DGs. In [27], the isolated longitudinal system was improved by applying different reactive compensation options. For the load-shedding-related strategy, [28, 29] demonstrated the effects of various undervoltage load shedding settings on the motor load, and the stability improvement was shown via simulation. In [23, 30-34], the optimal arrangement strategies for DGs and the related voltage regulation schemes are presented. The stability characteristics of load dynamics and reactive power compensation were analyzed in [35, 36]. An arrangement method for the current components was proposed to enhance the modification of the current limiters' dynamic voltage stability in [37-39]. In [40, 41], an optimized reactive power compensation strategy was proposed..

The purpose of this article is to determine and discuss the voltage stability analysis methods designed for renewable-dominated power systems. In particular, we focus on the

islanded microgrid, which has not been treated in detail in previous review papers. In addition, the voltage stability indices applied in microgrids are systematically analyzed, compared, and reviewed based on their different DG types. Specifically, the paper aims to

- Investigate the analysis and verification of voltage stability studies based on different renewable energy generation types;
- Classify and compare voltage stability analysis methods based on different microgrid operation modes and types of DGs; and

Evaluate voltage stability techniques and conduct a simulation verification to demonstrate the most suitable simulation platform with different microgrid settings.

The state-of-the-art voltage stability analysis methods applied in renewable-dominated power systems are presented in detail in this paper. This paper takes the form of five sections, including this introductory section. The classification and the mathematical models related to voltage stability analysis methods in terms of both static and dynamic analysis are presented in Section 2. The voltage stability index (VSI) models proposed by researchers in recent years are classified and compared in Section 3. Section 4 presents a comparative discussion of simulation tools and techniques that can be used to verify and apply voltage stability methods to simulations and experimental case studies. Section 5 concludes with the implications of the development with respect to future research recommendations on voltage stability analyses in renewable-dominated power systems.

2.4 Voltage Stability Methods of Analysis

The significance of voltage stability analyses is the determination of vulnerable parts of microgrids through appropriate evaluation methods. Improving voltage stability can identify reasonable solutions for further optimization, enhance the system's strength, and enhance the tolerance level of abnormal operation of the microgrids. The continuous replacement of synchronous generators by inverter-based units puts a limit on the reactive power capacity of the system, leading to an unstable voltage after the occurrence of external interference [42, 43]. The voltage stability analysis method can be selected based on the microgrid stability mechanism [44]. Reactive power Q and bus voltage V are direct measurement parameters of voltage stability for microgrid systems. When the V–Q sensitivity of all buses in the system is positive, the voltage of the power system is stable. If at least one current V–Q response is negative, the voltage of the power system is unstable.

Figure 2.2 shows the classifications of voltage stability analysis methods, including static and dynamic voltage stability analyses. Static analysis techniques analyze the voltage stability by using the static operating parameters of microgrids to determine the key factors affecting the stability. Static analysis techniques only consider the static operation of microgrid systems, and the real-time variable differential equation is set to zero. At present, static analysis techniques are commonly based on load flow analyses, such as P–V, V–Q analysis, and V–Q sensitivity analysis [45]. Dynamic voltage stability analysis methods are helpful when analyzing voltage collapse and testing the application effect of the control strategy. Dynamic analysis methods are similar to transient analyses of the power system,

where a set of differential equations is used for system modeling. As the dynamic influence on the system's stability usually changes relatively slowly, the system's static operating parameters are still used in most dynamic voltage stability studies.
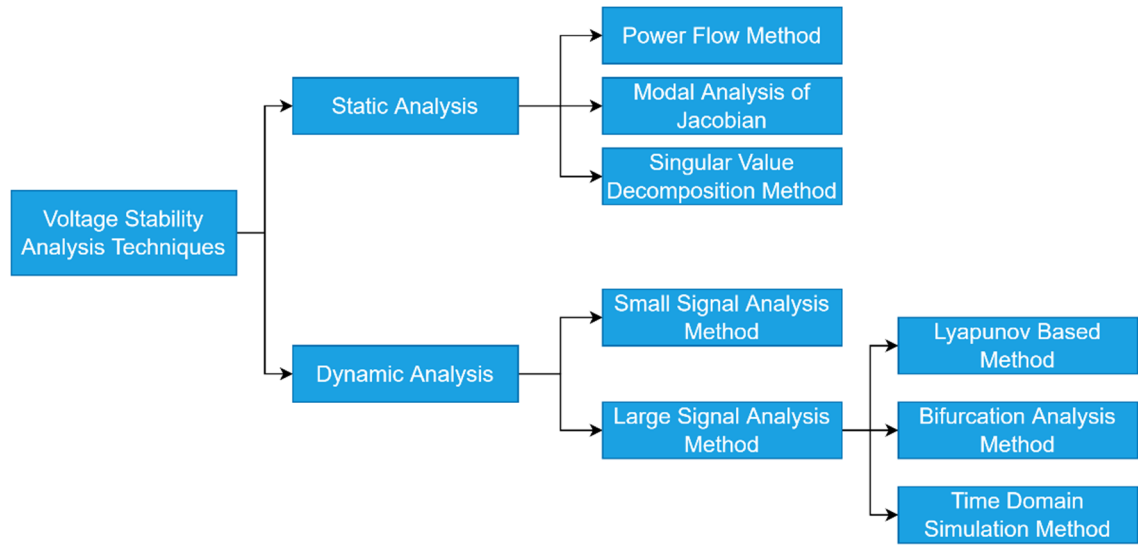
Figure 2.2 Classification of voltage stability analysis techniques

2.4.1 Static Voltage Analysis Techniques

At present, a series of the existing static voltage stability analysis methods of microgrids is based on the calculation and modification of the load flow equation. The microgrids are modeled by the following first-order differential equations [45]:

$$\dot{x} = f(x, V) \tag{1}$$

$$I(x, V) = Y_N V \tag{2}$$

where $\dot{x}$ is the state vector, V is the bus voltage vector, and Y_N is the admittance matrix of bus N.

In static analysis methods, when the value of $\dot{x}$ is zero, the system operates under steady-state conditions and represents the margin of stability. In load flow equations, a feasible solution is based on the judgement of system voltage stability, which means that the feasible solution to the load flow equation is the voltage stability limit of the microgrid. In addition, static voltage stability analysis methods can provide researchers with information on the system voltage stability margin and state variable sensitivity. Consequently, static voltage analysis methods for microgrids are generally divided into three categories: the load flow method, the modal analysis of the Jacobian matrix, and the singular value decomposition method. Several common static voltage analysis techniques are summarized below.

2.4.1.1 Continuation Load Flow Method Using P-V and V-Q Curves

By constantly updating the load flow equation and calculating the existence of a solution to the load flow equation, the convergence problem near the stable operation limit point can be solved, and the voltage stability limit can also be obtained. Moreover, the approximate voltage collapse point is rounded by the continuous prediction and correction process. This solution is the continuation load flow method based on the convergent solution to the load flow calculation. A set of load flow results are obtained by changing the load value P or Q of the selected bus and operating the microgrids with all other parameter settings unchanged. When the load flow algorithm cannot converge, the corresponding point is the voltage collapse point, which is the margin of the stable and unstable states of the microgrid. Figure 2.3 shows P–V and V–Q curves illustrating the

voltage characteristics in terms of both active power and reactive power [18].
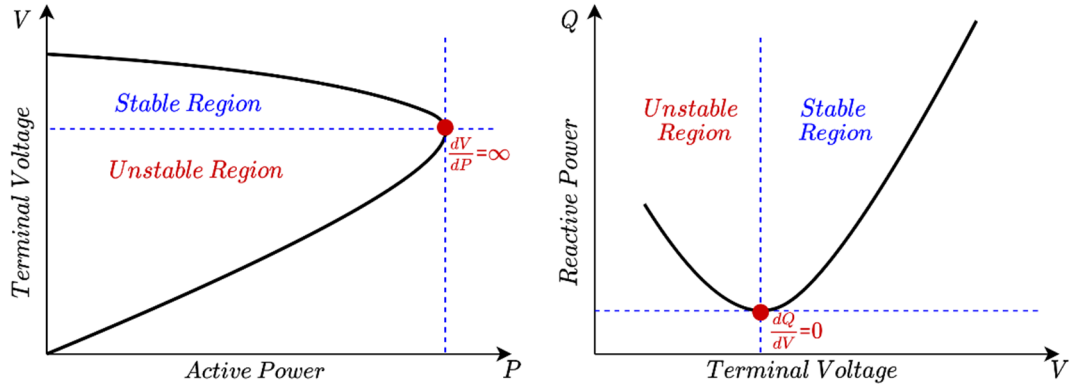
Figure 2.3 P-V and V-Q curves in voltage stability analysis of power systems showing stable and unstable regions

As one of the conventional methods, the continuation load flow method has been studied for a long time. It has been used extensively to calculate the critical voltage collapse point, helping to determine the voltage stability limit. However, this method is only suitable for simple microgrid systems and cannot be applied to large and complex systems, as the calculations are highly time consuming.

2.4.1.2 Modal Analysis of the Jacobian Matrix Based on V–Q Sensitivity

In the modal analysis method, the sensitivity matrix is obtained by linearizing the load flow equation of the system [46]:

$$\begin{bmatrix} \Delta P \\ \Delta Q \end{bmatrix} = \begin{bmatrix} J_{P\theta} & J_{PV} \\ J_{Q\theta} & J_{QV} \end{bmatrix} \begin{bmatrix} \Delta \theta \\ \Delta V \end{bmatrix} \tag{3}$$

where ΔP is the bus real power change, ΔQ is the bus reactive power change, $\Delta\theta$ is the bus voltage angle change, ΔV is the bus voltage magnitude change, and J is the Jacobian matrix.

By assuming that the real power P is constant in the calculation (due to the static nature of the analysis), the sensitivity matrix equation is inversed to obtain the following equations [44]:

$$J_R = (J_{QV} - J_{Q\theta} \times J_{Q\theta}^{-1} \times J_{PV}) \tag{4}$$

$$\Delta V = J_R^{-1} \Delta Q \begin{bmatrix} \Delta P \\ \Delta Q \end{bmatrix} = J_R^{-1} \Delta Q \begin{bmatrix} J_{P\theta} & J_{PV} \\ J_{Q\theta} & J_{QV} \end{bmatrix} \begin{bmatrix} \Delta\theta \\ \Delta V \end{bmatrix} \tag{5}$$

In the equations above, J_R^{-1} is the V–Q sensitivity matrix. Specifically, if the value of J_R^{-1} is positive, the system voltage is stable. If not, the system may be an unstable one.

In [7], a new and time-saving sensitivity-based voltage stability analysis method was proposed. This method deduces the Thevenin-Based Voltage Stability Margin based on the amplitude and angle of the node voltage for preventive control. Unlike other commonly used sensitivity methods, this method does not need complex calculations to consider the maximum loading point (MLP) in real-time applications. In the simulation results, the accuracy and rapidity of this method are successfully verified for power systems without emergencies. However, this method is unsuitable for systems with emergencies, allowing room for improvement.

In [47], a method for validating the sensitivity of the voltage stability margin was proposed. This method can be used to identify the weakest voltage stability bus and the node-set. This research extends the application of such a method to a multi-machine system from a Single Machine Infinite Bus (SMIB) system.

In addition, the standard P–V curve or V–Q curve method has been applied by many studies in the literature. In [48], Bonneville Power Administration power analysis platform (PSD-BPA software) was used to apply this method to a wind-power generation system. In [49], DIgsilent PowerFactory was used to analyze the impact of large-scale wind power on the state grid. PowerFactory was also used in [39] to analyze a power system with photovoltaic power generation. In [50], the influence of new energy generation on power system stability was studied by using continuation load flow (CPF) combined with a P–V curve analysis in the PSAT power system toolbox environment. The sensitivity modal analysis method is simple and easy to apply. It only needs a small amount of computing and is therefore more efficient for data processing. However, this method is not suitable for microgrids with complex network configurations because of the weak linear characteristic of the index.

2.4.1.3 Singular Value Decomposition Using Network-Load Admittance Ratio

If the load condition of microgrids is close to the critical state, the trend of the Jacobian matrix can be close to singularity. Therefore, the singular point of the Jacobian matrix of the load flow equation can represent the critical point of system voltage stability (voltage collapse point). In addition, this method plays a crucial role in static voltage stability analysis methods.

Y. Song et al. [8] proposed an index representing the load admittance ratio based on

the improved load flow Jacobian matrix for the voltage stability analysis of microgrids. In their paper, a simple two-bus system was used, as shown in Figure 2.4. The method was applied to a network with distributed generator systems (DGS) that could be simplified by equivalent admittances of the load and transmission lines. The ratio-based function presented in the literature is expressed as:

$$M_{n/d} = 1 - \frac{P_{L1}}{P_{L1}^{Lim}} = 1 - \frac{R_{n/d}|1\angle\alpha_{loss} + 1\angle\alpha_d|^2}{|1\angle\alpha_{loss} + R_{n/d}\angle\alpha_d|^2} \tag{6}$$

where $R_{n/d}$ approaches infinity when there is no load, and $R_{n/d}$ = 1 is the voltage stability limit point. As a result, the voltage stability index $M_{n/d}$ ranges from 0 to 1 (stability limit point to no load). Refer to [51] for the detailed linear index calculation.
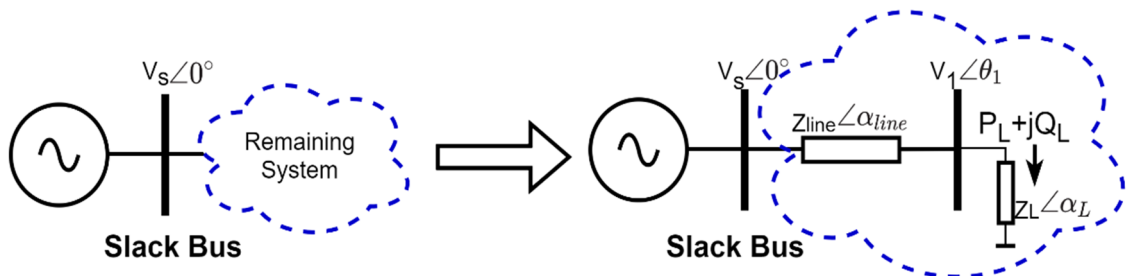
Figure 2.4 A typical two-bus system for load and transmission line equivalent admittance method.
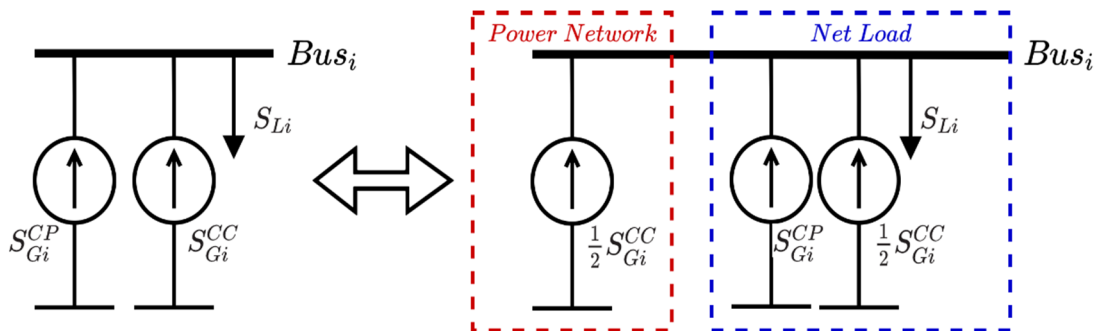
Figure 2.5 Illustration of CP-DGS and CC-DGS equivalents

The voltage stability analysis index is determined according to the parameters of the

power grid, load, and distributed generation. This concept is a generalization of the line load admittance ratio, representing the load state of the general distribution system considering the influences of constant-power distributed generators (CP-DGS) and constant-current distributed generators (CC-DGS), as illustrated in Figure 2.5. The admittance ratio represents the load state of the distribution system and considers the influence of distributed generation. It has been proven that the Jacobian load flow is singular when the network load admittance ratio is 1. Additionally, the Voltage Stability Index (VSI) has been verified on several IEEE test feeders. Simulation results have shown an excellent linear relationship between the network load admittance ratio and the load growth, and the voltage stability margin can be well estimated. In addition, the index reflects the influences of the DG access level and control mode on voltage stability. In [52], a voltage stability analysis technique was proposed based on the smallest eigenvalues and the associated eigenvectors of a reduced Jacobian matrix. The eigenvalue modules describe the voltage stability of the current state. This work is based on an early scheme of the singular value decomposition method, which has been improved and applied many times.

In summary, a singular value decomposition method based on the linearized load flow equation was proposed. Because of the high nonlinearity of the Jacobian matrix, this method cannot accurately analyze the voltage stability.

2.4.1.4 Transfer Capability Evaluation Using Static Analysis Methods

The overwhelming cost of power transmission network development and the need for

improved transfer capability has raised significant concerns regarding distributed energy system planning [53, 54]. Therefore, several correlational studies are being conducted to investigate the impact of voltage stability on the power transfer capability. The advantage of considering static voltage stability analysis is that both bus voltage and its voltage stability limits can be fully considered during the calculation. In [55], a static Thevenin equivalent method to estimate the voltage collapse point and the system stability margin with wind generation was proposed. This study evaluated the assessment methods at a wind hub connected to a medium-voltage transmission network. The wind hub was modeled using the Thevenin equivalent parameters to calculate the maximum power transfer capacity, and the simulation results show that the power transfer capability can be seen as a linear relationship with the voltage stability. In   [56], the power transfer capability was studied based on the continuation load flow analysis. The maximum loading factor can be calculated through continuation load flow analysis, and the power transfer capability limit can be obtained with a simulation. Although this method is effective and intuitive, it is unlikely to produce a global optimum, as the calculated loading factor presents a system-wide limit and finding the optimal settings for bus connections is challenging. In addition, only the voltage limit and line thermal limit can be considered when determining the power transfer capability, while other practical factors are neglected (e.g., the uncertain regional weather of the transmission network, which is important but not considered in the continuation power flow methods).

2.4.2. Dynamic Voltage Analysis Techniques

Static voltage stability analysis methods have been widely employed in voltage stability analysis cases. However, given that power systems are dynamic entities and voltage instability and collapse are also dynamic responses, the analysis of dynamic voltage stability is also of particular importance [57]. Dynamic voltage stability analysis is critical when investigating the long-term impacts of high time-varying components in microgrids. Dynamic voltage stability is the ability of the power system to maintain a balance between load demand and supply [58, 59]. Compared to static analysis methods, dynamic analysis methods can reflect the behavior of system components in a more practical manner.

The time-domain simulation method is the most suitable method for dynamic voltage stability analyses and is suitable for any power-system model. Different load models will lead to different conclusions by building different time-domain simulation dynamic models. In [60], a generalized load flow calculation model was proposed to simulate the behavior of a distributed generation system. In that study, a set of time-domain nonlinear equations was used to represent an islanded microgrid, and the V–Q sensitivity was analyzed. In [61], a voltage analysis index based on network loss sensitivity, which is used for online simulation and tests, is discussed. Although this method has broad application, there is still dispute over its use because of its different simulation characteristics for different load models; thus, it needs to be further optimized and studied. Short- and long-term voltage stability evaluations can be carried out through time-domain dynamic simulation of the microgrid system represented by differential-algebraic equations (refer to Equation (12)). The

differential equations in the transient response can be solved by using numerical integration techniques. Several dynamic voltage analysis techniques are reviewed below.

2.4.2.1. Small Signal Analysis Method

The small signal analysis method is applicable for minor disturbances. It is based on the linear differential equation of the distributed networks. It is suitable for determining the voltage stability influence of on-load tap-changing transformers, dynamic loads, and generators. By modeling the differential-algebraic equations, the system is linearized at the balance point, as shown below:

$$\Delta \dot{x} = A\Delta x + B\Delta y \tag{7}$$

$$0 = C\Delta x + D\Delta y \tag{8}$$

where $\dot{x}$ is the system state variable, and y is the algebraic variable.

When the algebraic variation is zero, the linearized system can be expressed as

$$\Delta \dot{x} = J\Delta x \tag{9}$$

$$J = A - BD^{-1}C \tag{10}$$

where J is the coefficient matrix of Δx. To this end, the voltage stability of the small disturbance system can be estimated by calculating the eigenvalue of matrix J.

The Jacobian matrix presented in Equation (3) retains the Q–V relationship in the power

system and expresses the linearized steady-state voltage equation in the static analysis. The modal analysis of the Jacobian matrix is usually used in static voltage stability analyses. Even though the small signal analysis method used in dynamic analyses is based on the modal analysis of the Jacobian matrix, there are still some differences between the modal analysis used in the static analysis and the small-signal-based dynamic analysis.

The first difference is the computational complexity. Dynamic analyses study the transient stability of the system, including the influences of the dynamic loads and generators, whereas static analyses focus on the solutions to algebraic equations of the system's state. Applying the small-signal analysis in dynamic studies can be more complex. However, the application of the modal analysis to static analyses mainly focuses on how far the stability margins move away from the voltage stability collapse point, a process that is computationally less extensive.

Secondly, dynamic analyses represent a kind of hybrid evaluation tool composed of the static analysis method and nonlinear analysis tools and are based on the use of fundamental modal analysis in static analysis methods. Small-signal voltage stability analyses usually involve the use of static analysis tools, such as the modal analysis of the Jacobian matrix and the power flow analysis. However, the small-signal-based dynamic voltage stability analysis method is a combination of linear and nonlinear analysis tools.

In [62], a reduced-order small-signal-analysis model was proposed for an islanded microgrid with multiple micro sources. The eigenvalues were obtained with the system

matrix by linearizing around the operation point. The simulation results were compared and verified with the PSCAD platform.

The bifurcation method is also a critical theory that is used to analyze the voltage stability for small signals. Bifurcation refers to a phenomenon that leads to a sudden system stability change when one or more parameters in the system change. The changed parameter value is called the bifurcation value. There are two main bifurcation structures in the mathematical representation of power systems: Hopf bifurcation and saddle-node bifurcation. Hopf bifurcation refers to the phenomenon where a pair of complex conjugate eigenvalues are on the imaginary axis, resulting a loss of stability and continuous oscillation in the power system. Saddle node bifurcation is a process in which a real eigenvalue is located on the imaginary axis, and the system completely loses stability with the continuation of bifurcation. Local bifurcation theories, such as P–V and P–Q curves, can be used to determine the characteristics of static parameters when bifurcation occurs. Bifurcation theory is an essential aspect of studying the dynamic stability of the power system. In [52], the Hopf bifurcation-related method for the system was developed. The authors of [63] used the bifurcation theory analysis on an AC islanded microgrid under loop control and detected Hopf bifurcation and the saddle-node bifurcation points in the power system. Furthermore, they predicted the unstable bifurcation margin, thereby increasing the computation efficiency for the voltage stability analysis and prediction.

2.4.2.2. Large Signal Analysis Method

Voltage stability analyses are generally restricted to small disturbance studies, where the

system has voltage instability issues due to slow changes in system parameters. However, researchers have found that transient phenomena, such as tripping incidents, short circuits, and blackouts, can lead to significant load voltage changes that cannot be kept constant [64]. In this context, large-signal voltage stability analysis methods play an important role.

The Lyapunov-based method is a large-signal voltage stability analysis method based on the dynamic performance of switched microgrid models. It is used to develop solutions to differential equations. If the switched system's state transition matrix has negative real eigenvalues, the system tends to stabilize [65]. The Lyapunov equation is shown below:

$$A_P^T P + P A_P \leq -Q \tag{11}$$

where P and Q are symmetric matrices.

A positive Q and a unique positive P exist for a switched linear system that can satisfy the Lyapunov equation [9]. In [66], a model consisting of nonlinear elements for the microgrid, including the loads and generators, was developed. Based on the Lyapunov stability theory for a closed-loop system, all eigenvalues in the Jacobian matrix should have negative real numbers. The research results prove that the dynamic voltage stability scheme could work well for the microgrid system. In [60], an energy-function-based voltage stability analysis method for the islanded microgrid was developed. The energy function method directly uses the Lyapunov theory to analyze the system's voltage stability. The whole model is divided into two parts: the energy function and the auxiliary function. The energy function considers the change in load, the solar radiation, and the energy storage system charging

conditions, allowing direct evaluation of the stability of the system's operating point. The energy function expression is [67]:

$$v(X^S, X^u) = \sum_{i=1}^{n} [\int_{\theta_i^S}^{\theta_i^u} f_i(\theta, V)d\theta_i + \int_{V_i^S}^{V_i^u} g_i(\theta, V)dV_i] \qquad (12)$$

where $v(X^S, X^u)$ is the measured value that indicates the system's energy balance, n is the system's node number, and f and g are the power values.

The researchers simplified the load model as a static model instead of using a dynamic model, so the dynamic characteristics of the load were not considered. The simulation results of the IEEE 37-bus test feeder show that the energy function is effective for voltage stability evaluation. Auxiliary function technology can improve the stability of the system when the intermittent power supply is configured in the microgrid area. The closer the energy measure value is to zero, the lower the voltage stability is. The method based on the energy function does not completely suffice for predicting load characteristics. Thus, the efficiency of this method remains to be proven. However, it presents an idea for combining static voltage stability and dynamic analyses.

2.5 Voltage Stability Analysis Indices

The voltage stability analysis techniques mentioned in Section 2 can be used to evaluate the voltage stability of microgrids. Nevertheless, such techniques cannot indicate how far the system is from the voltage collapse margin (i.e., the boundary between system voltage stability and instability). Therefore, the concept of the voltage stability index (VSI), through

which the level of system stability can be obtained, was introduced. This allows a comprehensive voltage stability analysis to be performed based on the inclusion of one or more voltage stability indices. To understand the voltage collapse proximity of the microgrid system more accurately, as well as the maximum load capacity of the system, and to identify the bus with the weakest stability, the use of the voltage stability index is essential. The voltage stability index, however, has a high calculation cost when quantifying stability. This section reviews the use of the voltage stability index in the current research field.

2.5.1. VSI Classification

This section systematically classifies the VSI and reviews the related methods according to different classifications to understand how the voltage stability analysis index is applied to microgrids. At present, there are many directions for VSI classification in the research field, among which the most common method is classification according to the variables used in the VSI definition formula. For example, in [45], VSIs are divided into the index class, eigenvalue decomposition class, and line data class based on system variables and the Jacobian matrix. In [68], the authors classified the indices as the Jacobian matrix index and system variable index according to the formulation mechanism. In addition, these indices can be classified according to the evaluation target, for example, according to the measurement target and the voltage instability mechanism. As per the voltage instability classification presented in [53, 54], the areas that are most prone to voltage collapse in the power system can be identified through different VSIs. In [69], classification according to offline or online VSI applications was proposed, in which offline is suggested for VSI

applications of buses and online is suggested for VSI applications of lines. Figure 2.6 shows

the VSI classification framework, including the mentioned categories.
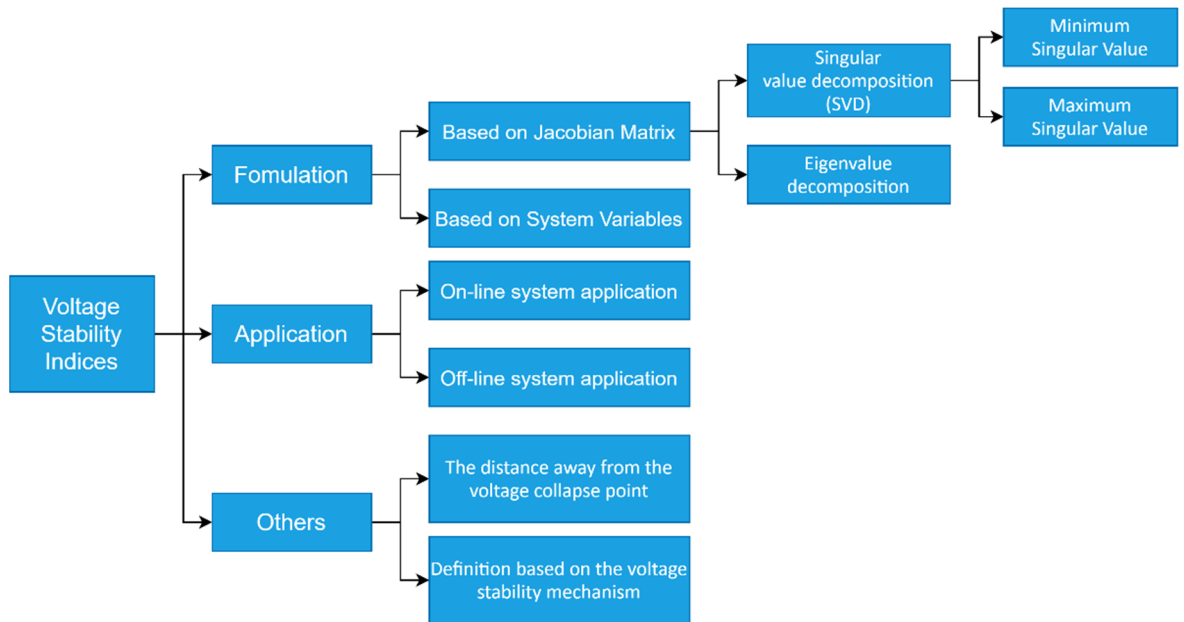
Figure 2.6 Voltage stability indices classification.

2.5.2. Voltage Stability Indices Review

Researchers have compared, analyzed, and classified the voltage stability indices from

different aspects [70]. At present, the most commonly used VSI classification scheme

involves dividing VSIs into two categories based on the Jacobian matrix and system

variables according to the VSI formula [71]. In addition, in [72-74], several common

indicators are compared and classified based on load shedding and optimal storage in

critical cases. This section reviews and analyzes the microgrid-based voltage stability indices

proposed in the literature.

2.5.2.1. Jacobian-Matrix-Based VSIs

A VSI calculation based on the Jacobian matrix needs all of the system's data. Its central theory involves singular values and the eigenvalue index. Based on the singularity of load flow, the Jacobian matrix is close to singular at the point of voltage collapse. It requires a significant amount of calculation and detailed power system information.

In [75], a singular value decomposition (SVD) method was developed, and the following equations illustrate the detailed formulation of this technique:

$$J = VSU^T = \sum_{i=1}^{2(n-1)} u_i s_i v_i^T \tag{13}$$

$$\begin{bmatrix} \Delta\theta \\ \Delta V \end{bmatrix} = \delta_{2(n-1)}^{-1} v_{2(n-1)} u_{2(n-1)}^T \begin{bmatrix} \Delta P \\ \Delta Q \end{bmatrix} \tag{14}$$

where J is the singular value, U is the left singular vector, V is the right singular vector, S is the singular vector, u_i, s_i, v_i^T are the values of the matrix from the ith column, $v_{2(n-1)}$ provides details about the critical bus, and $u_{2(n-1)}$ shows the power mismatch details for $\begin{bmatrix} \Delta P \\ \Delta Q \end{bmatrix}$.

Here, the vectors $v_{2(n-1)}$ and $u_{2(n-1)}$ provide information on the weakest bus and area of the power system, respectively. The minimum value of $v_{2(n-1)}$ illustrates which bus is the weakest.

Singular value decomposition has been demonstrated to be a superior method for voltage stability analysis in comparison to modal analysis in the following aspects: the SVD

method only has one mode in comparison with the modal analysis, which has several modes. It is hard to determine the weakest operating mode in the modal analysis. The SVD method uses the full Jacobian matrix instead of the reduced Jacobian matrix, which is used in the modal analysis. Even though the complexity of the question is reduced in the modal analysis, the P–V and Q–θ coupling issues cannot be focused on under the reduced matrix method. The SVD method is used to identify the weakest boundaries during voltage stability analysis, which is helpful when conducting the correction analysis in further steps.

In [44], the basic formulation and definition of the eigenvalue decomposition technique are shown. The following equations illustrate the detailed formulation used in this technique.

$$J_R = \in \Lambda \eta \tag{15}$$

$$\triangle V = \in \Lambda^{-1} \eta \triangle Q \tag{16}$$

$$\triangle V = \sum_I \frac{\in_i \eta_i}{\lambda_i} \triangle Q \tag{17}$$

$$v_i = \frac{1}{\lambda_i} q_i \tag{18}$$

where η is the right eigenvector of matrix J_R, $\in$ is the left eigenvector of matrix J_R, Λ is the diagonal eigenvalue matrix of J_R, v is equal to $\eta \triangle V$, q is equal to $\eta \triangle Q$, and v_i is the ith mode of the V–Q response. If λ_i is positive, the ith voltage and modal reactive power are directly proportional, and the system is stable. If λ_i is negative, the ith voltage and modal reactive power are not directly proportional, and the system is unstable.

In [76], the sensitivity of the steady-state power system model was analyzed based on the theorem that the Jacobian matrix J is a singular matrix at the critical point. Through the parameterization of the load flow equation and the correlation operation of the left eigenvector after Taylor's expansion, the approximate expression $S_{\lambda\omega}$ of the sensitivity matrix of the power system with new energy generation can be obtained [77, 78]:

$$S_{\lambda\omega} = \frac{\triangle\lambda}{\triangle\omega} = -\frac{MF|_\omega}{MF|_\lambda} \tag{19}$$

$$\triangle\lambda_i = \sum_r s_{ir0}\,\triangle\omega_r \tag{20}$$

where ω is the node power random disturbance coefficient, λ is the loading margin, and r is the node number.

The sensitivity matrix expresses the influence of the load margin on the power random disturbance coefficient. Combining the VSI calculation method with the cumulant-based maximum entropy method (CMEM) in probability theory, the randomness of wind power, PV, and other types of renewable energy power generation and the impact of power load consumption on the load margin can be measured. Compared with the series expansion method, this method has greater sensitivity under different levels of renewable energy permeability, leading to more accurate and effective analysis results. As this method considers the probability theory principle of accumulation and an increase in maximum entropy, it takes into account the correlation and uncertainty of power injection and consumption. Therefore, this method is more suitable for renewable energy power generation systems. Additionally, compared with the Monte Carlo method (MCM), this

method has a higher calculation speed. Comparative experimental results show that this method is up to 99.95% quicker than the MCM method. This is because the CMEM method can classify samples through K-means clustering technology, which significantly reduces the redundancy of repeated operations. Therefore, the scheme is suitable for microgrid systems with integrated renewable energy generators.

2.5.2.2. System-Variable-Based VSIs

In [79], a new stability index based on a two-bus equivalent circuit (SMIB system) was developed, as shown in Figure 2.7a. By simplifying the equations, the above basic index was developed in the presence of tap changers and DGs based on Figure 2.7b. The proposed index was obtained using the following equations:

$$VSI_1 = V_1^2 - 4(PR + XQ) \geq 0 \tag{21}$$

$$VSI_2 = V_1^2 t^2 - 4t^2(PR + XQ) \geq 0 \tag{22}$$

where t is the transformer ratio.
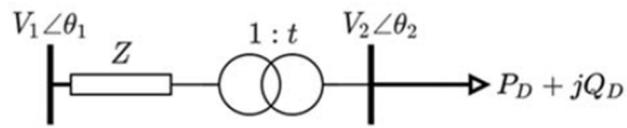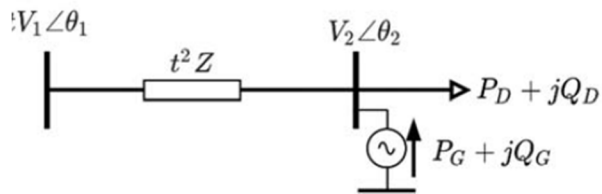
Figure 2.7 (a) Two-bus system (b) Equivalent circuit after removal of the transformer (elements transferred from the primary side to the secondary side) in the presence of tap chargers and DGs

Based on this improved VSI, researchers can easily detect the voltage stability level in the system with distributed generators. This method can be used to rank the voltage stability of the network bus through the calculation of VSI, and then the weakest bus can be identified. Unlike using the Jacobian matrix to obtain the stability index, the VSI calculation method does not calculate the Jacobian matrix and bus impedance matrix of the whole system. Instead, it directly uses the power value of the system from load flow calculations, and therefore the problems of low calculation speed and complex calculation are avoided to a great extent. Thus, this method has the advantages of involving simple calculation and high accuracy, which makes this index suitable for the study of the voltage stability of distribution networks with a large number of buses. In addition, this method is suitable for microgrids with tap changers. However, many system parameters, such as R, X, P, Q, the Jacobian matrix and the admittance matrix, are not considered in the calculation. Although this method improves the calculation efficiency, it ignores the influences of these

parameters on the system.

In [80], a novel VSI, named the fast voltage stability index (FVSI), was proposed to identify weak voltage stability areas or buses. In this method, for base load to peak line loading situations, each bus is evaluated by the FVSI to check if it is the weakest one in the whole system. If the FVSI is equal to one, the system is unstable. The lower the FVSI, the more stable the bus voltage is. The line index is calculated using the following equation:

$$FVSI_{ij} = \frac{4Z^2 Q_j}{|V_i|^2 X'} \tag{23}$$

where Z is the line impedance, X is the line reactance, V is the sending end voltage, and Q is the receiving end reactive power.

In [81], a quantitative transient voltage evaluation index based on the ultrahigh-voltage direct-current (UHVDC) transmission terminal that can analyze and determine the dynamic reactive power compensation capacity was proposed. With the high proliferation of renewable energy generation, several UHVDC projects have been designed to transmit renewable power from remote areas to the capital cities, which have great demands for electricity. Thus, research on voltage stability analyses for the UHVDC transmission system is also worthwhile. The voltage stability in each region is quantitatively compared using the approximate step function, absolute sensitivity, and relative sensitivity. The voltage stability index proposed in this paper is suitable for power systems with a UHVDC transmission system. It is used to evaluate the transient overvoltage state of the UHV transmitting power system. Here, the concepts of absolute sensitivity and relative sensitivity are proposed. The

parameters of this method are set according to the operational requirements of the UHVDC

transmission system rather than those of the distribution network. Therefore, this method

is more suitable for actual large-scale networks in the selection of parameters. However,

the analysis parameters proposed in this paper are based on a DC transmission system, so

this scheme is not suitable for AC microgrids, which means that the application scenario of

this scheme is relatively limited.

In [82], a voltage stability index based on sensitivity factors that consider the power

system load was proposed. The formula was defined as below:

$$d_i = \frac{1}{1 + \frac{\gamma(\Delta + \lambda)}{\pi_i}} \tag{24}$$

where Δ and γ are diversity and scale factors, π_i is the Lagrange multiplier for bus i, and

λ is the loadability for the current operating state.

The VSI index (d-index) shown above can indicate the stability state of the system with

a range of 0 to 1 (stable to unstable). Using ZIP and the exponential model and considering

the difference between the maximum power transmission point and load point, the voltage

stability of different bus loads under different stress conditions can be evaluated. The index

was improved by using the traditional L-index stability analysis method. The scheme uses

the concept of the Lagrange multiplier. Previous experimental results show that with an

increase in the load to voltage collapse, the Lagrange multiplier related to maximum

reactive power generation will decrease when the power system approaches the maximum

load limit. Therefore, one advantage of this scheme is that it can refine the exponential

response through multiple attempts to change the parameters. Compared with other similar VSIs, the d-index performs better. The L-index presented by P. Kessel, and H. Glavitsch [83] is the traditional method and can conservatively evaluate the steady-state of the system. However, when the L-index reaches the MPPT limit, this will cause a false alarm for the system state, leading to erroneous results. As the exponential response of the d-index is refined according to different parameters in different systems, it can better estimate the proximity of voltage collapse than the traditional L-index method.

To effectively present how voltage stability analysis can be employed in renewable-dominant power systems, a summary of the stability analysis methods, VSI, analytical foundation, equation, and the stability threshold is presented in Table 2.1.

Table 2.1 Voltage stability analysis techniques summary

Ref	VSI/Method	Analytical Foundation	Index Type	Equation	Stability Threshold
[84]	$J^C \in C^{2n \times 2n}$	Jacobian Matrix Singular Point	Static	$J^C = \begin{bmatrix} -I^n & V^n\, {}^-Y^b \\ -V^nY^b & I^n \end{bmatrix} =$ $\begin{bmatrix} V^n & \\ & -V^n \end{bmatrix} \begin{bmatrix} (V^n)^{-1}\, {}^-I^n & -Y^b \\ Y^b & (-V^n)^{-1}I^n \end{bmatrix}$ $\Lambda = (V^n)^{-1}Y^{b/n}V^n$	$\lambda^{cr} = \min_{\lambda_i}\|\lambda_i - 1\| = 0,$
[85]	L_s-index	Load flow Equation	Static	$L_i = \frac{1}{V_i}\sqrt{f^2 + g^2}$	$L_s \leq 1$
[81]	TVAI	Approximated Step Function	Dynamic	$F = F_1 + F_2 = \sum_{i=0}^{n}\sum_{j=1}^{m} K_j g_j(V\|t_i\|)\|V[t_i] - V_N\|\, \triangle$ $t + \sum_{i=1}^{n} \frac{k}{1+e^{\frac{(\|t_i\|-V_N-a)c}{b}}}$	$g_j(V\|t_i\|)$ $= \begin{cases} 1 & (V_{cr.j+1} \leq V[t_i] \leq V_{cr.j}) \\ 0 & (V[t_i] \leq V_{cr.j+1}\ or\ V[t_i] > V \end{cases}$
[79]	VSI	Two-bus Equivalent Circuit	Static	$VSI = V_1{}^2 - 4(PR + XQ)$	$VSI \geq 0$
[86]	VSI	Two-bus Equivalent Circuit	Static	$VSI = \frac{4R_i \times P_i{}^2}{(Q_iV_{i-1}sin\delta_i + P_iV_{i-1}cos\delta_i)^2} \times (P_i + \frac{Q_i{}^2}{P_i})$	$VSI \leq 1$
[87]	$v(X^S, X^u)$	Energy Function	Static	$v(X^S, X^u) = \sum_{i=1}^{n}[\int_{\theta_i{}^S}^{\theta_i^u} f_i(\theta, V)d\theta_i + \int_{V_i{}^S}^{V_i^u} g_i(\theta, V)dV_i]$	$v(X^S, X^u) \geq 0$
[88]	$M_{n/d}$	Load flow Jacobian matrix	Static	$M_{n/d} = 1 - \frac{P_{L1}}{P_{L1}^{Lim}} = 1 - \frac{R_{n/d}\|1\angle\alpha_{loss} + 1\angle\alpha_d\|^2}{\|1\angle\alpha_{loss} + R_{n/d}\angle\alpha_d\|^2}$	Ranges from 0 to 1 (Stability limit point to no load)
[89]	$cat_{VSI(n)}$	Saddle-node	Static	$cat_{VSI(n)} = (P_nR_{mn} + Q_nX_{mn} - 0.5\|V_m\|^2)^2 -$	Range from 0.25 to 0

Ref	VSI/Method	Analytical Foundation	Index Type	Equation	Stability Threshold
		& finite induced bifurcation		$Z_{mn}^2(P_m{}^2 + Q_m{}^2)$	(No load to collapse point)
[90]	Sensitivity matrix	Linearised load flow equation	Static	$\begin{bmatrix} \Delta P \\ \Delta Q \end{bmatrix} = \begin{bmatrix} J_{P\theta} & J_{PV} \\ J_{Q\theta} & J_{QV} \end{bmatrix} \begin{bmatrix} \Delta\theta \\ \Delta V \end{bmatrix}$ $\Delta Q = (J_{QV} - J_{Q\theta}J_{P\theta}{}^{-1}J_{PV})\Delta V$	If the sensitivity measure is positive, the system is stable; if not, the system is unstable.
[89]	GSA	Optimal Load flow and probabilistic model	Static	$PL_{ij} = -t_{ij}G_{ij}V_i{}^2 + V_iV_j(G_{ij}cos\theta_{ij} + B_{ij}sin\theta_{ij})$ $QL_{ij} = t_{ij}B_{ij}V_i{}^2 - \dfrac{B_{ij}V_i{}^2}{2} + V_iV_j(G_{ij}sin\theta_{ij} - B_{ij}cos\theta_{ij})$	$P_2L_{ij} + Q_2L_{ij} \leq S_2L_{ij,max}$
[90]	IB index	Traditional IB index	Dynamic	$IB_i = \dfrac{|Z'_{eq,i}|}{|Z'_{Li}|} = \dfrac{|Z'_{LLii} + Z_{coupled,i}|}{|r_i^2 Z_{Li}|}$	If the load impedance Z'_{Li} is located inside of the circle with a radius $|Z'_{eq,i}|$, the system is unstable.
[91]	MSV (Minimum Singular Value)	Singular point of Jacobian Matrix	Dynamic	$diag\left[\Delta\sum\right] = diag|[SU]^T \cdot [HP,V] \cdot [\Delta V] \cdot [SV]|$ $\sum Case = \sum BaseCase + \Delta\sum Casel$	$\Delta\Sigma$ is the change in singular value due to the uncertainty of wind power. MSV is used to assess the added wind turbine generator having a positive or negative effect on the voltage stability of the power system.
[92]	V-Q modal	V-Q modal	Static	$\Delta U = \xi \cdot u$	For modal analysis: Positive value

Ref	VSI/Method	Analytical Foundation	Index Type	Equation	Stability Threshold
	analysis, V-Q curve analysis	analysis, V-Q curve analysis		$\Delta Q = \xi \cdot q$	means the system is stable. A negative value means the system is unstable. For the V-Q curve, the reactive power margin can show the voltage collapse margin.
[93]	VSI_{ij}	P-V Curve theory	Static	$VSI_{ij} = V_i^4 - 4(P_j R_{ij} + Q_j X_{ij})V_i^2 - 4(P_j X_{ij} - Q_j R_{ij})$ $f_2 = \max(\min(VSI_{ij}))$	This essay uses the combined method to analyse voltage stability for the P-V curve; the active power margin can reveal the voltage collapse margin. For VSI, the larger the voltage stability index, the more stable the system is.
[94]	Monte Carlo based voltage stability analysis	Eigenvalue, reactive power margin, real and reactive power loss Monte Carlo Simulation	Static	$\Delta Q = \lambda \phi \zeta \Delta V$ $\Delta V = \phi \lambda - 1\zeta \Delta Q \Delta V = \sum i \phi i \lambda - 1 i \zeta i \Delta Q$ $Pki = \phi ki \zeta ki$ $P_{L,i}^{hr,k} = \mathbb{R}(\mathbb{P}_{L,i}^{hr,k} \sim \mathcal{N}(\mu_{L,i}^{hr,k}, \sigma_{L,i}^{hr,k^2}))$ $Q_{L,i}^{hr,k} = P_{L,i}^{hr,k} \tan(cos^{-1}(pf))$	For modal analysis: Positive value means the system is stable. A negative value means the system is unstable. For the V-Q curve, the reactive power margin can show the voltage collapse margin.
[95]	LILO	Integral-integral estimate theory, LIOS	Dynamic	$\theta \circ [\alpha_0^{IOS}(|x_0|) + \varphi^{IOS}$ $\circ \int_0^t (|\omega(s)|)ds] \leq \min[\Theta_{\widetilde{x_0}}, Y]$	The system outputs satisfy the equation

Ref	VSI/Method	Analytical Foundation	Index Type	Equation	Stability Threshold
		properties			
[96]	VPS	P-V and V-Q curve	Static	$$VPS = \left\|\frac{dV}{dP}\right\|$$	The active power margin can show the margin of the voltage collapse
[80]	FVSI, L_{mn}	Line stability index	Static	$$FVSI_{ij} = \frac{4Z^2 Q_j}{\|V_i\|^2 X'}$$ $$L_{mn} = \frac{4XQ_j}{[V_i \sin(\theta - \delta)]^{2'}}$$	$L_{mn} \leq 1$, the system is stable $FVSI \leq 1$, the system is stable FVSI is close to 1, and the system is close to instability.
[97]	Voltage Stability Condition	Steady-state load properties, Lyapunov stability theory	Static	$$(\beta_{s_i} - 2)Q_{s_i}(V_i) + \sum_{j \in N_G} w^Q_{\epsilon^{gl}_{j_i}}$$	Assuming that $\|\theta_i - \theta_j\| \leq \pi/2$ for any branch (i,j), the power system is at a QV regular operating point, if the condition is satisfied: $$(\beta_{s_i} - 2)Q_{s_i}(V_i) + \sum_{j \in N_G} w^Q_{\epsilon^{gl}_{j_i}} > 0 \ (i = 1, \dots, n)$$
[98]	P-V and V-Q curve	P-V and V-Q curve	Static	$$VPS = \left\|\frac{dV}{dP}\right\|$$	The active power margin can show the margin of the voltage collapse.
[14]	PV analysis	Continuation Load flow Algorithm	Static	$$P_{Di}(\lambda) = P_{Di0} + k_{Di}\lambda P_{Di0} = (1 + k_{Di}\lambda)P_{Di0}$$ $$Q_{Gi}(\lambda) = Q_{Gi0} + k_{Gi}\lambda Q_{Gi0} = (1 + k_{Gi}\lambda)Q_{Gi0}$$	The active power margin can show the margin of the voltage collapse.

Ref	VSI/Method	Analytical Foundation	Index Type	Equation	Stability Threshold
[99]	PV analysis	Continuation Load flow Algorithm	Static	$$\begin{bmatrix} \triangle V_{Re,k} \\ \triangle V_{Im,k} \\ \vdots \\ \triangle V_{Re,m} \\ \triangle V_{Im,m} \\ \triangle \gamma \end{bmatrix} = \begin{bmatrix} & J & & J_{I,\gamma} \\ & 0 & & 1 \end{bmatrix}^{-1} \begin{bmatrix} \triangle I_{Im,k} \\ \triangle I_{Re,k} \\ \vdots \\ \triangle I_{Im,m} \\ \triangle I_{Re,m} \\ \triangle \gamma \end{bmatrix}$$	The active power margin can show the margin of the voltage collapse.
[100]	Software-based Simulation method	Software function	Static	N/A	Compare the system voltage plots with voltage sag or UCAP between simulation software packages.
[101]	VSI	Optimal Load flow	Static	$$SI_{k+1} = \frac{4 \cdot [P_{k+1} \cdot X_k - R_k \cdot Q_{k+1}]^2 \cdot}{V_{M1}^4}$$ $$4 \cdot [P_{k+1} \cdot R_k + X_k \cdot Q_{k+1}] \cdot V_{M1}^2$$ $$VSI = MAX(SI_{k+1}) \text{ for k} = 1,2,3, \dots N$$	$VSI \leq 1$
[102]	Simulation Software-based method	Modal Analysis	Static	N/A	In the General Algebraic Modelling System (GAMS) optimisation software, analysed by CONOPT4 solver.
[103]	P-V and V-Q curve	P-V and V-Q curve	Static	$$P_L = VRIcos\theta_L = V_S^2 Z_L cos\theta_L Z_{TL}^2 + Z_L^2 + 2Z_{TL}Z_L cos(\theta_{TL} - \theta_L)$$ $$Q_L = VRIsin\theta_L = V_S^2 Z_L sin\theta_L Z_{TL}^2 + Z_L^2 + 2Z_{TL}Z_L cos(\theta_{TL} - \theta_L)$$	The active power margin can show the margin of the voltage collapse.

Ref	VSI/Method	Analytical Foundation	Index Type	Equation	Stability Threshold
[104]	L_k	P-V curve	Static	$$L_k = \frac{\sqrt{((R_S^2 + X_S^2)((P_r - P_{DG})^2 + Q_r^2))}}{||V_S|^2 - 2(R_S(P_r - P_{DG}) + X_S Q_r)|}$$	$L_k \leq 1$
[10]	$f(|\vec{U}|)$	Topological model	Static	$$f(|\vec{U}|) = \frac{|\vec{E}| \cdot Z_3}{|\vec{U}| \cdot (Z_1 + Z_3) - [\frac{P}{|\vec{U}|} + k \cdot [U_0 - |\vec{U}| \cdot j] \cdot \mathbb{Z}]}$$	The number of intersection points between the unit circle and the function's curve can show stability. Zero intersection point means unstable while two intersection point means stable. One intersection point is the stable margin.
[105]	VSI	Time-synchronised measurements	Dynamic	$$VSI = \min\left(\frac{P_{max} - P}{P_{max}}, \frac{Q_{max} - Q}{Q_{max}}, \frac{S_{max} - S}{S_{max}}\right)$$ $$P_{max} = \frac{QR}{X} - \frac{V_S^2 R}{2X^2} + \frac{|Z_{th}|V_s \sqrt{V_s^2 - 4QX}}{2X^2}$$ $$Q_{max} = \frac{PX}{R} - \frac{V_S^2 X}{4R^2} + \frac{|Z_{th}|V_s \sqrt{V_s^2 - 4PR}}{2R^2}$$ $$S_{max} = \frac{V_S^2 [|Z_{th}| - (\sin(\theta) X + \cos(\theta) R)]}{2(\cos(\theta)X - \sin(\theta) R)^2}$$	The system is stable if the VSI is 1. The system is unstable if the VSI is 0.

Ref	VSI/Method	Analytical Foundation	Index Type	Equation	Stability Threshold
[76]	$S_{\lambda\omega}$	Jacobian matrix singular point, PDF	Static	$$S_{\lambda\omega} = \frac{\triangle\lambda}{\triangle\omega} = -\frac{MF|_{\omega}}{MF|_{\lambda}}$$ $$\triangle\lambda_i = \sum_r s_{ir0}\,\triangle\omega_r$$	The formulation can measure the loading margin.

2.6 Verification Case Studies for the Voltage Stability Analysis

2.6.1 Analysis and Verification Case Studies with Integrated PV Generation Only

In [106], based on the Monte Carlo simulation and traditional voltage stability analysis methods, including the model analysis and V–Q curve model, a model framework for analysis was proposed. The aim was to improve the understanding of the relationship between photovoltaic energy penetration and power grid voltage stability. The critical eigenvalue, line loss, and reactive power were considered in the stability analysis. By changing the photovoltaic energy penetration in the IEEE 14-bus test system for model simulation and verification, the impacts of different photovoltaic energy penetration levels on the power grid voltage stability were analyzed. In [107], it was shown that photovoltaic power generation can easily lead to short-term voltage instability for a low-voltage distribution network. In [108], it was shown that with an increase in photovoltaic permeability, the intermittence of power generation will have a more significant impact on voltage fluctuations in the power grid. Therefore, starting from the existing photovoltaic power generation system, this study analyzed the voltage stability of different permeabilities using a new test model. We analyzed the voltage stability of a standard IEEE 14-bus system with five synchronous generators and three synchronous compensators. Through the V–Q curve analysis method, the reactive power margin of each bus was

calculated and measured. Bus 14 was the most unstable bus with the lowest reactive power margin and the highest bus participation coefficient. On the contrary, bus 4 was the most stable. After identifying the weakest and strongest nodes in the system through the V–Q curve method, the researchers converted all constant power loads into random loads and integrated the photovoltaic power generation system at the weakest bus. Through a sampling test of statistical data, the impacts of PV penetration on the overall system under different loads in different periods were obtained. The new framework presented in this paper can be used to evaluate the voltage stability of embedded photovoltaic systems. The novelty of this scheme is that it combines the traditional voltage curve method and the Monte Carlo simulation evaluation method to simulate uncertainty between photovoltaic energy and the system load.

In [109], a parametric model of effective reactive power (E-VAR) for evaluating the voltage stability of power systems with large-scale photovoltaic power generation is proposed. The high penetration of photovoltaic power generation reduces the flexibility of traditional power-system development. Moreover, due to the lack of E-VAR in the power grid, power system networks containing large-scale renewable energy are vulnerable to faults, affecting delayed voltage recovery. Therefore, using E-VAR as the research goal, several VAR resource contributions and load bus voltage recovery indices were quantified and a recovery index was designed. The New England power system (IEEE 39-bus) was tested with a simulation on the DIgSILENT power factory platform. The scheme is mainly applicable to power systems with single pieces of large-scale new energy generation equipment. The simulation results prove that the VSI can efficiently analyze the impact of

large-scale new energy on a system's transient stability. Furthermore, the optimal new energy integration location was obtained through the simulation analysis and can be used to help transmission system operators introduce more new energy generation resources without affecting the system's stability.

In [87], the dynamic voltage stability of a power system with large-scale photovoltaic power generation was studied. This method is different from the static voltage stability verification models mentioned above. This study examined the system's response to interference, identified the dynamic voltage characteristics, and determined the optimal location and scale of grid-connected new energy power generation according to the dynamic voltage stability analysis. Based on the investigation of the fault contribution of inverters, this analysis method forms a comprehensive framework that can be used to evaluate dynamic voltage characteristics. It was verified on the New England IEEE 39-bus test system using the DIgSILENT platform. Furthermore, by analyzing the SGs Var capability and the Var flow in the power system, the effects of different load conditions and PV penetration levels on the system's transient response were studied. The biggest highlight of this scheme is the realization of a dynamic voltage stability analysis on a system with large-scale photovoltaic power generation. In [106], a static voltage stability analysis model for photovoltaic power generation was proposed. This study used the traditional P–V and V–Q curves and the PowerWorld simulator for their analysis. The effects of variable power factor control, static voltage stability, generation power, and the threshold voltage distribution of photovoltaic power stations were studied. The change in voltage power sensitivity was used to optimize the configuration position of photovoltaic power

generation to optimize the static voltage stability of the whole system. This method is a verification test of the traditional curve analysis method that uses different software platforms to those used by other methods. The advantages and differences of several different simulation platforms can be obtained through comparison.

In [110], a dynamic voltage stability analysis evaluation frame was proposed for power systems with a high load capacity and a large-scale PV system. The model checks the power system's response to internal and external disturbances, understands the dynamic voltage characteristics, and determines the optimal location and scale of grid-connected renewable power generation units based on inverter resources. The dynamic voltage characteristic analysis framework uses the photovoltaic penetration level, load size, dynamic load percentage, and fault location to understand the system's dynamic voltage characteristics under different operating conditions. Using the DIgSILENT software platform, the proposed dynamic voltage stability analysis framework was applied to the IEEE 39-bus test system. The test results quantified the indicators of load bus voltage recovery to explore the steady state, transient response and voltage trajectory of the system.

In [111], the impact of the PV system on islanded microgrid static voltage stability analysis was researched. This study used the voltage collapse proximity index of the maximum deliverable power to conduct a quantitative stability analysis. The traditional P–V curve method was improved and verified using an improved IEEE standard 15-bus test model [112]. In addition, five different scenarios were applied to verify the system's ability to maintain the voltage stability. Using the coupling circuit breaker between buses to change the exchange power, the improved P–V curve method was used to evaluate the

impact of PV access on the system's voltage stability. In addition, the researchers considered different working conditions such as varying photovoltaic penetration levels, the impact of the PV power factor, and the impacts of different PV model units on the stability simulation.

In [113], a transient stability analysis and voltage stability compensation system based on reactive load flow control were proposed. This method was shown to provide increased power demand and improve stability. The authors connected photovoltaic power generation to the power grid in MATLAB Simulink to conduct stability studies. Three different fault types were applied, including single line to ground (LG), double line to ground (LLG), and three-phase line to ground (LLLG) faults. The transient stability analysis results were compared based on different photovoltaic power generation connection types. It was concluded that the rational use of photovoltaic power generation can effectively improve the stability of the power system.

2.6.2 Analysis and Verification Case Studies with Integrated Wind Generation Only

Hemmatpour et al. [114] developed a saddle-node and limited induced bifurcation-based voltage analysis model in which the wind turbine generator is considered in a microgrid. The index is based on the saddle-node and finite induced bifurcation, and the authors considered different load models. A new voltage stability margin of the islanded microgrid, called cat_VSI, was defined by catastrophe theory: the larger the index, the more stable the system is. In addition, a new concept called the reduced islanded microgrid network was proposed. The proposed index was extended to the N-bus islanded microgrid

by splitting the network. This method is called the maximum load margin of islanded microgrids. In the simulation, the performance and effectiveness of the proposed method were verified on 33 buses and 69 bus test systems with different load models. In this simulation model, both the wind turbine and the frequency deviation issues were researched. Two types were presented for the voltage stability index: saddle-node bifurcation (SNB) and limited induced bifurcation (LIB). The simulation process showed that the simplified static voltage stability analysis method proposed in this paper is comprehensive and detailed. Furthermore, the method was verified by simulating different test feeders with a wind turbine, showing that the voltage stability analysis model has very strong robustness and high generalization ability for wind-turbine-based islanded microgrids.

In [67], a method for short-term voltage stability analysis after the occurrence of a fault was proposed. This method is a system-level method for the quantitative analysis of voltage stability. In this method, the concept of integral estimation equivalent to the stability of the input state is used for quantitative analysis at the subsystem level. The authors studied the short-term voltage stability at the subsystem and system levels through a time-domain simulation, quantified the disturbance that the system can withstand, and provided a method for quickly conducting a system-level voltage stability analysis.

In [115], a voltage stability evaluation of power systems with wind power penetration was conducted. In this study, the P–V curve was used to determine the voltage stability limit of the system. DIgSILENT PowerFactory software was used for the simulation, and the results were analyzed with MATLAB. The verification results show that changing the settings

of the controllable series capacitor can change the circuit of the power grid, improving the voltage stability limit and ensuring the steady-state operation of the power system with an increase in wind energy penetration.

In [5], the influence of wind turbines connected to the power system on the static voltage stability was studied. Using the traditional P–V curve method, the static voltage stability of wind power incorporated into the traditional power grid was analyzed using psd-bpa software. The experimental results show that the influence of wind power on power grid voltage stability is closely related to the DG capacity. Although wind power grid connection will increase the load power limitation, it will reduce the voltage threshold. Therefore, when the system has enough reactive power, the wind power grid can improve the static voltage stability of the system. Combined with the existing Zhanjiang City power system, this paper studied the static voltage stability of the wind-power-connected grid.

The increase in wind energy in low voltage ride through or drop periods leads to power system instability and voltage quality problems. In [84], a microgrid with wind power generation was applied to various scenarios and simulated using Dlgsilent PowerFactory and MATLAB/Simulink. The voltage sag behavior and active and reactive power behaviors in the simulation models of the two platforms with and without capacitance were analyzed. The results show that combining a supercapacitor into a doubly fed wind power generation system can improve the voltage stability of the microgrid and provide a high-quality and stable power supply.

In [90], a voltage stability index for evaluating the grid connection effect of wind farms with doubly fed induction generators was proposed. The index based on impedance was

improved by using the voltage stability constrained optimal load flow calculation. Furthermore, a voltage stability analysis index considering the limit of the DFIG capacity curve and on-load tap changer behavior was proposed. In this study, simulation verification was carried out on the improved WSCC test system, the IEEE 39-bus system, the IEEE 57-bus system, and the Poland 2746 bus system. The experimental results show that this method can be used to analyze the instability behavior of a power system with a doubly fed induction turbine system.

In [91], a method for evaluating the voltage stability of a power generation system containing wind energy was developed. This method adopts the optimal load flow algorithm. By determining the Hessian matrix of the power balance equation, the minimum singular value of the system Jacobian matrix can be associated with the change in the actual power injection of the bus to evaluate the system's voltage stability. The method was applied to the IEEE 6-node, IEEE 57-node, and IEEE 118-node systems with wind-power generation. This study compared the minimum singular value method of the Jacobian matrix with a proposed optimized method via simulations and proved that the two schemes can effectively be used to analyze the voltage stability of a wind turbine system.

In [102], a new voltage stability constrained wind energy planning (VSC-WEP) model was proposed. The model is suitable for determining the optimal wind power penetration into a system based on the voltage stability. In this model, the modal analysis method is used to analyze the voltage stability of the system. The analysis results can be used to determine the best access location of the wind power module in the power system. The authors applied the proposed VSC-WEP model to the IEEE New England 39 bus test system.

The simulation results show that the voltage stability data can be obtained efficiently. On this basis, the model can maintain the system's voltage stability and optimize the capacity of the connected wind turbine.

In [116], a voltage stability analysis based on a control model was proposed. The method is suitable for large offshore wind farms integrated into the power system. Furthermore, a new low-voltage ride through the LVRT method was proposed suitable for the Taiwan power system. Researchers used the power-system engineering simulator PSS/E to simulate and analyze the off-peak systems of Taiwan power companies. The proposed LVRT curve was compared with the LVRT curve specified by the Taiwan power grid. The experimental results show that this method can prevent the turbine and power grid from decoupling when a fault occurs and can reduce the voltage drop at the PCC and the interference after fault removal.

2.6.3 Analysis and Verification Cases with Hybrid Distributed Generation

In [117], a Monte Carlo-based microgrid stability analysis model was proposed. The microgrid tested in this literature combines the wind turbine, PV, load, and energy storage system. A study investigated the internal and external errors in the transition process between the grid-connected and off-grid modes. A microgrid built with a 3000 Ah battery bank and a 335 kW wind turbine was simulated using the pseudo sequential sampling-based voltage stability analysis method. As the cut-out wind speed increased, the generation capacity increased, while the reliability index of the system decreased

dramatically. In this regard, it was concluded that the system's stability may not be improved by simply increasing the system's capacity.

In [85], the Monte Carlo sampling method was used to develop a voltage stability analysis method for renewable generation systems. In this literature, a simplified local area voltage stability index, the Ls-index, was proposed, and this was suggested to have higher accuracy and lower computation time than the L-index method. It uses the Monte Carlo and Nataf inverse methods to solve the sampling issue for power systems with renewable generators. By adding the PV model and the wind generator model into the IEEE 30-bus, the influence created by the DGs is viewed by the changing index. This method can only detect the system's voltage stability at the macro level. It evaluates the stability based on the load flow calculations, and the load flow equations have no solution when the system is unstable. Thus, this method can only detect stability caused by a loss of controllability. However, it cannot tell whether the loss of controllability is the reason for the voltage instability.

In [76], a static voltage stability analysis model combining probability theory and Jacobian matrix singular point theory was proposed. The scheme combines the cumulant-based maximum entropy method (CMEM) and nataf transform (NT) to analyze the steady-state voltage stability of a renewable-energy-based power system. The implementation of this method can be divided into four parts: (i) generate the injection power sample matrix and cluster the sample matrix through k-means; (ii) calculate the load flow by the Newton Raphson method and derive the sensitivity matrix of the load margin for random disturbances; (iii) judge whether the injection powers are independent of each other and

correct the sensitivity matrix VSI; and (iv) bring the origin moment into the maximum entropy model to obtain each cluster load margin's probability density function (PDF) and cumulative distribution function (CDF) curves. The above four steps form a CMEM analysis model based on probability theory. It can be used to conduct a steady-state voltage stability analysis of a power system. The researchers applied it to the improved IEEE 30-node and IEEE 57-bus system with wind power and photovoltaic power generation. They compared it with the sampling model based on the Monte Carlo method. It was concluded that the static voltage stability analysis model based on CMEM and the Newton Raphson method has a faster calculation speed. The test results drew the following four conclusions:

When a sampling method uses the standard error of the mean (SEM), the fitting probability ratio may be negative, while sampling methods using CMEM have greater effectiveness and accuracy;

The computational speed of the method based on CMEM is significantly higher than that of the Monte Carlo method, resulting in a time saving of 99.95%;

The higher the penetration rate of renewable energy, the greater the load margin fluctuation, leading to a more unstable system;

As the correlation degree of external weather factors, such as the wind speed and solar irradiation rate, increases, the mean value of the load margin is almost unchanged, but the fluctuation degree increases.

Overall, the verification experiment showed that this method is more accurate than the series expansion method, and the computational speed of this method is faster than that of the Monte Carlo method.

In [98], a P–V- and V–Q-based static voltage stability analysis simulation was developed with the IEEE 14-bus test feeder connected with the PV and wind power generator. It was shown that the system voltage profile reached the collapse point when the battery system's power capability was increased. Four different scenarios were simulated, and it was shown that systems with a wind turbine have broader stability spectra than systems with a PV generator.

In [118], a software-based static voltage stability analysis method to determine the maximum allowable penetration for solar and wind turbine generators on a specific power system, the Lesotho national electricity grid, was proposed. This study provides a good voltage stability analysis case study as it applied and verified the static voltage stability analysis model on a real system. The steady-state voltage stability of the power grid was studied under actual load in 2018 using the DIgSILENT PowerFactory simulation, which allows the basic models of photovoltaic and wind power generation to be connected to the national grid model for steady-state voltage analysis. The analysis results show that the maximum allowable capacity is 35 MW when only solar photovoltaic power is connected to a large-scale power grid. Similarly, when only wind power is connected to the large-scale power grid, the maximum allowable capacity was found to be 50 MW. Based on the load flow analysis model within the software, this study analyzed the relationship between the penetration of renewable power generation and the system's voltage stability.

In [119], a robust voltage tracking control method based on linear matrix inequality was proposed. This method is primarily aimed at power systems that use renewable energy. In this method, first, a nonlinear model of the renewable energy system is reconstructed into

a nonlinear combination of linear subsystems with state-related parameters. Then, the scheme uses the Lyapunov direct method to express the controller with the linear matrix inequality (LMI) formula. A verification experiment based on DSP was carried out with a buck converter, and the applicability of this method was verified. The scheme has many advantages: it is suitable for various renewable energy systems, it creates a unified design framework of the LMI for multiple control objectives, and it provides robust tracking control for multiple objectives. Furthermore, this scheme can be used to analyze the voltage stability of the power system and further optimize the tracking control based on the stability analysis to solve the stability problem.

In [120], a reactive power management system based on voltage sensitivity analysis that is suitable for new distributed generation systems with high penetration was proposed. The voltage sensitivity characteristics of the whole power system were analyzed, including measurements of the voltage change rate and reactive power under steady-state and transient conditions. The Newton Raphson method was used to solve the nonlinear load flow solution to obtain the voltage sensitivity. The researchers applied the voltage sensitivity model to the existing distribution system in South Korea. They set up three different simulation scenarios: all distributed energy sources are disconnected; photovoltaic generators in the system are disconnected; doubly fed wind power generation and photovoltaic generators in the system are disconnected. This was achieved with the use of typical power compensation devices to minimize the voltage change under steady-state and transient conditions.

In [92], a basic verification process of the voltage stability analysis method was

constructed. This method uses the V–Q curve analysis and V–Q sensitivity method of the small hybrid power grid containing grid-connected photovoltaic power generation, wind power generation, and small hydropower generation to determine the weakest bus. The reactive power margin indicates the distance between the load of the bus and the voltage collapse point. Therefore, the V–Q curve can be used to observe which bus has the lowest reactive power margin, and solutions need to be constructed to enhance the voltage stability around that bus. The following scenarios were implemented on the IEEE 39-bus test system: (1) Separate the photovoltaic power generation injection system; (2) separate the wind power injection system; (3) separate the wind power and photovoltaic hybrid injection system, and (4) separate the wind power and hydropower hybrid injection system. The control test results show that injecting wind power alone can help the system to reach a more stable voltage level. Substituting photovoltaic power generation for the traditional power supply will reduce the voltage stability of the system. Injecting two or more new energy generation systems into the power system will enhance the level of voltage stability. It was also found that the static distribution compensator can improve the stability level of the bus with low voltage stability.

In [93], an optimization technique based on hybrid analysis and meta-heuristic methods that can be used to analyze the voltage stability of a distribution network with DGS and optimize the configuration model according to the analysis results was proposed. The model can calculate the DG loss accurately and provide a distributed generation power specification design for a specific bus. In this method, the optimal DG location in the distribution network is selected and designed using a tree growth algorithm. A test system

including the IEEE 33-bus, 69-bus, and 94-bus was used for verification. The verification results show that this method can be used to calculate the optimal DG allocation and type selection with minimal power loss, which helps to determine the highest voltage stability level of a power system. This scheme can determine the most optimal solutions for power systems with distributed generation energy to obtain maximal voltage stability.

In [121], a synchro phasor-based voltage stability analysis model for a renewable-included power system was proposed. The algorithm can carry out early warning and independent stability tests on the power system and undergo real-time detection of the power system. It is an application of VSI at the prediction level. This method also avoids false alarms. The method was verified on the Quebec test feeder, which proved the reliability of the method.

In [79], a stability analysis index was developed based on the load flow calculation for power systems without DGs. On this basis, tap changers and DGs were incorporated into existing model equations to develop a voltage stability analysis index for a distribution network with multiple distributed generation systems. In the process of simulation verification, to explain the applicability of the designed indicators, the researchers compared them with other indicators used in previous studies. The following situations were considered in the simulation process: calculating the recommended indicators under base load conditions, calculating the recommended indicators of different load models, and comparing different indicators under the critical state. In the first case, the test system's weakest and most regular bus under normal conditions was judged. In the second case, the stability index was calculated by changing the active power of any bus in the two

distribution network models to study the reliability of the analysis method. The experimental results show that the VSI can be used to effectively analyze the stability change behavior of the system. The third case proved that the VSI developed by the authors performs well in terms of both calculation accuracy and calculation strength. The new index presented in this paper can be used to detect the necessary information regarding network stability in the shortest period of time and formulate the recommended index according to the utilization rate of the DGS in the distribution network to optimize the voltage stability of the system. This method no longer needs R, X, P, Q, and the impedance matrix, admittance matrix, and Jacobian matrix, so it is more suitable for use in the smart grid and effectively reduces the computational burden.

In [122], a hybrid voltage stability analysis scheme based on a probabilistic analysis approach was developed. The stability analysis model considers several components, including the load margin, the damping of critical eigenvalues, and the transient stability index. Different cases were studied to verify this voltage stability analysis model with the IEEE 68-bus test feeder and the New England Test System-New York Power System (NETS-NYPS) test system. The main process of the scheme involves generating a data set of the uncertain parameters in the system using the probability distribution function, determining the optimal load flow, calculating the stability index under different scenarios, and ranking and analyzing the stability of the system. This scheme can be used to identify the parameters affecting different stability problems and provide a more precise research direction for later stability improvements.

In [123], a voltage stability analysis of isolated DC–AC hybrid microgrids in the case of

emergency was studied. In this study, the authors designed several research cases to simulate the voltage collapse of microgrids during different serious emergencies, such as DC or AC circuit tripping between different bus connections. They analyzed the load voltage stability through the basic method of solving the load flow equations. Voltage stability was studied by drawing the P–V curve on the DC load bus. The simulation results of the IEEE 12-bus system show that the scheme can be used to accurately analyze the impact of emergencies on the voltage stability of the DC–AC microgrid. In addition, the analysis results also show that the DC–AC hybrid microgrid can reduce the impact by increasing the load capacity margin of the subgrid following unexpected events.

In [124], a short-term voltage stability evaluation formula model was established according to the definition of the rated power of distributed generator units and the X/R ratio theory. The simulation was applied to a simple test system containing a single DG unit and load. This study focused on the impacts of different control methods on the short-term voltage stability of the whole power system with new energy generation. The experimental results show that four different fault ride-through (FRT) control strategies of VSC-based distributed generators can affect the short-term voltage stability of a power system. The D/Q voltage control strategy was shown to have more robust load characteristics. This study provides a design idea for the voltage stability analysis of power systems, voltage stability enhancement, and the improvement of design in the later stage.

In [89], a global sensitivity analysis method based on the load margin calculation that prioritizes renewable energy distributed generation systems that affect power system voltage stability was proposed. This method adopts the random response method to

improve the calculation efficiency and is suitable for large renewable energy power penetration systems. In addition, the influence of critical variables on voltage stability was studied. The method was tested with the IEEE 9-bus system and the IEEE 118-bus system connected to a new energy generator set and compared with the commonly used gravitational search algorithm method in terms of accuracy and local sensitivity. The verification results show that the scheme has greater computational efficiency and accuracy.

In [101], a voltage stability analysis framework for a hybrid microgrid system was proposed. The VSI index used in this method is based on the basic definition of voltage stability, contains the active and reactive power information of all nodes in the radial distribution network system, and takes the maximum value from calculation of the nodes as the VSI. Through the load flow analysis of the IEEE 10-node hybrid energy microgrid, the VSI and load factor of the system were plotted, and the most sensitive node was identified. Furthermore, it was found that by placing the shunt capacitor at the node, the voltage stability could be effectively alleviated.

In [125], a voltage stability evaluation method for power systems containing renewable energy was proposed. This method estimates the bifurcation point in the holomorphic embedded load flow using the noniterative load flow method (HEPF). This scheme can greatly improve the efficiency of the analysis, because of the fast calculation speed of the HEPF. This study used a three-bus system to deduce the matrix formula and applied it to the IEEE nine-bus system for simulation verification. The verification results show that the scheme can accurately evaluate the load change near the critical point to carry out a practical voltage stability analysis.

In [84], a Jacobian matrix-based static voltage stability analysis model was proposed. This model is suitable for power systems with inverter-based generators. This method is based on the singular theory of the Jacobian matrix, and can be used to analyze the voltage stability. This method has several advantages. For example, it can be used to comprehensively simulate the inherent characteristics of the system, rather than regarding the system as a wireless bus for the stability analysis. In addition, the internal relationship between the inverter generator droop coefficient and the static voltage stability was revealed.

A summary of the verification platforms and operation modes of the networks is presented in Table 2.2.

Table 2.2 Summary of simulation tools in different operation modes with various DGs

Operation Mode	Type of DG (s)	References
Grid-Connected	PV	[8], [84], [94], [96], [103], [104]
	Wind	[14], [61], [80], [90], [91], [95], [100], [102]
	PV, Wind	[76], [85], [86], [89], [98]
	PV, Hydro	[81]
	PV, Wind, Hydro	[92]
Islanded	PV	[5]
	Wind	[87]
	PV, Wind	[43], [126]

2.6.4 Examples of Simulation Validation under Different Scenarios

In [79], different voltage stability analysis methods and indices were assessed and compared under the same simulation model for different scenarios. The Ranjan and Das voltage stability index based on solving power-flow equations (index 2003 [127]), the Banerjee and Das voltage stability index based on the Q–V curves (index 2014 [128]), and the developed novel index with the tap changers shown in Figure 7 were evaluated for the following cases:

1. Basic load condition;

2. Different load models;

3. The model works under the critical state.

All three indices are static stability analysis indices, and the IEEE 33-bus system and IEEE 69-bus system were used for the tests. Table 2.3 summarizes the Index formulation and the simulation details for the three VSIs. The formulation shows that only parameters P, Q, X, R, and V are considered in the novel index, thus making it simple. It may be noted that index 2014 considers the power loss P_{loss}, and Q_{loss} also increases the compilation time. Overall, the novel index is faster for analysis. For base loading under scenario 1, the simulation results show that the index based on the power flow equation method performs worse than the others, as this method considers too many system parameters such the impedance. The simulation runtimes of the first two indices are 2.5% slower than that of the novel index, which means that the latter has a higher computing speed than the others. For scenario 3, index 2014 showed that the system's instability level is higher than the others, as this method considers the power loss of the system. The simulation results show that the novel index enhances practical grids with renewable energy generation.

Table 2.3 Comparison of the assessed voltage stability indices

Voltage Stability Index	Formulation	Calculation Runtime (Units)
Index 2003	$SI = 0.5|V_2|^2 - PR - QX$	0.8171
Index 2014	$VSI = V_1^2 - 2PR - 2QX - RP_{loss} - XQ_{loss}$	0.8172
Novel Index	$VSI = V_1^2 - 4(PR + XQ)$	0.7997

In [129], three commonly used static voltage stability analyses were reviewed: V–Q curves, sensitivity analysis and minimum singular value, and modal analysis. The assessment results were drawn under the following two simulation scenarios:

1. A two-node power system model with a 90-degree initial voltage angle for a flat start;

2. A 1900 MW pure active load connected at the receiving end of the power system.

The assessment results show that the simulation results based on these three different analysis methods are not always consistent. When the value of the critical voltage stability point is near the nominal voltage, the sensitivity analysis and minimum singular value method may give wrong assessment results. This is different from the other two methods. Additionally, the flat start can aid the power-flow iterative calculation in the V–Q curve method to reach the stable range. For example, in scenario 1, the Jacobian determinant is positive with an initial angle of 90°. Additionally, the Jacobian matrix can give a more reliable result than the others.

In [130], different static voltage stability analyses, the Q–V sensitivity analysis, the P–V curve method, the Q–V curve method, and the time-domain method were tested in an IEEE

39-bus system under the following scenarios:

1. Bus 8–9 outage;

2. G3 outage;

3. Bus 12 load increment.

The simulation results show that the static voltage stability analysis methods are more conservative than the dynamic voltage stability analysis method. Additionally, the dynamic analysis method can provide greater accuracy under severe conditions. However, the limitation of the dynamic voltage stability analysis is that overlapped time-domain actions may exist in the interconnected networks. Additionally, the time-domain dynamic stability analysis simulation could not calculate the stability margin for each bus. Therefore, the combination of time-domain analysis and traditional static voltage stability analysis methods can avoid the above limitations and obtain more accurate evaluation results. Using the simulation results of different voltage stability analysis methods under the various scenarios, Table 2.4 summarizes the characteristics of these methods.

Table 2.4 Summary of the various voltage stability analysis methods

Voltage Stability Analysis Method	Simulation Results
L-index method	This method requires the least amount of calculation and retains good consistency with most other methods.
Modal analysis	The method is most suitable for determining the strongest and the weakest buses of the system.
V-Q sensitivity analysis	This scheme finds it difficult to distinguish different stability modes of the system; it may be misleading when applied to large systems with multiple regions.
Power flow-based methods	It is a traditional analysis method which is easy to understand and apply in the power system. However, too many system parameters need to be considered in the calculation, and the accuracy is relatively poor.
Dynamic voltage stability analysis	Cannot accurately calculate the stability margin for each bus. Overlapping time-domain actions in the interconnected networks may exist, which can lead to a wrong conclusion.

2.7 Conclusion

This paper presents a systematic review of the state-of-the-art literature on voltage stability analyses of renewable-dominant power systems from various perspectives. Useful information, including analysis methods, voltage stability indices, and case studies involving simulation verification, is summarized and compared to demonstrate how each analytical method and voltage stability index can be applied to DG-penetrated networks. The advantages and limitations of different mathematical methods and VSIs are also discussed in the respective subsections. The background, motivation, aims, and the current literature review are briefly illustrated in Section 1. The commonly used voltage stability analysis methods are reviewed and classified in the second section. In Section 3, other VSIs used for specific power systems are reviewed and compared. We describe how the voltage stability analysis methods and the voltage stability analysis indices, including both the static and dynamic methods, have been applied to different simulation models in Section 4.

The discussions in this paper led to the following inference: static voltage stability analysis is the core of voltage stability analysis. Firstly, because it focuses on the analysis of the algorithm, it can accurately quantify the voltage stability of the system. Additionally, this type of analysis method can calculate the distance between each node's voltage and the voltage collapse point relatively accurately, so it can be used to improve and optimize the power system's stability. Therefore, the static analysis method is still the mainstream direction for voltage stability analysis.

The computing complexity of different methods is also discussed in this paper, thus

providing guidance on choosing proper analysis methods and voltage stability indices to perform stability assessments for renewable-energy-dominated networks.

The discussions above lead to the below suggestions for further studies:

Systematic development of dynamic voltage stability analysis methods: Although several dynamic methods to evaluate the voltage profile of a system are available, additional work needs to be performed to improve their accuracy and efficacy levels.

Online real-time techniques for assessing the state of the system's voltage and the threshold of instability: It can be anticipated that power systems can be further optimized in an efficient and timely manner if the voltage collapse is detected at an early stage.

Coping with increasing asynchronous generation from renewables: The increasing complexity of the network due to the higher level of renewable penetration may lead to more stability issues. Increasing the integration of DGs may exponentially increase the risk of large disturbance instability. Therefore, it may become important to coordinate the expanding asynchronous power supplies with the current synchronous generation.

3 Modelling of Islanded Microgrids

3.1 Introduction for PSCAD

PSCAD (Power Systems Computer Aided Design) is a powerful and flexible graphical user interface software, which enables user to build a power system, run a simulation, and view the results in an integrated environment. It has a large library which consists of pre-programmed and tested simulation models, ranging from simple elements to complex

devices. In the main library, the pre-programmed models include passive elements, sources, miscellaneous I/O devices, breaker and faults, HVDC, facts and power electronics, imports, exports and labels, transformers, machines, Control Systems Modelling Functions (CSMF), transmission lines, cables, meters, protection, external data recorders and readers, sequences, logical, and PI sections. Users can also create their own libraries and import them as they require them, which can greatly reduce the modeling time.

According to the numbers of nodes that can be run, the platform has three different versions, including free version, educational version, and professional version. PSCAD is a flexible design environment which is suitable for students, researchers, engineers, and scientists. It incorporates several excellent functions which is better than other simulation software. For example, it can translate other power flow-type data including PSS/E, DigSilent, PowerFactory, and so on. Also, it has a parallel and high computing performance. In addition, it can utilise the Python script language. In conclusion, PSCAD is an advanced platform for power system simulations, and it has various functions. As a result, PSCAD is selected as the simulation environment in this research.

3.2 Islanded Microgrid Model

In this section, an islanded microgrid with diesel generator, PV generation, wind turbine generation, Energy Storage System (ESS), and loads is developed in PSCAD environment. The theoretical assumptions, basic formula, control principle and model structure are discussed in detail.

3.2.1 IEEE 14-Bus Model

As shown in Figure 3.1, the standard IEEE 14-bus test feeder represents an approximation of the American electrical power system in 1962, which contains 14 buses. In this research, an islanded microgrid network is built based on the modified IEEE 14-bus test feeder.

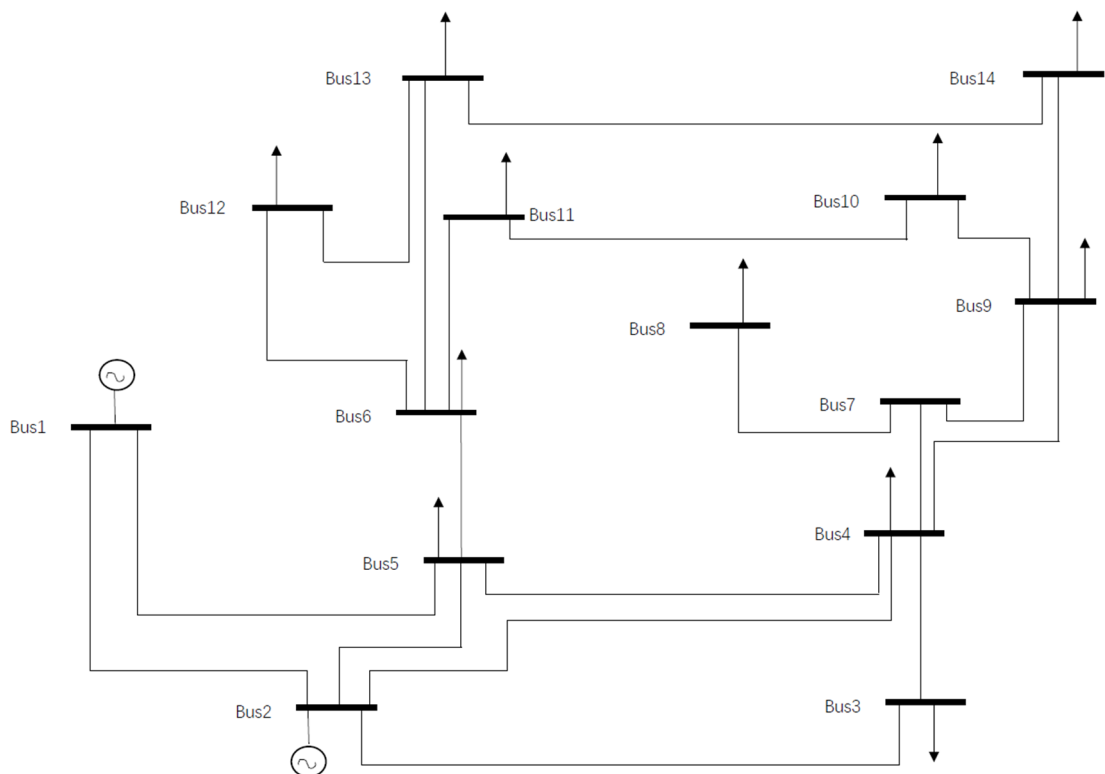**Figure 3.1** Standard IEEE 14-bus test feeder

The standard IEEE 14-bus distribution network has three feeders, which means the IEEE-14-bus network has 16 branches. However, since the distribution network usually operates under open-loop conditions, three branches can be deleted to obtain a simplified islanded microgrid design. As a result, we can get the modified 14-bus model, as shown in Figure 3.2 [131].
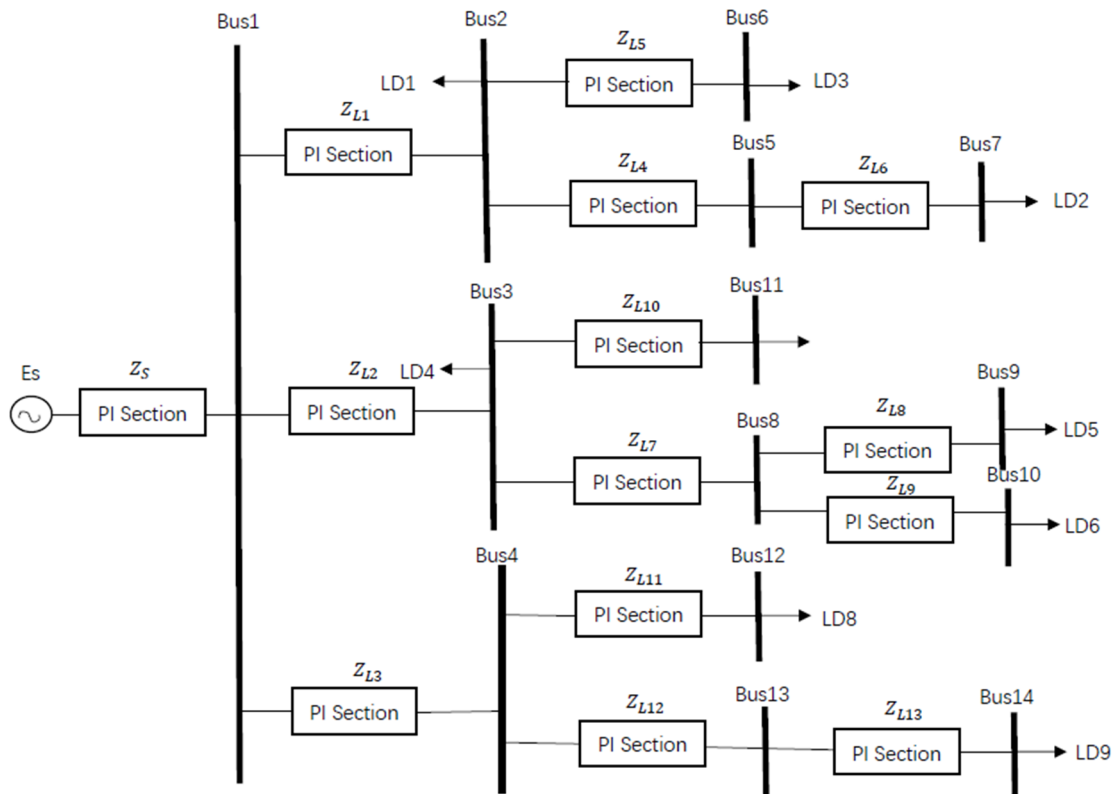
Figure 3.2 Modified 14-bus distribution network [131]

The 14-bus distribution network shown in Figure 3.2 has 14 nodes and 13 branches. As the slack bus is bus 1, the diesel generator is connected to node 1. The islanded microgrid system is modelled by connecting the photovoltage system, wind turbine, and energy storage system at various buses.

Table 3.1 below lists the impedance parameters of each branch while Table 3.2 shows the node power in the network. These parameters are used in the PSCAD modelling. Z is the line impedance between two buses, Es is the voltage setting of the diesel generator.

Table 3.1 Impedance parameters in the 14-bus network[131]

Name	Positive (p.u.)	Negative (p.u.)	Zero (p.u.)
Z_S	0.1+j0.1	0.1+j0.1	0.3+j0.3
Z_{L1}	0.075+j0.1	0.075+j0.1	0.225+j0.3
Z_{L2}	0.11+j0.11	0.11+j0.11	0.33+j0.33
Z_{L3}	0.11+j0.11	0.11+j0.11	0.33+j0.33
Z_{L4}	0.09+j0.18	0.09+j0.18	0.27+j0.54
Z_{L5}	0.08+j0.11	0.08+j0.11	0.24+j0.33
Z_{L6}	0.04+j0.04	0.04+j0.04	0.12+j0.12
Z_{L7}	0.08+j0.11	0.08+j0.11	0.24+j0.33
Z_{L8}	0.08+j0.11	0.08+j0.11	0.24+j0.33
Z_{L9}	0.11+j0.11	0.11+j0.11	0.33+j0.33
Z_{L10}	0.11+j0.11	0.11+j0.11	0.33+j0.33
Z_{L11}	0.09+j0.12	0.09+j0.12	0.27+j0.36
Z_{L12}	0.08+j0.11	0.08+j0.11	0.24+j0.33
Z_{L13}	0.04+j0.04	0.04+j0.04	0.12+j0.12

Name	Value	Name	Value
E_S /kV	10.5	LD7 / kVA	1000+j900
LD1 / kVA	2000+j1600	LD8 / kVA	1000+j700
LD2 / kVA	1500+j1200	LD9 / kVA	2100+j1000
LD3 / kVA	3000+j1500		
LD4 / kVA	4000+j2700		
LD5 / kVA	4500+j2000		
LD6 / kVA	600+j100		

3.2.2 Synchronous Generator

This work uses a 10MVA standard synchronous generator based on the sixth-order model. Figure 3.3 shows the complete representation of the diesel generator.
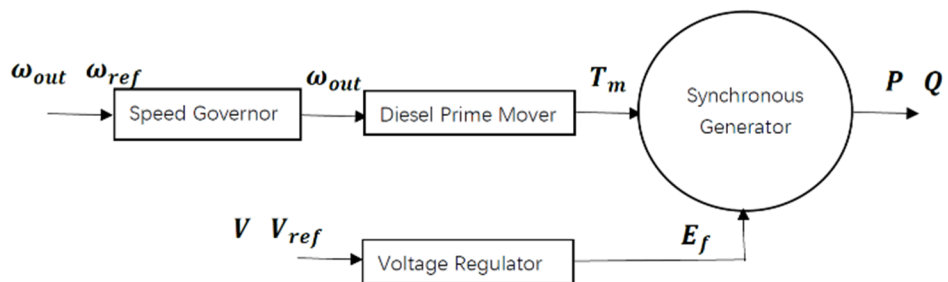
Figure 3.3 The principle diagram of diesel generator

In Figure 3.3, ω_{out} and ω_{ref} represent the real speed and the reference speed of the generator. T_m is the output torque of the diesel prime mover. V and V_{ref} represent the real voltage and the reference voltage of the generator. E_f is the output excitation voltage of the voltage regulator. Based on the principle diagram of diesel generator, the practical diesel generator in PSCAD model is designed as shown in Figure 3.4 and Figure 3.5 below.
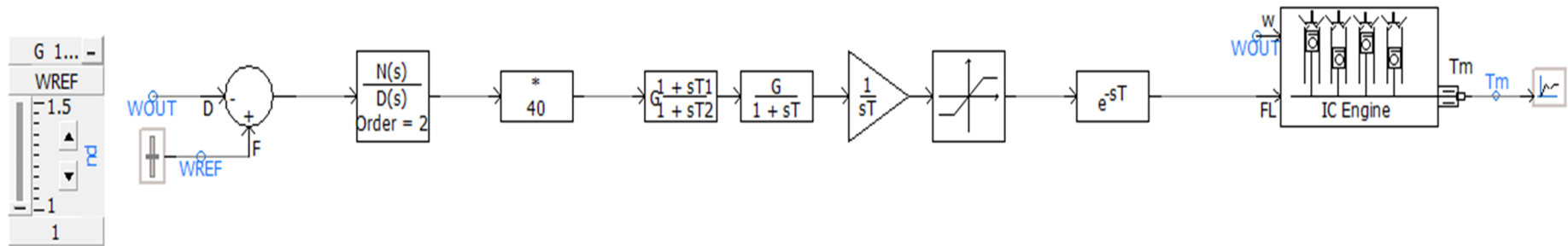
Figure 3.4 Diesel generator control system
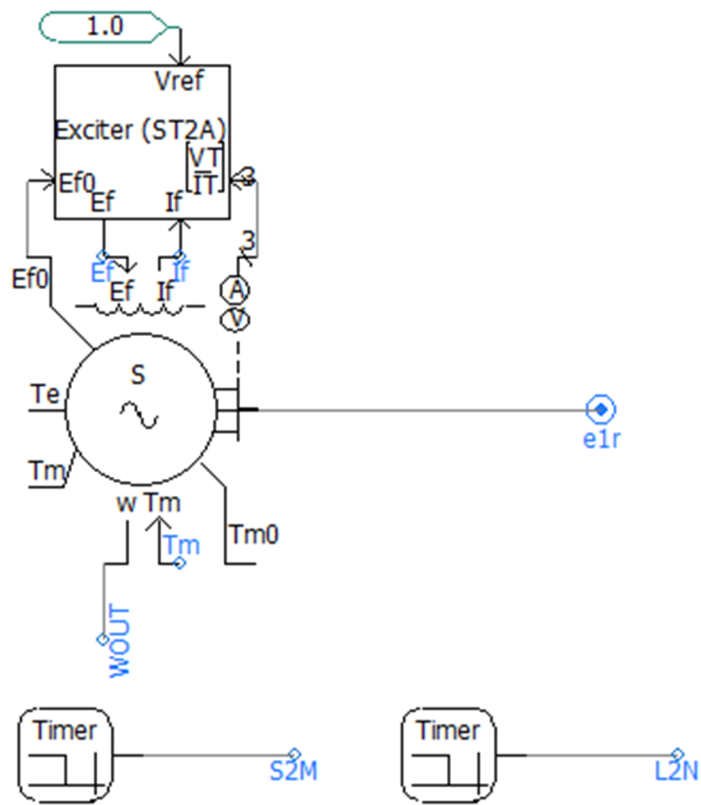
Figure 3.5 Synchronous generator structure

In the PSCAD model, signals are transferred between different parts through labels. The blue words in the above figures are labels. Part of the variables can also be transferred to the integrated model by setting the same signal name. For example, Figure 3.6 is the setting interface of the synchronous generator. By defining the same label name, the output value can be transferred to other parts easily.
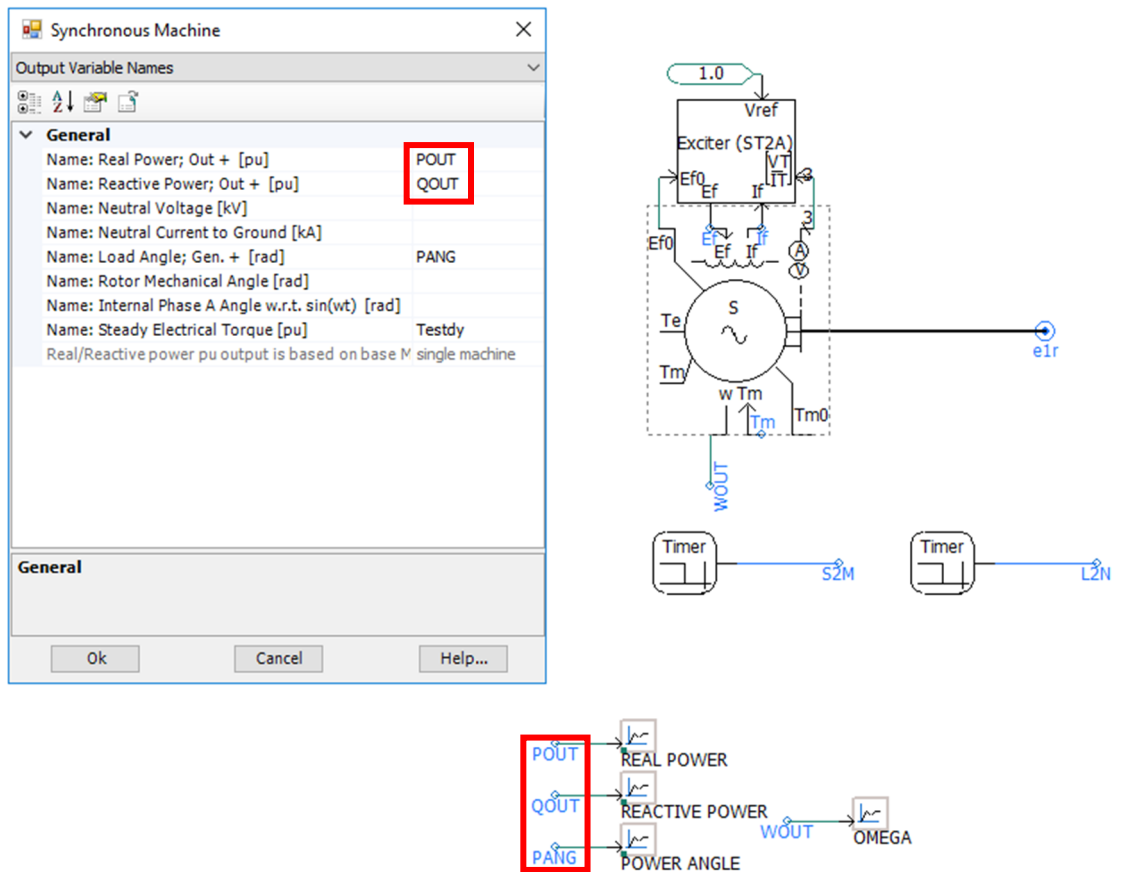
Figure 3.6 Variable names setting

Through the simulation, the output data of the diesel generator can be viewed as shown in the figures 3.7 and 3.8. Figure 3.7 shows the power output of the diesel generator. Figure 3.8 shows the real speed ω_{out} of the generator. The reference speed ω_{ref} is set to 1 p.u. Figure 3.8 shows that ω_{out} reaches 1 p.u.. Thus, the diesel generator meets the design requirements.
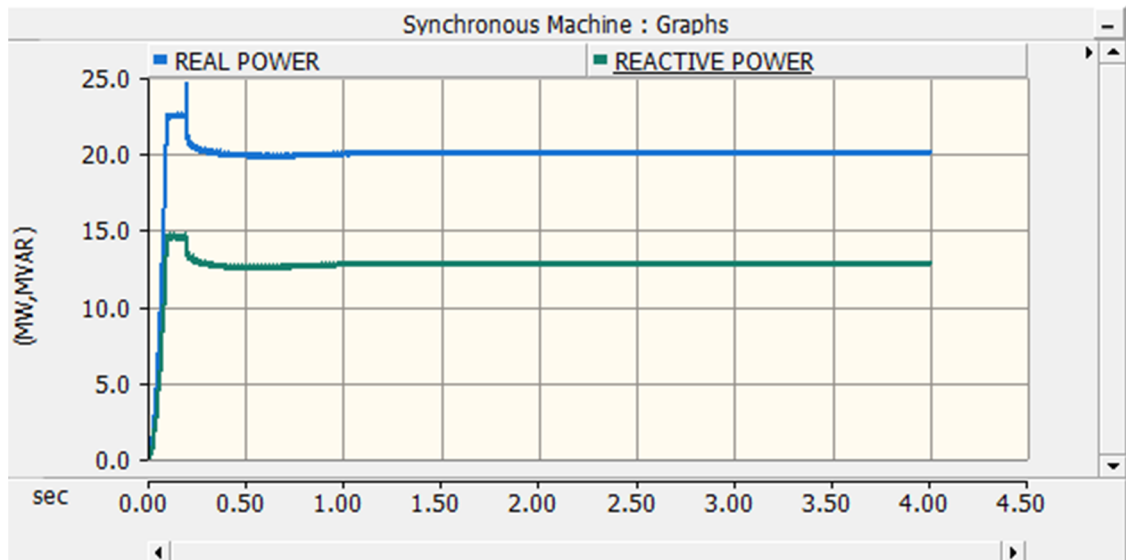
Figure 3.7 Power output of the diesel generator
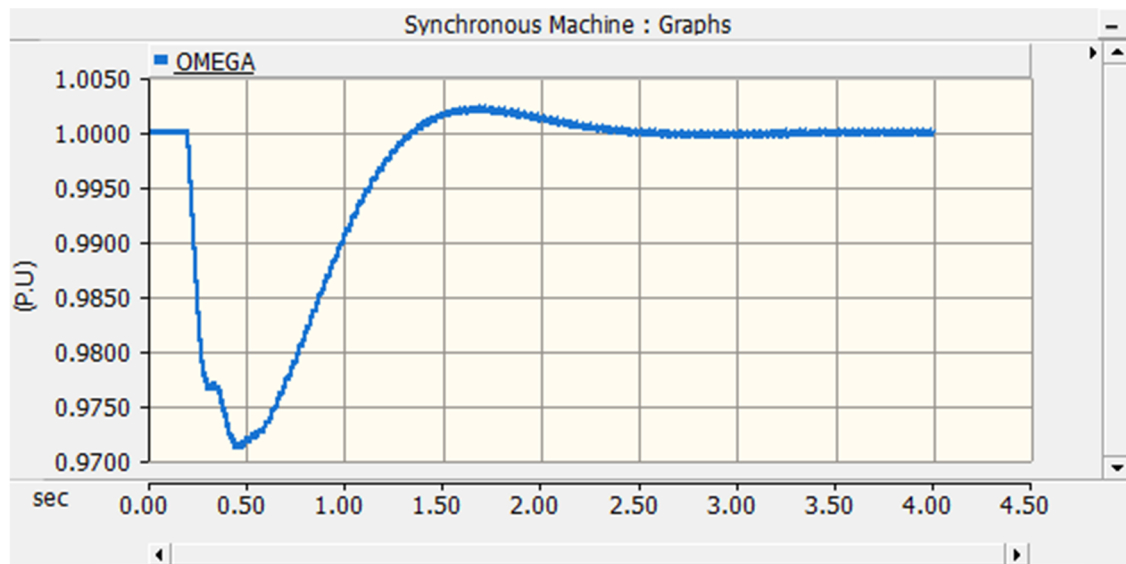
Figure 3.8 Rotor real speed of the diesel generator

3.2.3 Wind Turbine Generation

This work uses a direct-drive permanent magnet synchronous wind turbine generation system (PMSG). The topology of the wind turbine generation system is shown in Figure 3.9. In order to simplify the design, the distributed generators in the microgrid adopt the design of an aggregation circuit. A DG with high output power can be composed of multiple single-unit DGs through the aggregator. By changing the aggregator scaling factor, the

85

output power can be changed. For example, if a single unit DG output power is 0.2 MW, with an aggregator whose scaling factor is 25, the designed DG output is 5 MW. Thus, the change of distributed generation output power can be simplified in the simulation. A basic schematic diagram of the aggregator is shown in Figure 3.10. The aggregator structure is equivalent to amplifying a current source 25-fold, which means amplifying the output power by 25 times while keeping the voltage unchanged.
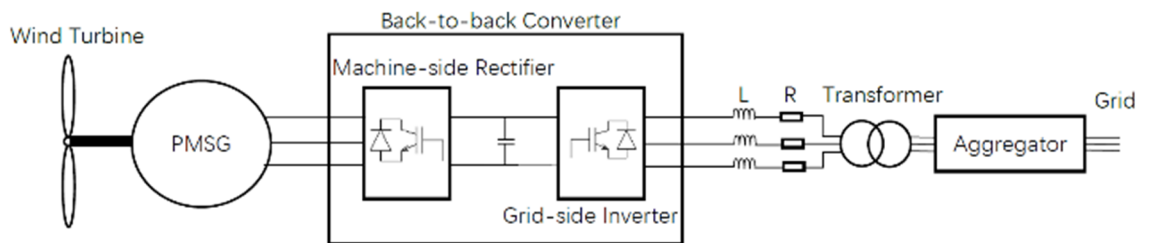
Figure 3.9 The principle diagram of the wind turbine generation system
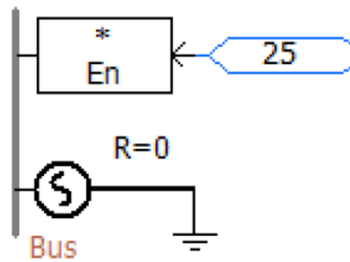
Figure 3.10 The basic schematic diagram of aggregator

The wind turbine part is the pneumatic part of the wind generation system, which can be seen as a prime mover of the wind turbine generation system. The principal formula of wind turbine output can be expressed as follows:

$$P = 0.5 \times A_{swept} \times D_{air} \times C_p \times V_w^3 \tag{25}$$

where A_{swept} is the swept area that the wind passes through with the rotor radius set as 40 in this case (3-60 in average), D_{air} is the air density, which is 1.225, C_p is the capacity factor, which is 0.43 in this case (0.26-0.52 in average), V_w is the wind speed.

By converting the power into torque, the machine torque T_m can be obtained. Through the shafting motion in the wind turbine section, which is the gearbox in the practical application, the speed ω_m can be obtained. Therefore, the wind turbine section aims to convert the detected wind speed into the machine speed and transmits the value to the PMSG. The PMSG generates power based on the ω_m and T_m. The power output P, Q and the voltage V are detected by the multimeter connected to the PMSG. The output voltage is fed to the distribution network through the back-to-back converter. Based on the principle diagram of wind turbine generation, the practical direct drive doubly fed wind turbine model in PSCAD is shown in Figure 3.11. As we can observe in Figure 3.12, the power output of the wind turbine system achieves the original design requirements, i.e., 5 MW.
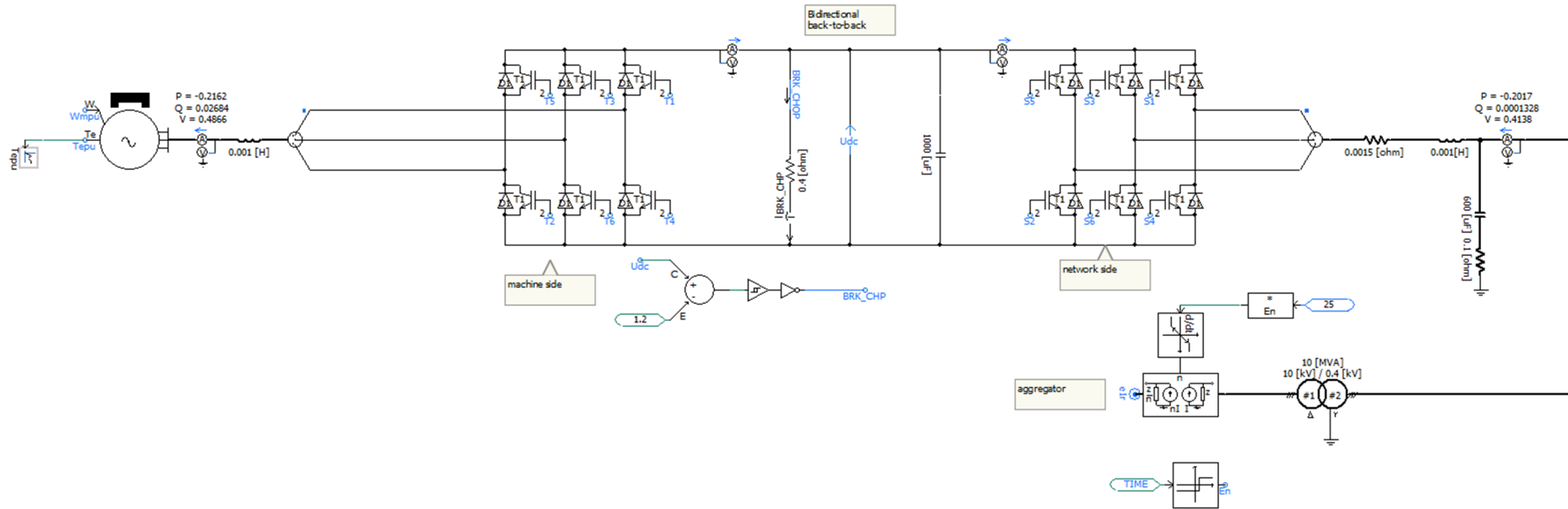
Figure 3.11 Direct drive doubly fed wind turbine model in PSCAD
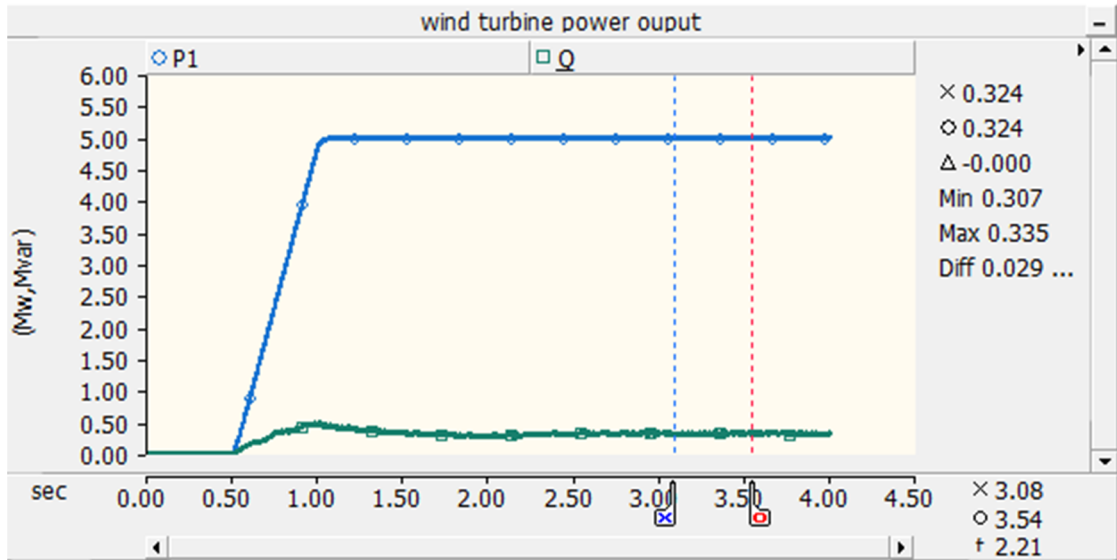
Figure 3.12 Power output of wind turbine system

3.2.4 Solar Power Generation

In this work a standard photovoltaic system is employed. The topology of the photovoltaic (PV) system is shown in Figure 3.13.
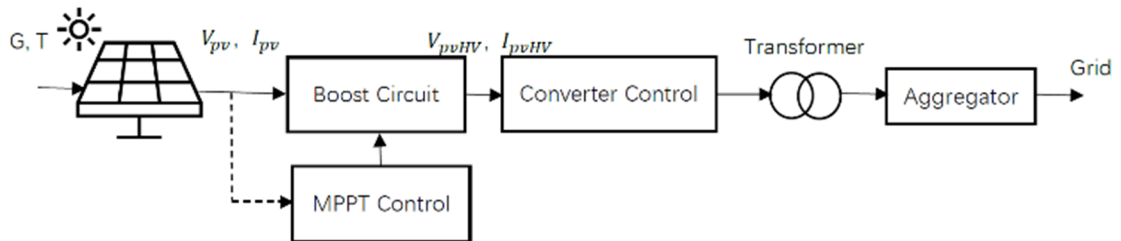
Figure 3.13 The principle diagram of the photovoltaic system

In Figure 3.13, G and T are the parameters received by the solar panel. G is the irradiation, and T is the cell temperature. MPPT control is used to track the maximum power output. Figure 3.14 illustrates the I-V and P-V characteristics of the PV array [132]. V_{pv} is the voltage value generated by the solar panel, and I_{pv} is the current value generated by the solar panel. V_{pvHV} is the voltage value generated by the boost circuit, and I_{pvHV} is the current value generated by the boost circuit.

89
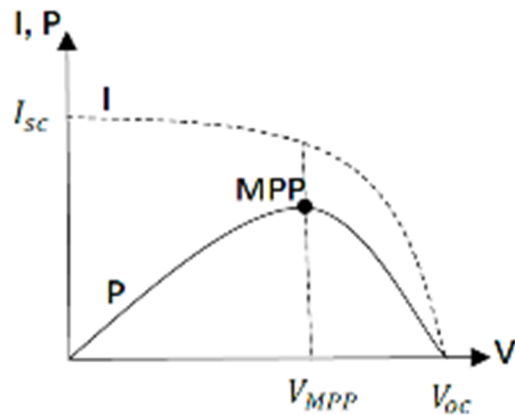
Figure 3.14 The I-V and P-V characteristics of the PV array

As shown in Figure 3.14, the output voltage of the PV array is V_{MPP} when the output power is the maximum value. I_{SC} means the short circuit current value, and V_{OC} means the open circuit value. V_{MPP} is the reference signal for the boost circuit. Thus, the PV system collects the maximum panel output power as the system output power. The converter control block comprises the Vdc-Q control block and LCL filter. Vdc-Q control provides signals that can control the opening and closing of diodes in the converter to convert the DC signals generated by PV panels into AC signals that can be connected to the grid. The PV power generation system with a specified output power can be built through the transformer and aggregator. Based on the principle diagram of the PV generation, the practical PV model in PSCAD is designed as shown in Figure 3.15.
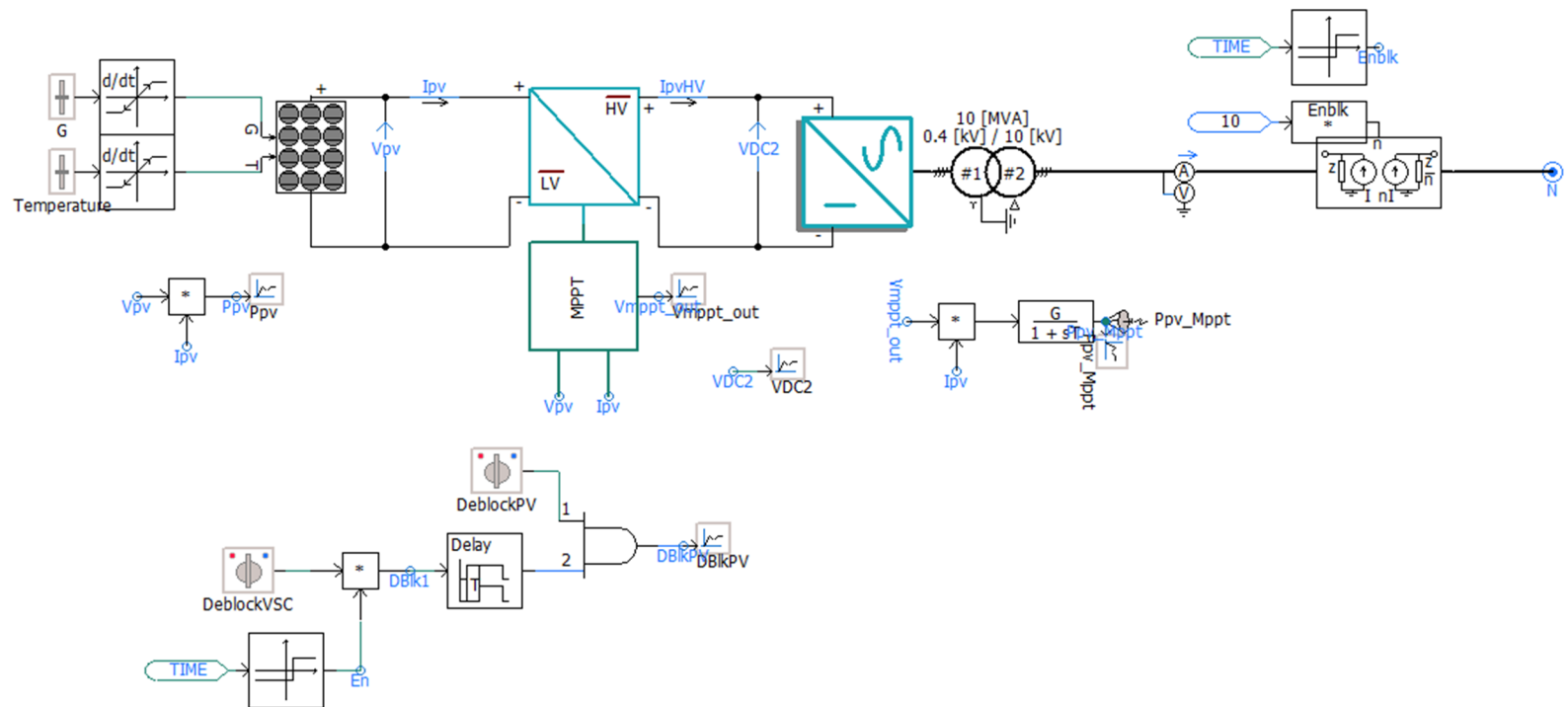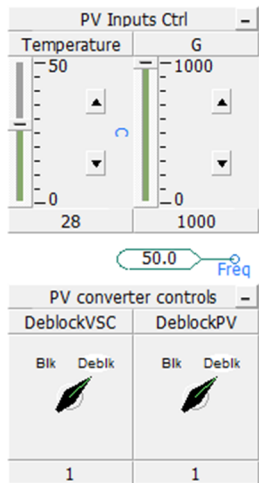
Figure 3.15 Photovoltaic generation model in PSCAD

In this case, the solar irradiation constant G is set as 1000 W/m^2, which is the standard test condition [133]. The cell temperature T is set as 28 ℃. Here, the per unit PV system output is designed as a 0.2 MW. The aggregator factor is set as 10, which means the total output of the PV system should be 5 MW. Figure 3.16 shows the power output of the PV system. As we can see from Figure 3.16, the power output of the PV system achieves the original design requirements.
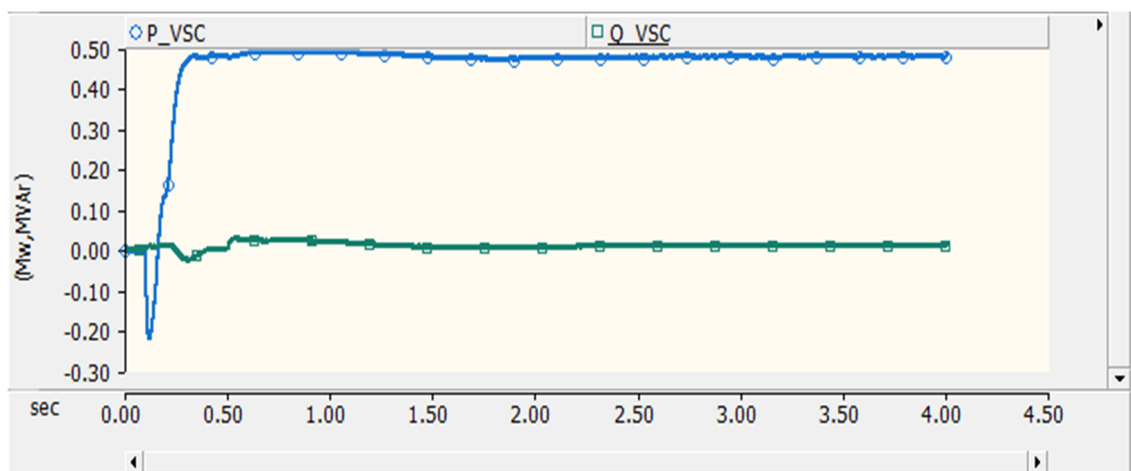
Figure 3.16 Photovoltaic generation model power output

3.2.5 Energy Storage System

The energy storage system (ESS) is essential in the islanded microgrid. Normally, ESS can be batteries, flywheels, and supercapacitors [2]. The complete energy storage system representation is shown in Figure 3.17.
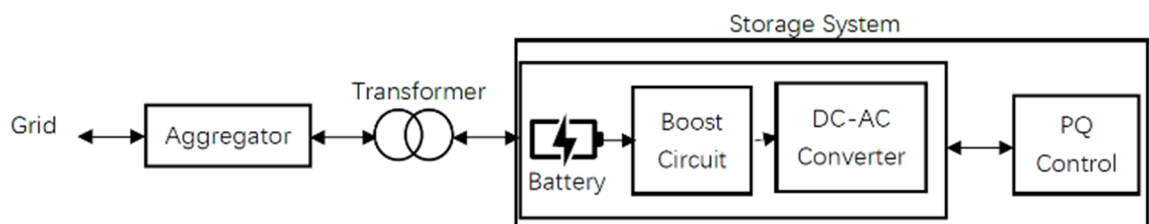
Figure 3.17 The principle diagram of the energy storage system

In this work, a generic secondary electrochemical battery model is used. The

mathematical model of the battery can be expressed as follows [134]:

$$E = E_0 - K\frac{1}{SOC} + Ae^{-BQ(1-SOC)} \tag{52}$$

where E is the no-load voltage, E_0 is the battery constant voltage, K is the polarisation

voltage, SOC is the state of charge in percentage, A is the exponential zone amplitude,

and B is the exponential zone time constant inverse, Q is the reactive power.

The boost circuit is designed to amplify the battery terminal voltage. DC-AC converter

is used to convert the battery voltage from DC to AC for network connection. PQ control

block is used to set the constant power charging and discharging of the ESS. Based on the

principle diagram of the energy storage system, the practical battery model in PSCAD is

designed as illustrated in Figure 3.18.
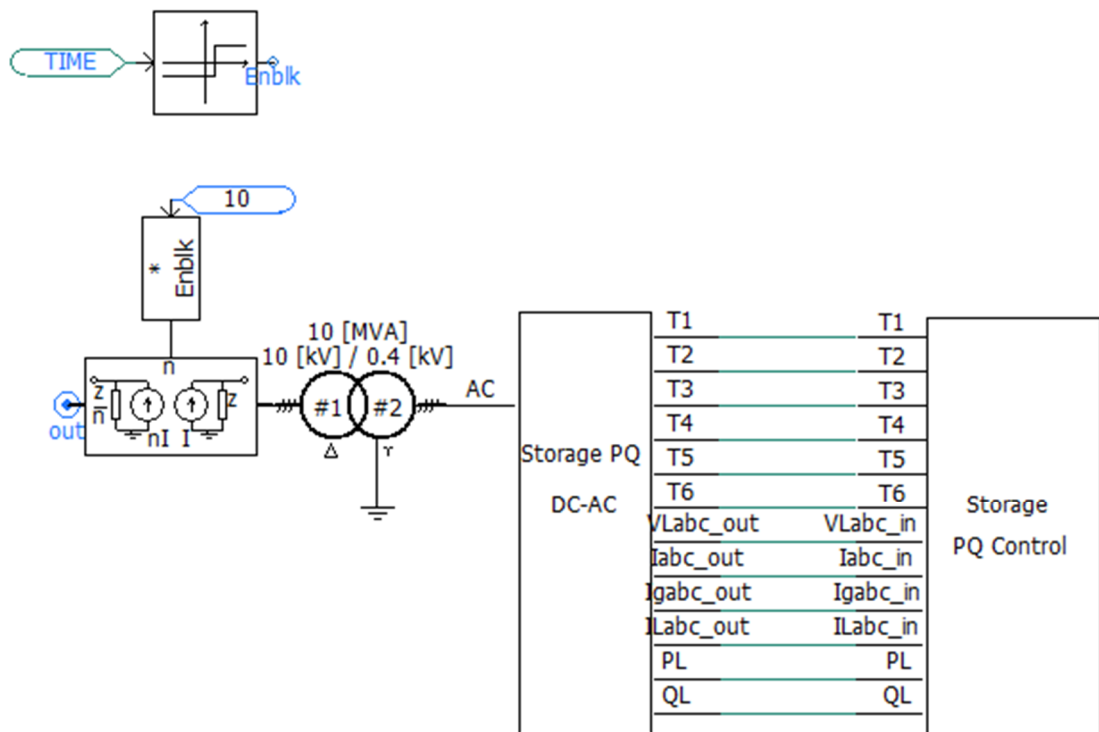
Figure 3.18 Energy storage system design in PSCAD
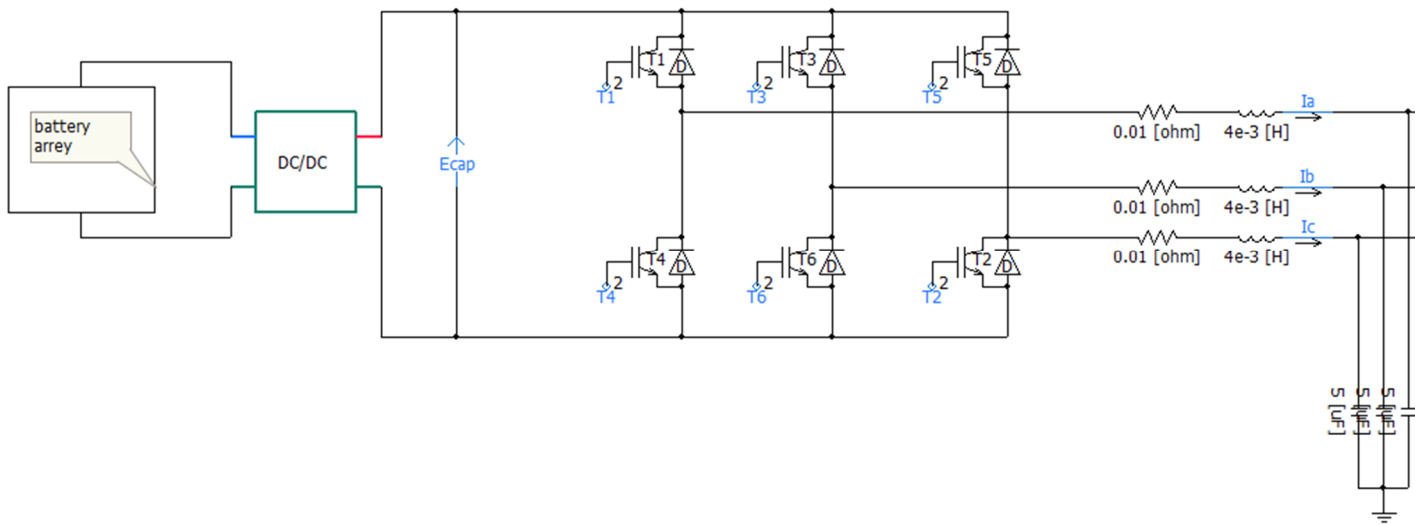
Figure 3.19 Storage PQ DC-AC subsystem inner structure in PSCAD

94

Figure 3.19 depicts the inner structure of the storage PQ DC-AC subsystem. As shown in figure 3.17, the inner structure includes a standard battery array, a DC/DC boost circuit, a DC/AC converter, and impedances. The battery part uses the general lithium battery model, and the relevant Fortran code is presented in Appendix A. With the aggregator factor, which is 10 in this case, the power output of this ESS can be designed to be 5 MW as shown in Figure 3.20.
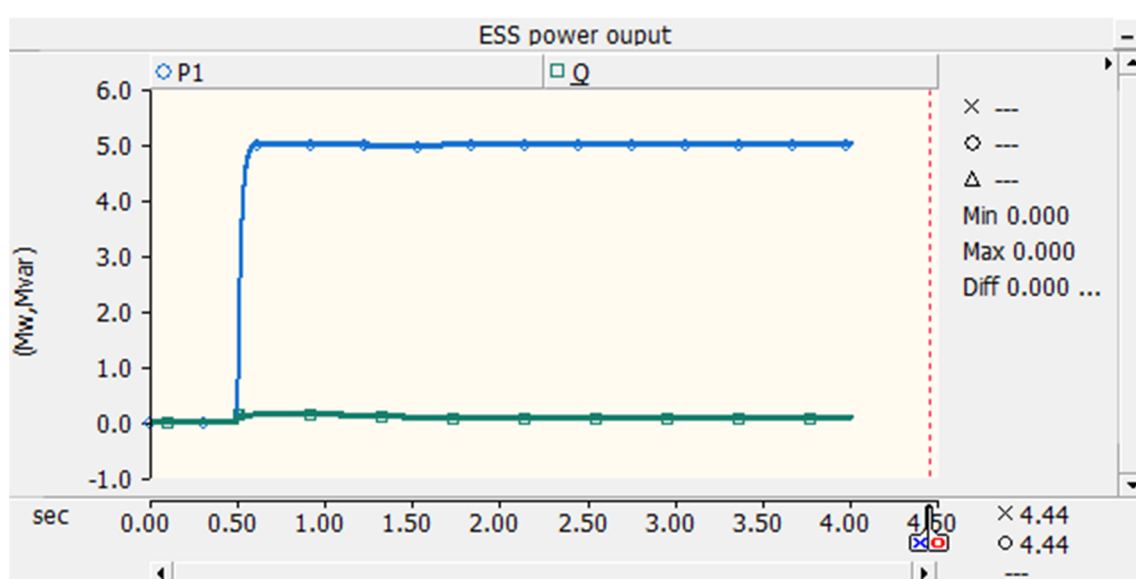
Figure 3.20 ESS power output

3.3 Simulation Scenarios

According to the modeling process of each subsystem described in the above sections, an islanded microgrid with multiple DGs can be build, as revealed in Figure 3.21. In this case, the diesel generator built in section 3.2.2 is connected to bus 1, the slack bus. The PV DG, designed in section 3.2.4, is connected to bus 8. The wind turbine DG, designed in section 3.2.3, is connected to bus 5, while the energy storage system, discussed in the last section, is connected to bus 4. By running the simulation, load flow analysis can be done in the

PSCAD simulation environment, and the results can be viewed from the scopes. Figure 3.22 illustrates the load flow analysis results for bus 2. From the figure, we can observe that the RMS bus voltage value can be stabilized to 10.4KV when the simulation run time is close to 4s. Since the islanded microgrid is designed based on a 10kV distribution network [131], and according to Table 3.2, the rated power of the diesel generator connected to the slack bus is designed as 10.5KV, the RMS voltage of bus 2 is reasonable and appropriate. Besides, from the analysis results for other buses in the PSCAD, the steady-state bus voltage values are also within acceptable ranges. Overall, the 14-bus model is tested for its design as an islanded microgrid.
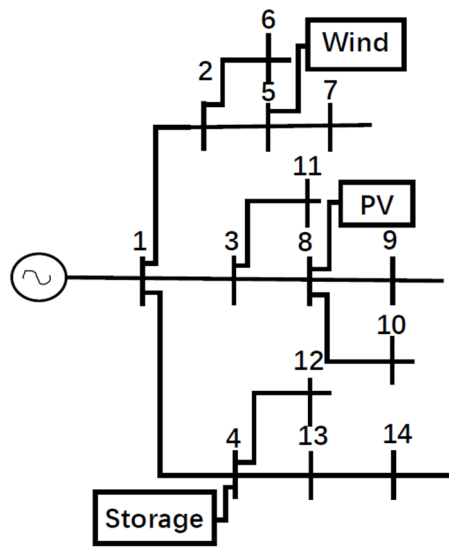
Figure 3.21 14-bus Islanded microgrid test feeder structure
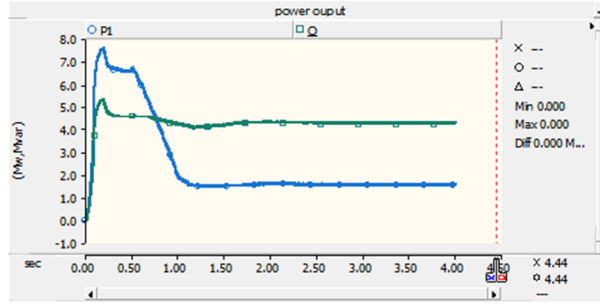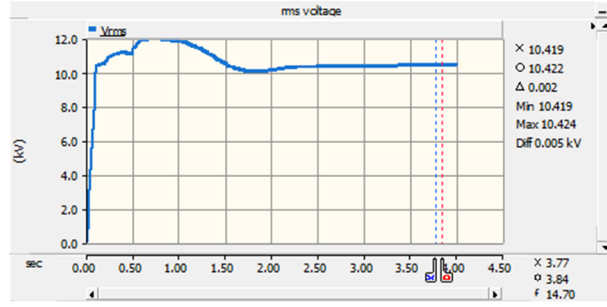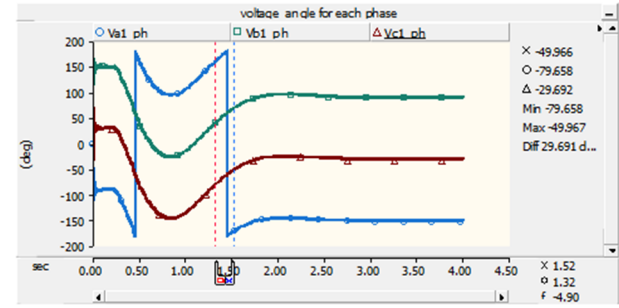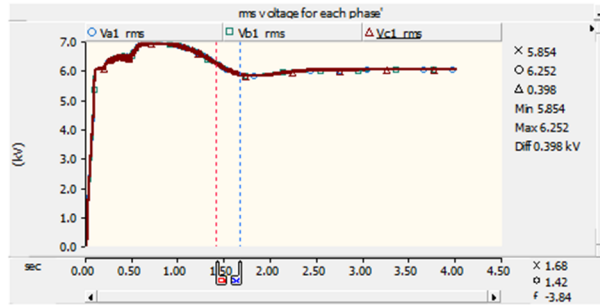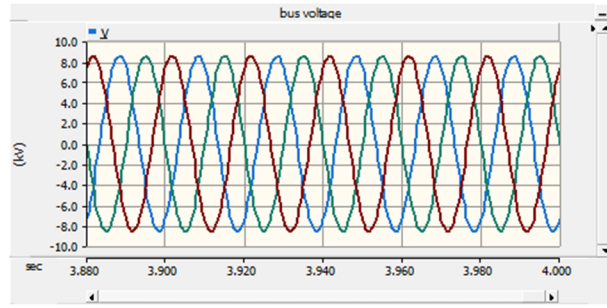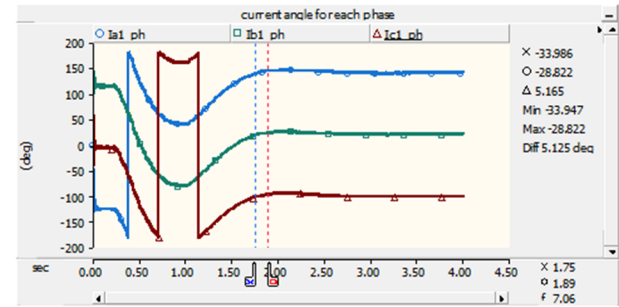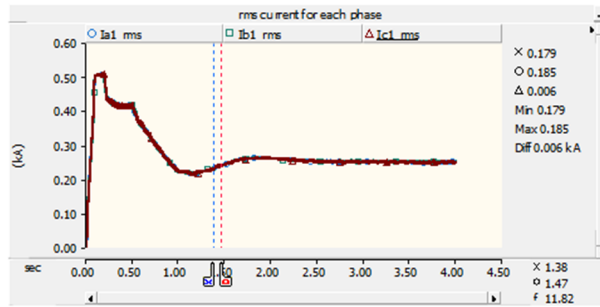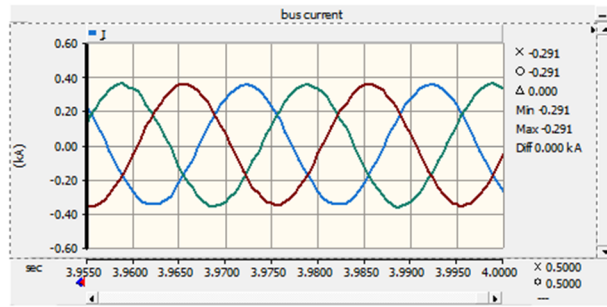
Figure 3.22 Load flow analysis results for bus 2

Different simulation scenarios are set in order to carry out the comparison experiments. Table 3.3 describes four scenarios used. To maintain the integrity of the control experiment, the control variable method is considered to establish the simulation scenario settings. In scenarios 1, 2, and 3, the power output is kept consistent while the connection buses are changed. Conversely, in scenarios 2 and 4, the connection buses remain the same, but the power output settings are altered.

Table 3.3 Scenarios settings

DG	Type	S1	S2	S3	S4
PV	Power	5 MW	5 MW	5 MW	1MW
PV	Connection	Bus 14	Bus 9	Bus 8	Bus 9
Wind	Power	5 MW	5 MW	5 MW	3MW
Wind	Connection	Bus 13	Bus 8	Bus 5	Bus 8
ESS	Power	5 MW	5 MW	5 MW	10MW
ESS	Connection	Bus 5	Bus 12	Bus 4	Bus12

3.4 Conclusion

In this chapter, an islanded microgrid based on IEEE 14-bus network built in PSCAD simulation environment was described. As a professional and flexible graphical user interface simulation tool, the suitability of PSCAD functions and pre-programmed models for power system modelling and simulation was assessed. Then, the modelling of photovoltaic generation, doubly fed wind turbine generation, and energy storage system were discussed in detail. Variables used in the model were defined and explained based on

the practical modelling. Through the simulation verification, the power output of the renewable energy distributed generations is found to meet the design requirements.

In addition, three different simulation scenarios were proposed to obtain a more accurate experimental outcome. By changing the power output settings for different DGs and changing the DGs connection bus randomly, three simulation scenarios were designed. In the following chapters, comparison experiments will be conducted based on these three scenarios.

Some of the work described in this chapter has been presented and published in:

X. Liang, and J. Ravishankar, "Voltage Stability Indices for Islanded Microgrids", *AUPEC 2022*.

4 Comparison Study on State-of-the-Art Static Voltage Stability Analysis Techniques

4.1 Theoretical Background

4.1.1 Eminoglu and Hocaoglu Voltage Stability Index

Eminoglu and Hocaoglu presented a voltage stability analysis index based on the distribution network's transferred active and reactive power [135]. Figure 4.1 below shows a 2-bus distribution line model. Using the load flow analysis, the quadratic equation (53) calculates the line sending end voltage. V_s is the voltage magnitude of the sending end, $\angle\delta_s$ is the voltage angle of the sending end, V_r is the voltage magnitude of the receiving end, $\angle\delta_r$ is the voltage angle of the receiving end, Z denotes the line impedance between sending bus and receiving bus, P stands for the real power received by the receiving end, Q is the reactive power received by the receiving bus.
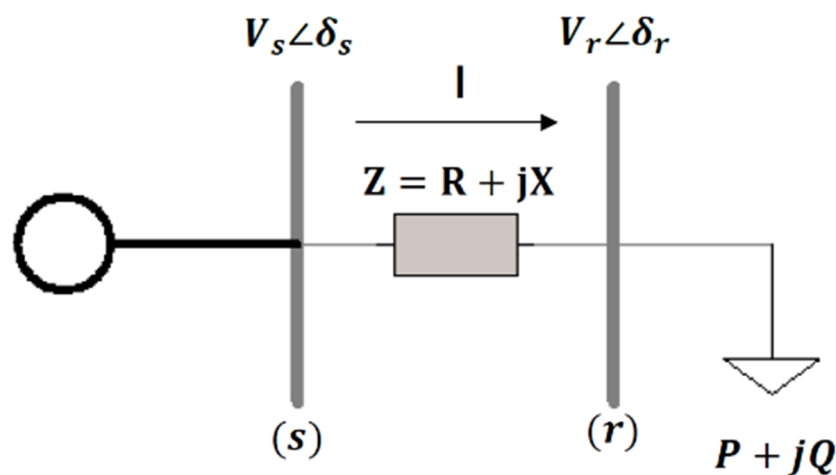
Figure 4.1 2-bus equivalent distribution line model

$$V_r^4 + 2V_r^2(PR + QX) - V_s^2V_r^2 + (P^2 + Q^2)|Z|^2 = 0 \qquad (53)$$

$$P = \left[-\cos(\theta_z)\,V_r^2 \pm \sqrt{\cos^2(\theta_z)V_r^4 - V_r^4 - |Z|^2Q^2 - 2V_r^2QX + V_s^2V_r^2}\right]/|Z| \qquad (54)$$

$$Q = \left[-\sin(\theta_z)\,V_r^2 \pm \sqrt{\sin^2(\theta_z)V_r^4 - V_r^4 - |Z|^2P^2 - 2V_r^2PR + V_s^2V_r^2}\right]/|Z| \qquad (55)$$

According to (54) and (55), the conditions required to obtain the real value of active and reactive power at the receiving end are:

$$\cos^2(\theta_z)V_r^4 - V_r^4 - |Z|^2Q^2 - 2V_r^2QX + V_s^2V_r^2 \geq 0 \qquad (56)$$

$$\sin^2(\theta_z)V_r^4 - V_r^4 - |Z|^2P^2 - 2V_r^2PR + V_s^2V_r^2 \geq 0 \qquad (57)$$

Summing (56) and (57), we can get:

$$2V_s^2V_r^2 - V_r^4 - 2V_r^2(PR + QX) - |Z|^2(P^2 + Q^2) \geq 0 \qquad (58)$$

From (58), we can observe that the equation value decreases with an increase in the active and reactive powers, and line impedance. The lower the value of this equation (58), the weaker is the bus voltage stability. This subsequently becomes the index (VSI) and can be written as:

$$VSI_a = 2V_s^2V_r^2 - V_r^4 - 2V_r^2(PR + QX) - |Z|^2(P^2 + Q^2) \qquad (59)$$

4.1.2 Banerjee and Das Voltage Stability Index

Based on the same 2-bus distribution line model, Banerjee and Das developed a new voltage stability analysis index based on the load flow calculation [127]. From Figure 4.1,

the following equations can be written:

$$I_{sr} = \frac{V_s - V_r}{R + jX} \tag{60}$$

$$P - jQ = V^*_r I_{sr} \tag{61}$$

where P is the sum of the real power load beyond the bus r, the bus r real power load, and all the real power losses beyond the bus r. Q is the sum of the reactive power load beyond the bus r, the bus r reactive power load, and all the reactive power losses beyond the bus r.

From (60) and (61) we can derive the following equation:

$$|V_r|^4 - (|V_s|^2 - 2PR - 2QX)(|V_r|^2) + (P_r^2 + Q_r^2)(R^2 + X^2) = 0 \tag{62}$$

The real and reactive power losses can be expressed as:

$$P_{loss} = \frac{P^2 + Q^2}{|V_r|^2} R \tag{63}$$

$$Q_{loss} = \frac{P^2 + Q^2}{|V_r|^2} X \tag{64}$$

From (62), (63) and (64), we can get:

$$|V_r|^2 = |V_s|^2 - 2PR - 2QX - RP_{loss} - XQ_{loss} \tag{65}$$

In order to get the real value of the receiving end voltage, the value of RHS of (65) should be non-negative:

$$|V_s|^2 - 2PR - 2QX - RP_{loss} - XQ_{loss} \geq 0 \tag{66}$$

In conclusion, the index can be expressed as:

$$VSI_b = |V_s|^2 - 2PR - 2QX - RP_{loss} - XQ_{loss} \tag{67}$$

4.1.3 Ranjan and Das Voltage Stability Index

Ranjan proposes another modified load flow method for voltage stability analysis at each node [136]. Based on the original load flow algorithm developed by Das [137], the composite load model and variation in load level are considered in this novel index. Balanced loads can be considered as constant power, constant current, constant impedance or exponential load. Exponential loads are a combination based on the proportion of different types of consumer loads. When taking into account either load or combinations of the above loads, the loads for each node can be modelled according to the following equations:

$$P^0 = P_0(\alpha_0 + \alpha_1 V_r + \alpha_2 V_r^2 + \alpha_3 V_r^{e1}) \tag{68}$$

$$Q^0 = Q_0(\beta_0 + \beta_1 V_r + \beta_2 V_r^2 + \beta_3 V_r^{e2}) \tag{69}$$

With the conditions that:

$$\alpha_0 + \alpha_1 + \alpha_2 + \alpha_3 = 1 \tag{70}$$

$$\beta_0 + \beta_1 + \beta_2 + \beta_3 = 1 \tag{71}$$

Where e1 and e2 are the exponential load, e1=1.38 and e2=3.22 [138]. α_0 and β_0 denote the constant power load. $\alpha_1 V_r$ and $\beta_1 V_r$ represent the constant current load. $\alpha_2 V_r^2$ and $\beta_2 V_r^2$ represent the constant impedance. $\alpha_3 V_r^{e1}$ and $\beta_3 V_r^{e2}$ stand for the

exponential load. P^0 and Q^0 are the nominal real and reactive loads at the receiving bus.

With the scaling factor ξ, any load variations at the receiving bus can be modelled:

$$P_1^0 = \xi P_0(\alpha_0 + \alpha_1 V_r + \alpha_2 V_r^2 + \alpha_3 V_r^{e1}) \tag{72}$$

$$Q_1^0 = \xi Q_0(\beta_0 + \beta_1 V_r + \beta_2 V_r^2 + \beta_3 V_r^{e2}) \tag{73}$$

where ξ can vary from 0 to any value when the voltage collapse occurs.

The mathematical expressions of P and Q for the receiving bus are:

$$P = \sum_{i=2}^{N} PP_{LOSS}(i) + \sum_{i=2}^{N-1} P_{LOSS}P(i) \tag{74}$$

$$Q = \sum_{i=2}^{N} QQ_{LOSS}(i) + \sum_{i=2}^{N-1} Q_{LOSS}Q(i) \tag{75}$$

From the basic mathematical model (74) and (75), we get:

$$|V_r| = \sqrt{B - A} \tag{76}$$

$$A = PR + QX - 0.5|V_s|^2 \tag{77}$$

$$B = \sqrt{A^2 - Z^2(P^2 + Q^2)} \tag{78}$$

$$B - A \geq 0 \tag{79}$$

$$(B - A)^2 \geq 0 \tag{80}$$

Thus:

$$B^2 - A^2 + 2A^2 - 2BA \geq 0 \qquad (81)$$

Simplifying (81) with (77) and (78) we obtain:

$$Z^2(P^2 + Q^2) \leq -2A(B - A) \qquad (82)$$

Z^2 and $(P^2 + Q^2)$ must be non-negative, and from (79), $B - A \geq 0$. Therefore, A must be negative:

$$A = PR + QX - 0.5|V_s|^2 < 0 \qquad (83)$$

$$0.5|V_s|^2 - PR - QX > 0 \qquad (84)$$

In conclusion, the index can be expressed as:

$$VSI_c = 0.5|V_s|^2 - PR - QX \qquad (85)$$

With the condition that:

$$P = \sum_{i=2}^{N} PP_{LOSS}(i) + \sum_{i=2}^{N-1} P_{LOSS}P(i) \qquad (86)$$

$$Q = \sum_{i=2}^{N} QQ_{LOSS}(i) + \sum_{i=2}^{N-1} Q_{LOSS}Q(i) \qquad (87)$$

4.1.4 Sadeghi and Foroud Voltage Stability Index

Based on the above load flow equations, Sadeghi and Foroud invested in a new voltage stability method suitable for smart distribution networks [132]. The following shows how the mentioned indices are derived.

According to Figure 4.1, the system equations can be obtained as follows:

$$I = \frac{|V_s|\angle\delta_s - |V_r|\angle\delta_r}{R + jX} \tag{88}$$

$$P + jQ = V_r I^* \tag{89}$$

$$I = \frac{P - jQ}{|V_r|\angle-\delta_r} \tag{90}$$

By equalising (88) and (90), we get:

$$(P - jQ)(R + jX) = |V_s||V_r|\angle\delta_s - \delta_r - |V_r|^2\angle\delta_r - \delta_r \tag{91}$$

$$(PR + XQ) + j(PX - QR) = |V_s||V_r|\big(COS(\delta_s - \delta_r) + jsin(\delta_s - \delta_r)\big) - |V_r|^2\angle 0 \tag{92}$$

As the bus voltage angles are small, so $\delta_s - \delta_r \approx 0$.

$$(PR + XQ) + j(PX - QR) = |V_s||V_r| - |V_r|^2 \tag{93}$$

As the right part of the (94) can only have real values, (93) can be simplified as follows:

$$V_r{}^2 - V_s V_r + PR + XQ = 0 \tag{94}$$

In order to find the solution to (94), we can use the delta formula:

$$\Delta = \frac{V_s \pm \sqrt{V_s^2 - 4(PR + XQ)}}{2} \tag{95}$$

So, we get:

$$V_s^2 - 4(PR + XQ) \geq 0 \tag{96}$$

In conclusion, in a normal distribution network, the voltage stability index is:

$$VSI_{d1} = V_s^2 - 4(PR + XQ) \tag{97}$$

Considering the development of the smart distribution network, high speed and efficiency in the detection process are necessary. In calculating the previous indices, a lot of information is needed such as line resistance, line impedance, received real power and reactive power by the node, the impedance and admittance matrices, and the Jacobian matrix. These huge amounts of data increase the calculation time and limit the indices application in the smart power system.

This paper [132] also proposed a modified VSI by considering the approximate equation for Figure 4.1 as written below:

$$|V_s|\cos(\delta) = |V_r| + R|I|\cos(\varphi_r) + X|I|\sin(\varphi_r) \tag{98}$$

where φ_r is the phase angle difference between the voltage and current of receiving bus.

$$|V_s|\cos(\delta) - |V_r| = R|I|\cos(\varphi_r) + X|I|\sin(\varphi_r) \tag{99}$$

$$|V_s||V_r|\cos(\delta) - |V_r|^2 = R|V_r||I|\cos(\varphi_r) + X|V_r||I|\sin(\varphi_r) \tag{100}$$

$$|V_s||V_r|\cos(\delta) - |V_r|^2 = RP + XQ \tag{101}$$

By substituting (101) in (102) the new index is:

$$VSI_{d2} = V_s^2 - 4(|V_s||V_r|\cos(\delta) - |V_r|^2) \tag{102}$$

As shown in (102), VSI_{d2} only considers the voltage magnitude value and the voltage angle. This is also applicable for systems with DGs and tap changers.

4.2 Simulation and Results

This section describes the performance evaluation results of the previously introduced VSIs. To evaluate the capability of the VSIs, the 14-bus islanded microgrid model developed in Chapter 3 is used. Furthermore, to investigate the performance of VSIs in different cases, the following DGs connection scenarios are considered. The power output and location are changed in different scenarios:

- Scenario 1: PV system (5 MW) connected to bus 14, Wind turbine system (5 MW) connected to bus 13, ESS (5 MW) connected to bus 5.

- Scenario 2: PV system (5 MW) connected to bus 9, Wind turbine system (5 MW) connected to bus 8, ESS (5 MW) connected to bus 12.

- Scenario 3: PV system (5 MW) connected to bus 8, Wind turbine system (5 MW) connected to bus 5, ESS (5 MW) connected to bus 4.

- Scenario 4: PV system (1 MW) connected to bus 9, Wind turbine system (3 MW) connected to bus 8, ESS (10 MW) connected to bus12.

To make the experimental analysis more comprehensive, the following control groups were set up. As shown in the above scenario settings, Scenarios 1, 2, and 3 have the same DG power output settings, but different connection bus settings. Scenarios 2 and 4 have the same connection bus settings, but different DG power output settings.

4.2.1 Calculation of VSIs under Scenario 1

In this section, without any changes in power capacity or DGs connection position, the

introduced four indices are calculated and compared with each other. After the load flow is

executed on the 14-bus microgrid by PSCAD simulation, the VSI values calculated are listed

in Table 4.1. Based on the data presented in the table, we can get the bus index comparison

graph, as shown in Figure 4.2.

Table 4.1 VSIs values under scenario 1

Bus No.	Index a	Index b	Index c	Index d2
2	0.872224402	0.876522961	0.934347857	0.971069469
3	0.596106569	0.586116666	0.793236476	0.920685941
4	0.802971593	0.808581938	0.911198714	0.999428653
5	0.822108108	0.837207133	0.925136714	0.986900327
6	0.881325545	0.896479517	0.945024143	0.965446612
7	0.947782584	0.962530821	0.980154857	0.9801
8	0.781077051	0.814469945	0.903242095	0.929846939
9	0.771523006	0.816394546	0.903936143	0.918676608
10	0.875123754	0.92769783	0.962625952	0.939976417
11	0.87474391	0.914012432	0.954814	0.948304989
12	0.957614565	0.96096298	0.981413619	0.999619084
13	0.930036848	0.933332659	0.968170619	0.999619084
14	0.970778245	0.972629992	0.986403619	0.998096145

As shown in Figure 4.2, every bus index value is above 0 and below 1, which satisfies

the VSI range. Based on the voltage stability index theory, if the value is closer to 1, the

system has better stability characteristics. Figure 4.3 gives a clear view of the difference

between the indices VSI_a, VSI_b, VSI_c and VSI_{d2}.
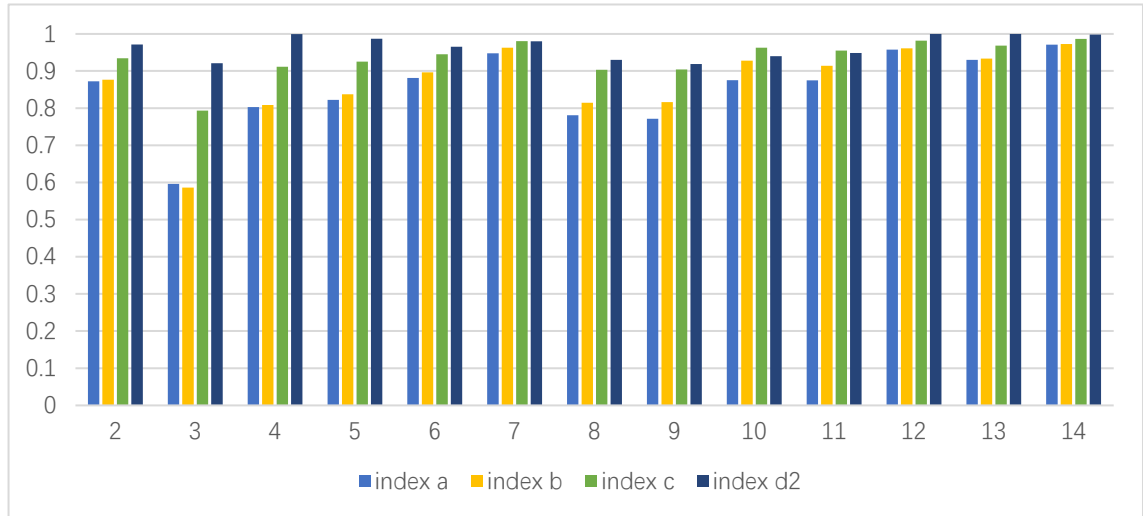
Figure 4.2 Calculated bus index values under scenario 1

In Figure 4.3, the light blue line represents the value of index 'a', the yellow line illustrates index 'b', the green line shows index 'c', and the dark blue line is index 'd2'. In this case, indices 'a', 'b', and 'c' have their minimum values at bus 3, while index 'd2' has its minimum value at bus 9. Consequently, bus 3 is identified as the weakest bus by indices 'a', 'b', and 'c', while bus 9 is identified as the weakest bus by index 'd2'. It should be noted that indices 'a', 'b', and 'c' have reasonable values close to 1 and exhibit a similar trend, which indicates that index VSI_{d2} is not accurate enough under scenario 1 as it exhibits a different trend compared to the other three indices. However, VSI_a identifies bus 9 as the second weakest bus, VSI_b recognizes this as bus 4, and VSI_c shows bus 8 as the second weakest. These differences arise from the algorithm used for each index. Furthermore, based on the calculation process times shown in Table 4.2, it can be seen that VSI_a can save a lot of time compared to VSI_b and VSI_c, as the formula does not consider power loss during the calculation. As a result, VSI_a is the most reasonable and highly efficient voltage stability analysis technique under scenario 1.
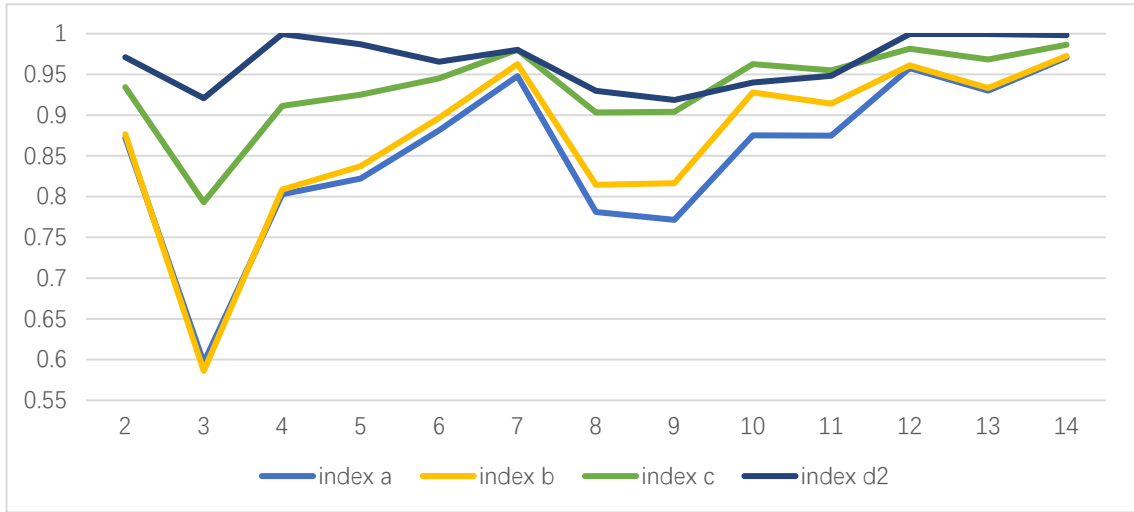
Figure 4.3 Index a, b and d2 values comparison under scenario 1

Table 4.2 General comparison of the VSIs in the study

	Comparison Items		
	Used Variables	Calculation Process Time[a]	Comprehensive Performance
VSI_a	V_s, V_r, X, R, P, Q	0.600	Medium
VSI_b	$V_s, V_r, X, R, P, Q,$ P_{LOSS}, Q_{LOSS}	0.725	Medium
VSI_c	$V_s, X, R, P, Q,$ P_{LOSS}, Q_{LOSS}	0.975	Medium
VSI_{d2}	V_s, V_r, δ	0.241	Worst

[a]Calculation process time in per-unit value on a base of 480s.

4.2.2 Calculation of VSIs under Scenario 2

In this section, the power outputs of different DGs remain unchanged while the

connection positions of DGs are changed. Four types of VSIs are applied for calculation and analysis in the new scenario. Therefore, the voltage stability level of the microgrid is analyzed with different connection positions under the same power output. After the load flow is executed on the 14-bus microgrid by PSCAD simulation, the VSI values calculated are listed in Table 4.3. Based on the data presented in the Table 4.3, we can get the bus index comparison graph, as shown in Figure 4.4.

Table 4.3 VSIs values under scenario 2

Bus No.	Index a	Index b	Index c	Index d2
2	0.791179664	0.7925233	0.891825833	0.955925224
3	0.848478764	0.851958596	0.923328714	0.967506431
4	0.908114639	0.913706018	0.957817857	0.994673778
5	0.879254853	0.901463825	0.947736048	0.960213342
6	0.867219085	0.88894239	0.941222619	0.957974866
7	0.914733688	0.945412238	0.971587429	0.963388989
8	0.907844051	0.925955791	0.965201238	0.987846676
9	0.845303257	0.857895294	0.927420476	0.968818367
10	0.953419255	0.968651352	0.983578333	0.981231755
11	0.919889616	0.937855564	0.966920238	0.9720082
12	0.953330265	0.958679856	0.977604095	0.986711111
13	0.931243159	0.936288066	0.965803714	0.982930612
14	0.952220447	0.963135803	0.980308381	0.983308336

Figure 4.4 Calculated bus index values under scenario 2

Under scenario 2, index 'd2' again has a different trend with others, which means VSI_{d2}

has a lower accuracy. The weakest bus analyzed by index 'a', 'b', and 'c' is bus 2, all three

VSIs follow a similar trend and reasonable range, as shown in Figure 4.5.

In conclusion, under the different scenarios, VSI_a, VSI_b, and VSI_c are appropriate for

the voltage stability analysis for the 14-bus islanded microgrid. VSI_a is the most suitable

one because it has a higher analysis efficiency and accuracy than others. Also, judging by

the calculation results, P_{LOSS} and Q_{LOSS} did not significantly affect the VSI value. In the

subsequent study of voltage stability analysis techniques, we can reduce attention paid to

the P_{LOSS} and P_{LOSS} values to concentrate on optimising the algorithm.
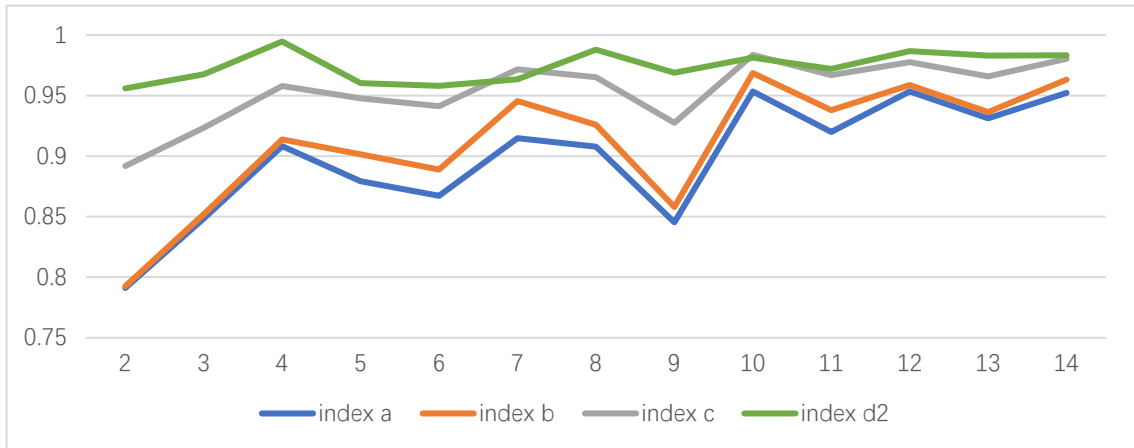
Figure 4.5 Index a, b, c and d2 values comparison under scenario 2

4.2.3 Calculation of VSIs under Scenario 3

In this subsection, the outputs of different DGs remain unchanged while the connection buses continue to vary. By analyzing scenario 3 with different VSIs, the weakest bus is identified. Based on the analysis results of the three scenarios, the influence of the DGs' connection on the voltage stability of the system is also analyzed.

After executing the load flow simulation of the 14-bus microgrid with PSCAD, the calculated VSI values are listed in Table 4.4. Based on the data presented in the table, we can obtain the index comparison graph as shown in Figure 4.6.

Figure 4.6 shows that parameters a, b, and c still have the same trend of change, and the values are within a reasonable range. The calculation results indicate that bus 3 is the weakest node under the scenario 3, followed by bus 8.

Table 4.4 VSIs values under scenario 3

Bus No.	Index a	Index b	Index c	Index d2
2	0.873143157	0.879492137	0.936424643	0.9720082
3	0.72100599	0.720451787	0.855008476	0.938130612
4	0.872872588	0.880363382	0.942326952	0.99391405
5	0.889818907	0.906651516	0.956196381	0.990119764
6	0.88032836	0.895968421	0.94467019	0.964511057
7	0.950369546	0.963862578	0.980825524	0.981420444
8	0.795856699	0.823948152	0.911105952	0.949789469
9	0.796427634	0.830588111	0.911454714	0.933524036
10	0.901369781	0.941625109	0.969959286	0.95462205
11	0.889529609	0.921902681	0.958740762	0.955739002
12	0.950360363	0.957160517	0.976937429	0.9855762
13	0.928333478	0.934789987	0.96505281	0.981420444
14	0.949282496	0.961637278	0.979554476	0.981797878
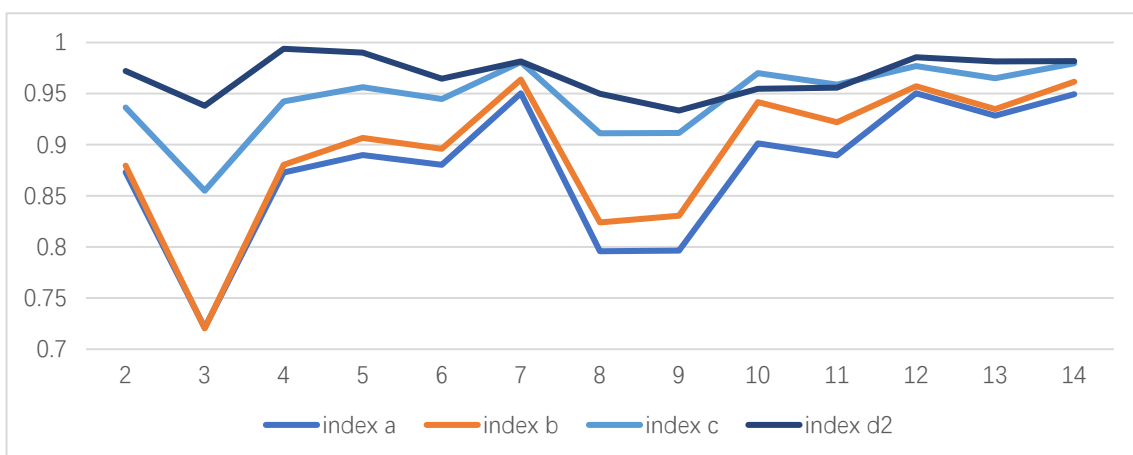
Figure 4.6 Calculated bus index values under scenario 3

In order to visually compare the voltage stability of the three scenarios, the calculation results of index 'a' under three scenarios are plotted and analyzed. Figure 4.7 shows the voltage stability analysis results of index 'a' under scenarios 1, 2, and 3.
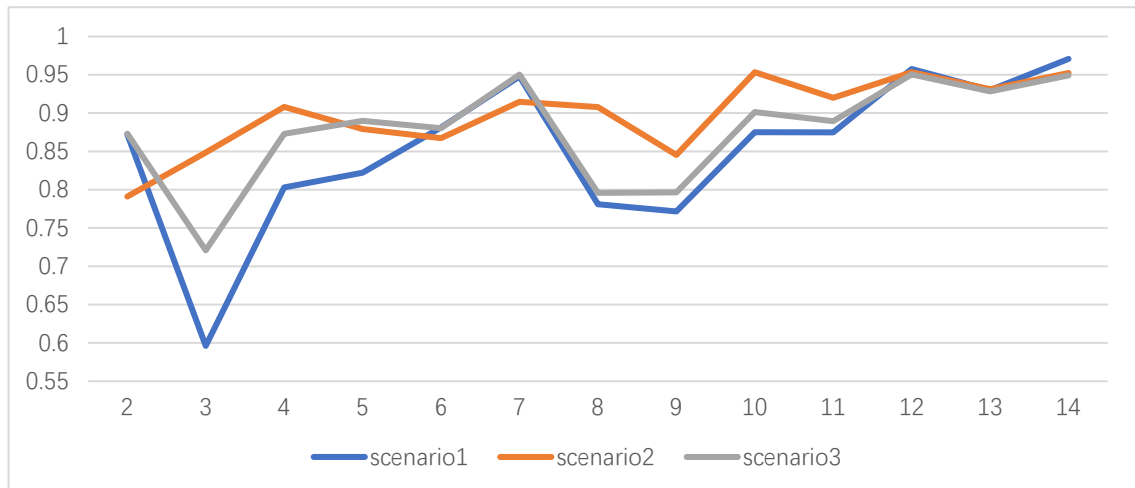
Figure 4.7 Calculated bus index values under scenario 1,2 and 3 with index a

Under scenario 3, with the same power output settings, DGs are connected closer to bus 3, which improves the voltage stability of bus 3 and its neighboring buses. As a result, the index 'a' calculation results of buses 3, 4, and 5 are greatly improved compared with scenario 1, making the system more stable.

Similarly, the connection scheme changes made in scenario 2 results in a significant improvement in the index calculation results of bus 3, no longer making it the weakest bus in the system. The analysis results show that scenario 2 is the best configuration scheme that can achieve the highest stability of the entire system among the three scenarios. The above analysis demonstrates that VSI_a can effectively perform static voltage stability analysis of the power system, and based on the comparison of analysis results, the most stable DGs connection scheme can be selected.

4.2.4 Calculation of VSIs under Scenario 4

In this section, the differences in voltage stability of the system are examined when DGs alter their output settings. Based on the connection schedule in Scenario 2, Scenario 4 changes the output of the PV from 5MW to 1MW, while the output of wind power is modified from 5MW to 3MW. Additionally, the output of the ESS is adjusted from 5MW to 10MW. Upon operating the system with this new scenario, four VSIs are utilized for analysis. After executing the load flow simulation of the 14-node microgrid with PSCAD, the calculated VSI values are listed in Table 4.5. Based on the data presented in the table, we can obtain the index comparison graph as shown in Figure 4.8.

According to Figure 4.8, we can observe that the index 'd2' still exhibits a significant deviation from the results calculated using other VSIs, leading to a low analysis reliability. Therefore, we only compare the calculated results of parameters a, b, and c. In Scenario 4, bus 3 is the weakest bus, followed by bus 9 as the second weakest bus. Buses 7 and 10 exhibit the highest stability.

Next, we will compare Scenario 2 and Scenario 4, both of which have the same bus connection settings. In both scenarios, the PV is connected to Bus 9, wind power generation is connected to Bus 8, and the ESS is connected to Bus 12. Figure 4.9 compares the results of the VSI_a calculation results in these two scenarios.

Table **4.5** VSIs values under scenario 4

Bus No.	Index a	Index b	Index c	Index d2
2	0.790010262	0.791925335	0.891427143	0.954808163
3	0.703659038	0.701318974	0.846651381	0.939607111
4	0.788195403	0.794246145	0.904551238	0.99923824
5	0.877533846	0.900578799	0.947382095	0.959653478
6	0.865482045	0.888017287	0.940754429	0.957042939
7	0.913304135	0.944662837	0.971111238	0.962267574
8	0.815578534	0.843347216	0.920505286	0.953505751
9	0.801116663	0.833212533	0.912788048	0.936102322
10	0.906339054	0.944236122	0.971102143	0.956484
11	0.892351118	0.92340075	0.959597905	0.957602041
12	0.953095177	0.956798908	0.979366143	0.99923824
13	0.93458655	0.938259567	0.970500381	0.999619084
14	0.97046393	0.972455603	0.985364	0.994103955

Figure **4.8** Calculated bus index values under scenario 4
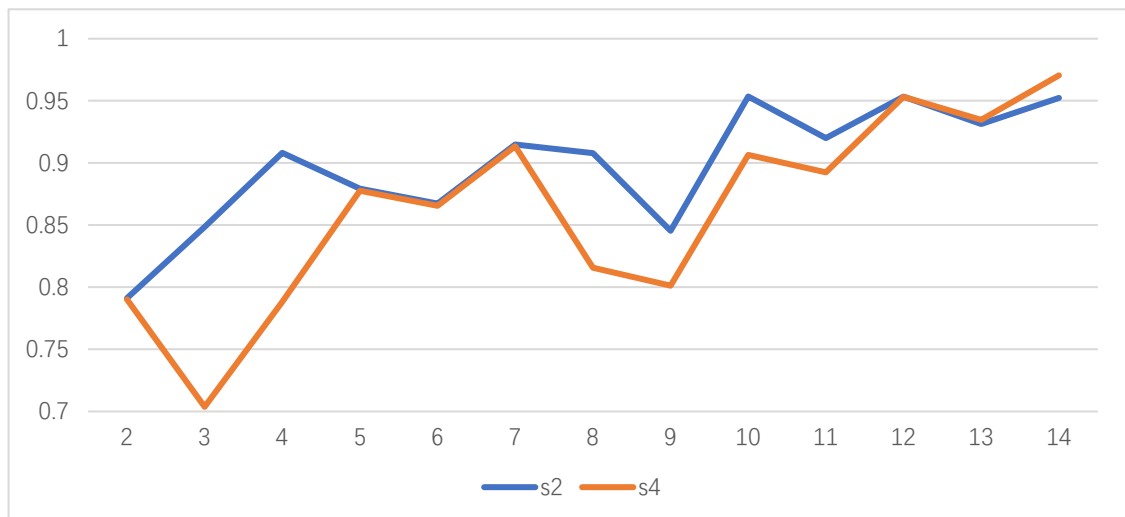
Figure 4.9 Calculated bus index a values under scenario 2 and 4

Since the output settings for PV and wind power generation in scenario 4 are much lower than in scenario 2, the index analysis results for Buses 3, 4, 8, 9, and 10 in scenario 4 are all lower than the calculated values in scenario 2. This indicates that as the output settings of DGs increase, the stability of the surrounding buses also increases. Therefore, among the four scenarios, the DG settings in scenario 2 can provide higher voltage stability for the entire 14-bus islanded microgrid. Overall, by applying the four VSIs to analyze the voltage stability of each bus in the aforementioned different scenarios, we can efficiently evaluate the voltage stability of each bus in the power system. The voltage stability index enables us to identify the weakest buses and devise better configuration planning.

4.3 Conclusion

This chapter studied the voltage stability analysis techniques for islanded microgrids. In the first section, literature-based case studies were investigated. The applications of different voltage stability analysis techniques in different types of power systems were classified and discussed. Based on the case studies, some of the voltage stability analysis

indices were chosen for further analysis. Four types of VSIs were discussed. The 14-bus islanded microgrid model developed in Chapter 3 served to undertake the accuracy test of these VSIs. The obtained results verify the effectiveness of the different VSIs. Advantages and disadvantages of different VSIs were explained. These indices are designed for general power systems instead of islanded microgrids and therefore do not include the effect of DGs on voltage stability. Besides, these indices consider the bus-level voltage stability status alone, rather than the system-level stability. The next chapter will analyse and improve these VSIs to address the above limitations and propose a new voltage stability analysis technique applicable to islanded microgrids.

Some of the work described in this chapter has been presented and published in:

X. Liang, and J. Ravishankar, "Voltage Stability Indices for Islanded Microgrids", *AUPEC 2022*.

5 An Improved Voltage Stability Analysis Technique for Islanded Microgrids

5.1 Introduction

With the development of renewable energy generation, the stability issue of power systems becomes increasingly complex. For islanded microgrids with a high penetration level of DGs, research on the influence of DGs on power system voltage stability becomes more important. In Chapter 2 and Chapter 4, the voltage stability analysis methods applicable to microgrids were classified and summarised. In Chapter 4, four VSIs selected from the literature were compared and studied through the simulation with the islanded

microgrid model. Limitations of these indices are:

1. Most of these indices do not really consider renewable energy generations. Therefore, the voltage stability analysis is unsuitable for islanded microgrids. For instance, the tap changers, which are interconnected between the DGs and the network, have not been extensively considered in prior methodologies. In summary, by addressing this aspect, the precision of calculations can be significantly enhanced.

2. Some indices have poor calculation accuracy and calculation efficiency. These limitations were studied in section 4.2. In the prior comparative analysis, the index 'd2' exhibits lower computational accuracy, demonstrating a distinct value compared to the other three indices. Furthermore, while certain indices, such as 'b' and 'c', take complex variables into consideration, the overall impact of these variables on the final results is less, indicating that there is potential for improving computational efficiency by simplifying the algorithm.

3. The computational complexity is high. In addition to analysing bus voltages, these VSIs also need to consider other parameters or matrices such as P, Q, R, and X. This means the run time will be high and furthermore shows these VSIs are difficult for application to complex power systems.

4. These indices can only analyse the single bus voltage stability, which means these VSIs cannot accurately assess the overall voltage stability of the entire power system. This implies that if two configuration planning exhibit comparable bus voltage stability levels, it can be better to incorporate system-level voltage stability analysis during the planning stage to ensure a comprehensive assessment.

This chapter proposes a novel index to study the voltage stability for islanded microgrids. The main motivation to develop this novel VSI is not only to identify the weakest bus but also to rank the voltage stability level of all buses. This will lead to the ideal DG configuration of the islanded microgrid by comparing the overall system voltage stability level. Albeit, the computational performance of the index increases significantly.

This chapter is structured as follows. Section 5.2 proposes the derivation process of the novel VSI. Section 5.3 presents the simulation results and the comparison with the other VSIs. The 14-bus islanded microgrid in PSCAD software is used in the simulation for comparison under different scenarios. Section 5.4 summarises this chapter showing the efficacy of the novel method.

5.2 Development of the Novel Voltage Stability Index

5.2.1 Bus Voltage Stability Index

Considering the penetration of renewable energy generations in the islanded microgrid, voltage stability analysis is not as simple as the analysis process in the normal power system. The VSIs presented in the literature may result in inaccuracies when analyzing voltage stability for islanded microgrids. It is essential to take into account the presence of distributed generators when formulating such indices to ensure a more accurate assessment. In this section, the proposed VSI is developed using Figure 5.1. In Figure 5.1, V_s is the voltage magnitude of the sending end, $\angle \delta_s$ is the voltage angle of the sending end, V_R is the voltage magnitude of the receiving end, $\angle \delta_R$ is the voltage angle of the

receiving end, Z denotes the line impedance between sending bus and receiving bus, P_R stands for the real power received by the receiving end, Q_R is the reactive power received by the receiving bus, P_D is the real power generated by the generator connected to the receiving bus, and Q_D is the reactive power generated by the generator connected to the receiving bus.

Figure 5.1 2-bus equivalent distribution line model considering the DG

Based on the 2-bus equivalent distribution system single line model, the following equations can be written:

$$I = \frac{V_s \angle \delta_s - V_R \angle \delta_R}{Z} \tag{103}$$

$$P + jQ = (|V_R| \angle \delta_R) \cdot I^* \tag{104}$$

$$I = \frac{P - jQ}{V_R \angle - \delta_R} \tag{105}$$

$$\begin{cases} P = P_R - P_D \\ Q = Q_R - Q_D \end{cases} \tag{106}$$

By combining equations (103) and (105) we get:

$$\frac{V_s \angle \delta_s - V_R \angle \delta_R}{Z} = \frac{P - jQ}{V_R \angle - \delta_R} \tag{107}$$

$$|V_s||V_R|\angle\delta_s - \delta_R - |V_R|^2\angle 0 = RP - jRQ + jXP + XQ \tag{108}$$

$$|V_s||V_R|[\cos(\delta_s - \delta_R) + j\sin(\delta_s - \delta_R)] - |V_R|^2\angle 0 = RP - jRQ + jXP + XQ \tag{109}$$

As the angles of voltages are small in the distribution network [79], we can assume that $\angle\delta_s - \delta_R \approx \angle 0$. Thus, we get:

$$\cos(\delta_s - \delta_R) \approx 1 \tag{110}$$

$$\sin(\delta_s - \delta_R) \approx 0 \tag{111}$$

By combining equations (109), (110) and (111) we get

$$|V_s||V_R| - |V_R|^2 = RP + XQ + j(XP - RQ) \tag{112}$$

Equating the real parts in (112):

$$|V_s||V_R| - |V_R|^2 = RP + XQ \tag{113}$$

$$V_R{}^2 - V_s V_R + RP + XQ = 0 \tag{114}$$

Equation (114) is a quadratic equation between the sending bus and receiving bus. In order to have a reasonable solution of V_R, the following equation must be satisfied:

$$(-V_s)^2 - 4(RP + XQ) \geq 0 \tag{115}$$

Therefore, the VSI when considering DGs can be defined as equation (116). The range of VSI is (0,1) and the closer the VSI_{DG} value is to 0, the more unstable the bus is:

$$VSI_{DG} = V_s{}^2 - 4[R(P_R - P_D) + X(Q_R - Q_D)] \geq 0 \tag{116}$$

When the generator is a renewable energy-based distributed generator, such as photovoltaic (PV) or wind turbine systems, it is more probable that a tap changer will be integrated between the generator and the network. Consequently, the subsequent condition entails the index considering the presence of tap changers. In this case, V_S is the voltage magnitude of the sending end, $\angle\delta_S$ is the voltage angle of the sending end, V_R is the voltage magnitude of the receiving end, $\angle\delta_R$ is the voltage angle of the receiving end, Z_T denotes the line impedance and the tap changer impedance, P_D is the real power generated by the generator connected to the receiving bus, and Q_D is the reactive power generated by the generator connected to the receiving bus.
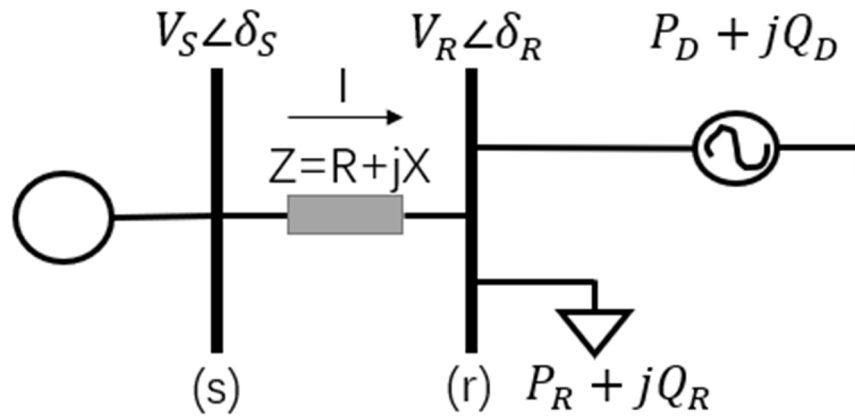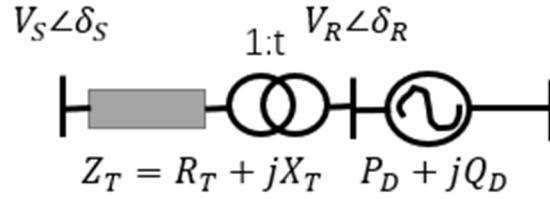

Figure 5.2 2-bus equivalent distribution line model considering the tap changer

Based on the Figure 5.2, the following equations can be written:

$$I = \frac{tV_S\angle\delta_S - V_R\angle\delta_R}{t^2 Z_T} \tag{117}$$

$$P_D + jQ_D = (|V_R|\angle\delta_R) \cdot I^* \tag{118}$$

$$I = \frac{P_D - jQ_D}{V_R\angle-\delta_R} \tag{119}$$

By combining equations (117) and (119) we get:

$$|V_S||V_R|t[\cos(\delta_S - \delta_R) + j\sin(\delta_S - \delta_R)] - |V_R|^2\angle 0 = t^2(R_T + jX_T)(P_D - jQ_D) \tag{120}$$

As the angles of voltages are small in the distribution network [79], we can assume that

$\angle \delta_S - \delta_R \approx \angle 0$. Thus, we get:

$$\cos(\delta_S - \delta_R) \approx 1 \tag{121}$$

$$\sin(\delta_S - \delta_R) \approx 0 \tag{122}$$

By combining equations (120), (121) and (122) we get

$$t|V_s||V_r| - |V_r|^2 = t^2[R_T P_D + X_T Q_D + j(X_T P_D - R_T Q_D)] \tag{123}$$

Equating the real parts in (124):

$$V_r^2 - tV_s V_r + t^2 R_T P_D + t^2 X_T Q_D = 0 \tag{124}$$

Equation (124) is a quadratic equation between the sending bus and receiving bus. In order to have a reasonable solution of V_r, the following equation must be satisfied:

$$t^2 V_S^2 - 4t^2(R_T P_D + X_T Q_D) \geq 0 \tag{125}$$

Therefore, the VSI when considering DGs can be defined as equation (126). The range of VSI is (0,1) and the closer the VSI_{DG} value is to 0, the more unstable the bus is:

$$VSI_{DG\_T} = t^2 V_S^2 - 4t^2(R_T P_D + X_T Q_D) \geq 0 \tag{126}$$

In conclusion, depending on the existence of a tap changer between the sending bus and the receiving bus, different voltage stability index formulas can be applied to analyze the bus stability level more accurately.

5.2.2 System Voltage Stability Index

This section uses the developed VSI_{DG} and VSI_{DG_T}, to compare the voltage stability

of the selected buses under different DG configurations. The weakest bus can be found through the index. However, we cannot observe the overall voltage stability level for the entire system under different scenarios. For this reason, we still do not know which configuration can maximise the stability of the islanded microgrid. In this section, a system voltage stability index is defined. Combining both bus voltage stability index and system voltage stability index, the voltage stability level of a specific islanded microgrid can be thoroughly analysed.

A system voltage influence parameter ε is defined based on the sum of the squared error, to quantitively analyse the influence of DGs connection to islanded microgrids. The definition is expressed as follows:

$$\varepsilon = \sum_{i=2}^{n}\left(VSI_{DGi} - VSI_{DG\_R}\right)^2 \tag{127}$$

where n is the bus number of the network; VSI_{DGi} is the VSI value of bus i. If a tap changer exists, the formula for VSI_{DG_T} should be applied; otherwise VSI_{DG} should be utilized. VSI_{DG_R} is the rated value of the stable state, which is 1.0 p.u. in the definition. The smaller ε is, the better will be the voltage quality of the system, and vice versa.

In conclusion, the expression for the novel voltage stability index can be written as equation (128):

$$\begin{cases} VSI_{DG} = V_s^2 - 4[R(P_R + P_D) + X(Q_R + Q_D)] \geq 0 \\ VSI_{DG\_T} = t^2 V_S^2 - 4t^2(R_T P_D + X_T Q_D) \geq 0 \\ \varepsilon = \sum_{i=2}^{n}\left(VSI_{DGi} - VSI_{DG\_R}\right)^2 \\ VSI_{DG\_R} = 1 \end{cases} \tag{128}$$

5.3 Simulation and Results

This section describes the performance evaluation results for the novel voltage stability index. Three scenarios are applied during the simulation. To this end, the new index is compared with other available indices discussed in Chapter 4.

The 14-bus islanded microgrid illustrated in Figure 3.22 is used for the analysis. Apart from showing the index's improvement, its results are compared with other VSIs studied in Chapter 4. In the test system, the novel VSI and other VSIs are studied based on different DGs' configurations in the islanded microgrid model. The following scenarios are chosen to investigate the novel index's performance:

1. Calculation of the proposed index in the power system with no DGs (Scenario 0).

2. Calculation of the proposed index under scenario 2: PV system (5 MW) connected to bus 9, Wind turbine system (5 MW) connected to bus 8, ESS (5 MW) connected to bus 12.

3. Calculation of the proposed index under scenario 3: PV system (5 MW) connected to bus 8, Wind turbine system (5 MW) connected to bus 5, ESS (5 MW) connected to bus 4.

4. Calculation of the proposed index under scenario 5: Synchronous generator (5 MW) connected to bus 8, Synchronous generator (5 MW) connected to bus 5, Synchronous generator (5MW) connected to bus 4.

In the above simulations, firstly, the load flow should be run in the PSCAD simulation environment, and then the indices should be calculated in different buses. Finally, the

system voltage stability index can be calculated based on the bus VSIs.

5.3.1 Outcome of the Proposed Index in the Power System with no DGs (Scenario 0)

In this section, without any connection of the DGs to the 14-bus network, as shown in Figure 5.3, the proposed index can be calculated after the load flow is executed.
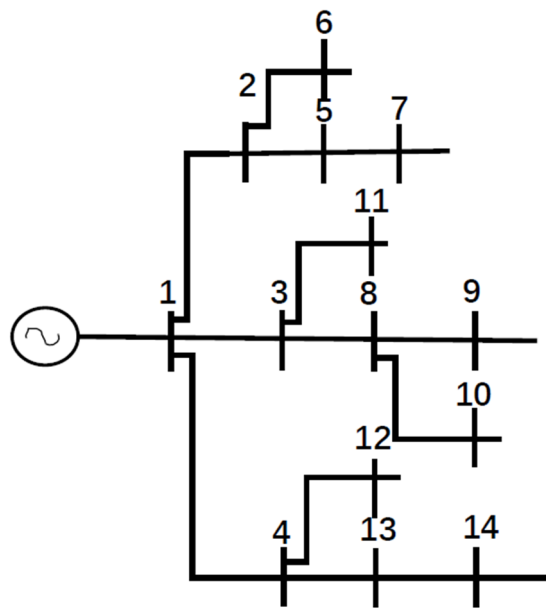
Figure 5.3 14-bus test feeder structure without DGs

After the load flow is executed on the 14-bus network, the novel VSI value for buses can be calculated. Other indices are also used in the comparison test, and the calculation results are listed in Table 5.1. To clearly demonstrate the distinctions among various voltage stability indices, Figure 5.4 presents a visual representation of the index values for comparison. As seen in this scenario, all indices, except the index 'd2', devote their minimum value to bus 3, which is 0.258. It can be concluded here that all indices, except the index 'd2', have similar evaluation results, i.e., bus 3 is the weakest bus.
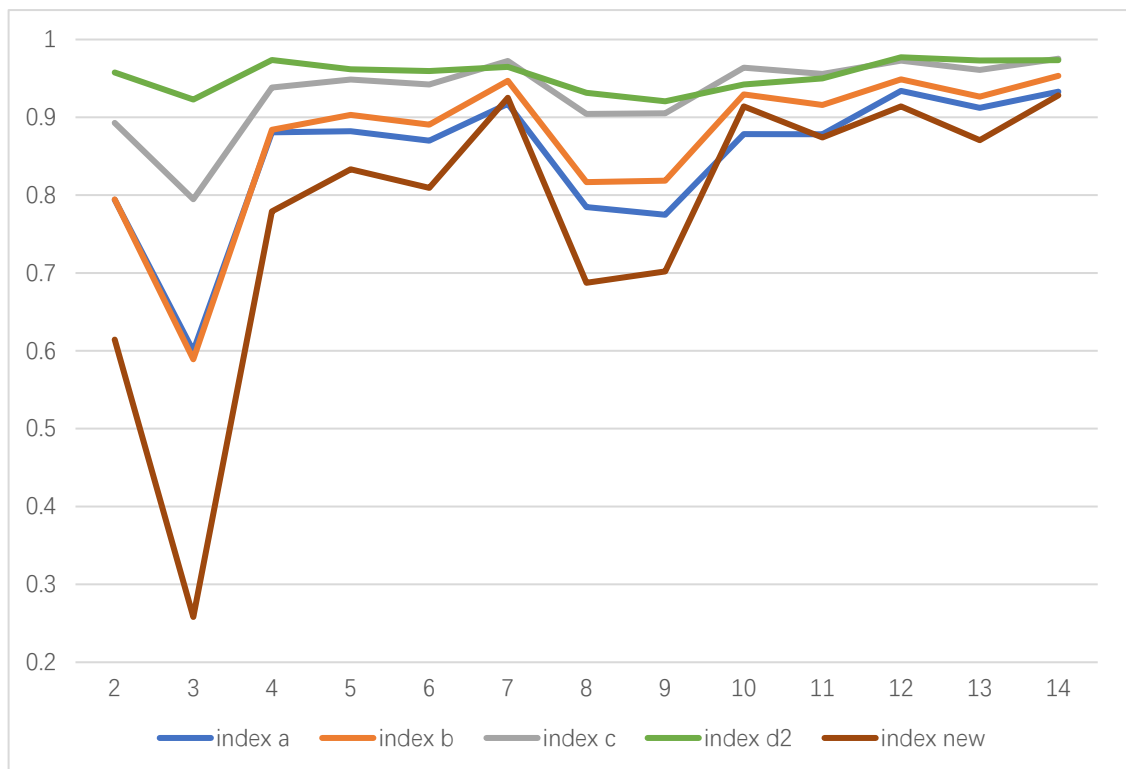
Figure 5.4 The index value in the 14-bus network under scenario 0

Firstly, as depicted in Figure 5.4, it is evident that the weakest bus identified for both

the indices 'a', 'b', 'c', and the new index is bus 3. Moreover, for indices 'b', 'c', and the new

one, the second weakest bus is bus 8, followed by bus 9. This feature suggests that the new

index offers a reliable and accurate analysis. For index 'd2', the lowest value is 0.9206, which

means bus 9 is the weakest bus. The second lowest value is 0.9226, indicating that bus 3 is

the second weakest bus. In addition, the results calculated by index 'd2' for buses 2 to bus

14 are similar, ranging from around 0.92 to 0.97. The numerical curve for index 'd2' is flat

and has a different trend compared to the others, suggesting that the index 'd2' is

challenging to use for clearly distinguishing the voltage stability of each buses and it has

the worst calculation accuracy among these five indices.

The changing trends of numerical curves for indices a, b, c, and the new index reveal

that the bus stability analyzed with these indices is nearly identical. However, the value

difference between different buses calculated by the new index is greater than that determined by other VSIs. This suggests that the new index can more effectively highlight the voltage stability differences between buses and more accurately identify and rank the voltage stability of each bus within the entire power system.

Table 5.1 VSIs' values in the 14-bus network

Bus	Index a	Index b	Index c	Index d2	New
2	0.7940	0.7945	0.8929	0.9574	0.6145
3	0.5999	0.5893	0.7948	0.9227	0.2581
4	0.8806	0.8838	0.9381	0.9735	0.7790
5	0.8820	0.9030	0.9485	0.9615	0.8331
6	0.8699	0.8905	0.9420	0.9593	0.8093
7	0.9173	0.9468	0.9723	0.9647	0.9250
8	0.7845	0.8167	0.9043	0.9315	0.6874
9	0.7748	0.8185	0.9051	0.9207	0.7020
10	0.8783	0.9294	0.9636	0.9420	0.9140
11	0.8781	0.9159	0.9558	0.9500	0.8741
12	0.9339	0.9488	0.9727	0.9771	0.9140
13	0.9121	0.9264	0.9608	0.9729	0.8706
14	0.9328	0.9532	0.9753	0.9733	0.9281

Based on the aforementioned analysis and in conjunction with the recorded computation times of each index, Table 5.2 summarizes the ranking of the calculation time

and accuracy for each index. It can be observed that the new index exhibits relatively high computational efficiency and accuracy. Consequently, it can be demonstrated that the new index operates reliably and efficiently under the scenario 0.

Table 5.2 General comparison of the VSIs

	Comparison Items		
	Used Variables	Calculation Process Time[a]	Calculation Accuracy
VSI_a	V_s, V_r, X, R, P, Q	0.600	Medium
VSI_b	$V_s, V_r, X, R, P, Q,$ P_{LOSS}, Q_{LOSS}	0.725	Medium
VSI_c	$V_s, X, R, P, Q,$ P_{LOSS}, Q_{LOSS}	0.975	Medium
VSI_{d2}	V_s, V_r, δ	0.241	Worst[b]
VSI_{DG} (new)	V_s, V_r, X, R, P, Q	0.600	Best

[a] Calculation process time in per-unit value on a base of 480s.

[b] Numerical curve for index 'd2' is flat and has a different trend compared to others.

5.3.2 Calculation of the Proposed Index under Scenario 2 and Scenario 3

In scenarios 2 and 3, a 5 MW photovoltaic system, a 5 MW wind turbine, and a 5 MW energy storage system are connected into the original network, while the loads and line

settings remain unchanged as the scenario 0. Figure 5.5 illustrates the islanded microgrid model structure under scenario 2, and Figure 5.6 depicts the islanded microgrid model structure under scenario 3. The proposed index can be calculated after the load flow is executed. In scenario 2, a 5 MW PV system is connected to bus 9, a 5 MW wind turbine system is connected to bus 8, and a 5 MW energy storage system is connected to bus 12. In scenario 3, the PV system is moved to bus 8, the wind turbine system is moved to bus 5, and the energy storage system is moved to bus 4.

After executing the load flow on the 14-bus network, the novel VSI values for buses under scenarios 2 and 3 can be calculated, as depicted in Figure 5.7. According to the values under scenario 3, bus 3 exhibits the minimum index value, which means that it is the weakest bus in this situation as well. Furthermore, by comparing the index results between subsections 5.3.1 and 5.3.2, it can be observed that the voltage stability of almost all buses demonstrates an improvement, especially for bus 3, which sees its index value increase from 0.2581 to 0.4829. In conclusion, this modeling configuration enhances the stability of the original system.

In Figure 5.7, the blue line represents the calculated values under scenario 2, while the orange line displays the index values calculated under scenario 3. In scenario 2, the lowest value is for bus 2, which is 0.6118. As Figure 5.5 illustrates, there are no DGs connected near the bus 2 branch. To enhance the voltage stability level of bus 2 in scenario 3, the wind turbine is relocated to bus 5, which is in proximity to bus 2, as shown in Figure 5.6. In this new configuration, the index value of bus 2 increases to 0.7739.

Comparing the configuration diagrams 5.5 and 5.6, it can be observed that from

Scenario 2 to Scenario 3, there is no longer a DG connection at bus 9, which implies that loads connected to bus 3 lose additional power supply. While maintaining the impedance of each line and connected loads, the stability of several buses near bus 3 will be affected as well. This can be verified by the calculation results shown in Figure 5.7. It can be seen that the VSI calculation results for buses 3, 8, and 9 are lower in the Scenario 3 case than in Scenario 2. This confirms that when the power provided by the diesel generator and the power consumed by the loads are unchanged, the relocation of the DGs makes the voltage supply of bus 3 and bus 7 less stable. In conclusion, the new VSI can reliably determine the voltage stability level of each bus in the entire islanded microgrid.
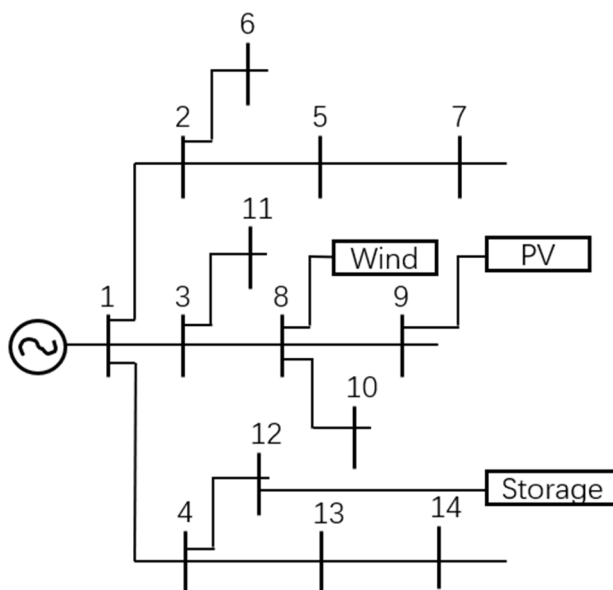
Figure 5.5 14-bus test feeder structure under scenario 2
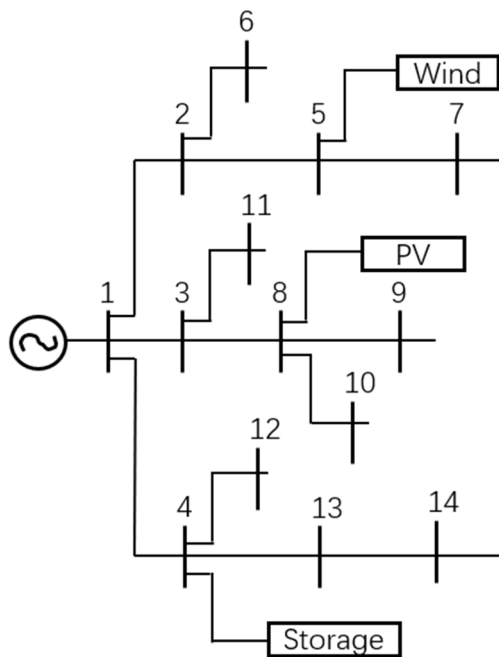
Figure 5.6 14-bus test feeder structure under scenario 3
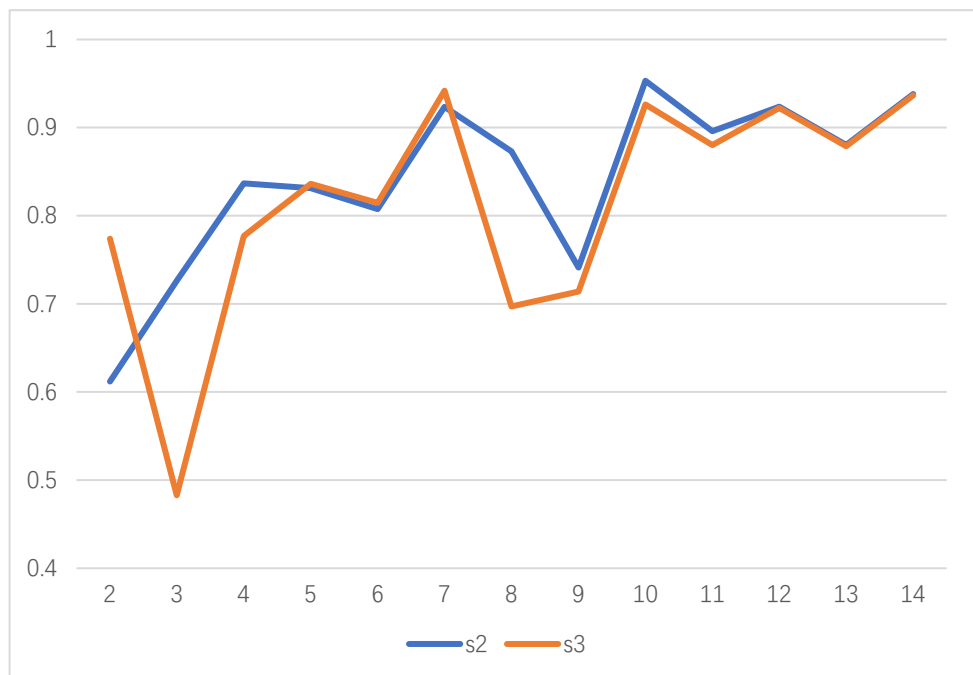
Figure 5.7 The novel index value comparison in the 14-bus network

5.3.3 Calculation of the Proposed Index under Scenario 5

In order to verify whether the new index is more suitable for voltage stability analysis of

islanded microgrids with renewable energy distributed generation systems, a set of control tests has been designed. In Scenario 5, the 5 MW PV, 5 MW wind turbine, and 5 MW ESS system from Scenario 3 are replaced with three identical 5 MW diesel generators, as shown in Figure 5.8.

Figure 5.9 displays the results of analyzing the voltage stability levels of each bus in Scenario 1 and Scenario 5 using the new index. The blue line represents the voltage stability of each bus under Scenario 5, while the orange line represents the voltage stability of each bus in a basic islanded microgrid configuration. It can be observed that there are some slight differences in voltage stability between the two situations, and it is clear that the stability of the system connected by three diesel generators is relatively high. The voltage stability of buses 2, 3, 4, and 8, 9, 10 in the case of the islanded microgrid is comparatively low compared to Scenario 5. This is because the new index analysis process takes into account not only the input power of each bus but also the bus voltage and the presence of tap changers. These experimental results confirm that the new index can identify the difference between diesel generators and renewable energy generators through the voltage stability analysis and it is suitable for the voltage stability analysis of islanded microgrids.
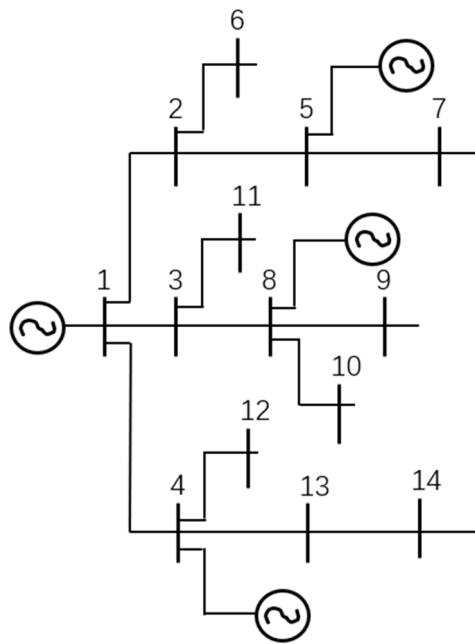
Figure 5.8 14-bus test feeder structure under scenario 4

Figure 5.9 The novel index value comparison in the 14-bus network

5.3.4 System Voltage Stability Analysis under Four Scenarios

One of the design aims of the new VSI is to analyse the voltage stability of the entire power system. In this section, the system index of the above three simulation models are calculated to rank the voltage stability levels of the three configurations. The calculated results of the system voltage influence parameter ε are listed in Table 5.3.

Table 5.3 Comparison of system voltage influence parameter

Scenario	Configuration	ε
0	No DGs	1.05668
2	5 MW PV – bus 9	
	5 MW wind – bus 8	0.44378
	5 MW ESS – bus 12	
3	5 MW PV – bus 8	
	5 MW wind – bus 5	0.65306
	5 MW ESS – bus 4	
5	5 MW diesel generator – bus 8	
	5 MW diesel generator – bus 5	0.41156
	5 MW diesel generator – bus 4	

It can be seen from the table that the parameter value of scenario 0 is the largest, and the parameter value of scenario 5 is the smallest. According to the definition of system voltage influence parameters, the higher the parameter value, the lower the system voltage stability level. It appears that the system under scenario 5 is the most stable one. This is reliable and consistent with the actual situation, as in the same 14-bus network, Scenario 0 has only one diesel generator connected to bus 1, which can supply power to the entire system, while Scenario 5 has three more stable diesel generators connected to the system to provide power. Consequently, it is logical for Scenario 5 to be more stable while the overall system loads and line impedance remain unchanged.

In Scenario 2 and Scenario 3, which are the basic islanded microgrids, three renewable

energy generators are added into the original IEEE 14-bus network, which was labelled as Scenario 0. As a result, both Scenario 2 and Scenario 3 should be more stable than the power system in Scenario 0, which only has one diesel generator. The system parameter results verified this statement. Furthermore, by comparing the calculation results of system parameters, it can be concluded that the configuration of Scenario 2 is more stable than that of Scenario 3.

As all four scenarios have the same diesel generator connected to bus 1 and same load settings, the connection of DGs has shown to increase the system's power supply and thus improve the voltage stability of the system. Additionally, system parameters can be employed to compare two configuration schemes with similar bus voltage stability levels. This process synthesizes the voltage stability levels of all buses, assisting designers in determining the optimal configuration. These analyses show that the novel index is reliable and can be used to analyse the static voltage stability on the system level.

5.4 Discussion and Summary

In this chapter, a novel static voltage stability analysis index is posited. Firstly, the theoretical background and derivation process was illustrated in detail. Then, four scenarios were applied in the simulation to verify the evaluation capability of the new VSI. The original 14-bus distribution network was used firstly in section 5.3.1 and in that section the proposed index was compared with four other indices. The performance of VSIs was summarised in Table 5.2. Scenario 2 and Scenario 3 were applied in section 5.3.2 to verify the evaluation accuracy of the novel VSI. PV, wind turbine and ESS were connected to the

original 14-bus network in these scenarios with different location. In this process, the bus stability index value is seen to increase as the power supply to the islanded microgrid increases.

In addition, after replacing the three DGs with diesel generators composed of synchronous generators, while maintaining the same power output settings, the bus voltage stability results analyzed using the new index differ slightly from the calculation results under Scenario 3. This demonstrates that the new index, which takes into account the presence of tap changers, is more suitable for islanded microgrids that include DGs with tap changers. Therefore, the results prove that the new VSI can effectively analyse and evaluate the static voltage stability of islanded microgrid on bus level. In section 5.3.4, the system voltage stability was compared and analysed under four different network configurations. The results show that the overall system stability of scenario 2 is higher than scenario 3. It is very convincing that the proposed voltage stability analysis technic can undertake a reliable system-level analysis. In summary, the new index system solves some of the limitations of the other four VSIs and has the following advantages:

1. The new index introduces the concept of analyzing voltage stability at both the bus and system levels, making the static voltage stability analysis more comprehensive and reasonable. It provides a method for comparing configurations with similar voltage stability at the bus level, further enhancing decision-making capabilities in islanded microgrid design.

2. The new index also considers the tap changer connected between the bus and the renewable energy generators. This makes the new index more suitable for islanded

microgrids with DGs in static voltage stability analysis, thereby improving the reliability and accuracy of the VSI. This suggests that the new index can more effectively highlight the voltage stability differences between buses and more accurately identify and rank the voltage stability of each bus within the entire power system.

3. The new index minimizes the types of variables that need to be considered, thereby reducing the complexity of computation and maintaining a relatively high computational efficiency. This is important in static voltage stability analysis.

Some of the work described in this chapter has been submitted in:

X. Liang, and J. Ravishankar, " A Novel Optimised Static Voltage Stability Analysis Technique for Islanded Microgrids," Submitted to Universal Journal of Electrical Engineering (UJEE).

6 Conclusion and Future Study

6.1 Conclusion

The aim of this thesis is to develop a novel static voltage stability analysis technique for islanded microgrid. The research process includes literature review, state-of-the-art voltage stability indices study and comparison, islanded microgrid modelling, novel VSI development, and simulation-based verification of the proposed VSI.

Chapter 2 presents a detailed literature review of analytical methods of voltage stability in renewable dominated power systems. A systematic classification of voltage stability

analysis methods is provided in this chapter. The computing complexity of different methods is also discussed, thus providing guidance on choosing proper analysis methods and voltage stability indices to conduct stability assessments for renewable-energy-dominated networks.

Chapter 3 develops a 14-bus islanded microgrid in PSCAD software. As a professional and flexible graphical user interface software, PSCAD is an advanced power system simulation platform. A detailed modelling process is presented in this chapter. Diesel generator subsystem, PV subsystem, wind turbine subsystem, and energy storage system modelling process are presented. This chapter provides a detailed theoretical basis and model structure for the modeling of islanded microgrids in PSCAD.

In Chapter 4, literature-based case study of the voltage stability analysis techniques and simulation-based case study of four appropriate voltage stability indices suitable for distribution network are proposed. Through the literature-based case study, state-of-the-art voltage stability analysis techniques are classified and summarised according to the applicable power system types. Then, four techniques are selected. Based on the simulation model established in Chapter 3, the advantages and disadvantages of these four methods are explained. The limitations are improved in Chapter 5. This chapter provides an important basis for proposing a new static voltage stability analysis index.

Chapter 5 develops a novel static voltage stability analysis technique designed for islanded microgrids. In this chapter the proposed index is compared with four indices presented in Chapter 4. Through the simulation process the performance of the proposed index is verified. The new index has high accuracy and it can be easily used to analyse the

weakest bus in the islanded microgrid. By ranking the stability level of buses, the configuration or connection position of DGs can be changed accordingly, so in effect improving the voltage stability of the bus and the whole system. Also, the proposed index can be used to analyse and compare the system's voltage stability level. The work has demonstrated that the new VSI is an improved voltage stability analysis method with high accuracy and applicable to islanded microgrids.

6.2 Future Work

This thesis leads to the following suggestions for further research on this subject:

1. Systematic development of dynamic voltage stability analysis methods: This thesis mainly focuses on static voltage stability analysis. Due to the advantages of low complexity and high efficiency, the research of static analysis method is more common. Although static voltage stability analysis is currently the primary focus of analysis, incorporating dynamic analysis will provide a more comprehensive understanding of microgrid behaviour. Dynamic voltage stability analysis enables researchers to investigate the system's response to transient events such as faults, startups, and shutdowns, resulting in a better understanding of the system's stability and performance. This understanding can lead to more profound improvements in decision-making concerning microgrid design and operation. Further research can be conducted to develop new techniques for dynamic voltage stability analysis or to improve existing ones. Although several dynamic methods to evaluate the voltage profile of a system are available, additional work needs to be done to improve their efficacy levels.

2. Simulation modelling optimization with less black boxes: The black box in islanded microgrid modelling refers to the use of pre-defined, generic models for DGs sources, synchronous generator, and loads provided in PSCAD library. They offer a simplified and efficient starting point for modeling, but their internal workings and parameters are hidden from the user. There are some limitations associated with using these black-box models: (i) Transparency is a critical issue with black-box models that can negatively impact the accuracy of experimental results. (ii) The internal control system and structure of the black box module cannot be viewed and modified, so researchers are unable to verify the accuracy and applicability of the simulation results. (iii) Another issue with black-box models is their inability to capture dynamic behaviour accurately. While static voltage stability analysis is only one aspect of microgrid voltage stability analysis, future research should focus on developing dynamic voltage stability analysis. However, black-box models struggle to capture the dynamic behaviour of DG units, such as transient responses during faults, startups, or shutdowns.

In summary, black-box models offer convenience and efficiency in simulation and research, but accuracy and reliability should be the ultimate goal. To achieve more accurate and effective simulation results, custom models or more detailed component-based models should be used instead, even if this requires more time and expertise. This approach will ultimately support better decision-making in microgrid design and operation.

3. Online real-time techniques for assessing the state of the system's voltage and the threshold of instability. It is anticipated that power systems can be further optimised in an efficient and timely manner if the voltage collapse is detected at an early stage.

7 Reference

[1]   S. Abhinav, H. Modares, F. L. Lewis, and A. Davoudi, "Resilient cooperative control of DC microgrids," *IEEE Trans. Smart Grid,* vol. 10, no. 1, pp. 1083-1085, 2018.

[2]   S. Sen and V. Kumar, "Microgrid control: A comprehensive survey," *Annual Reviews in control,* vol. 45, pp. 118-151, 2018.

[3]   L. Aththanayake, N. Hosseinzadeh, A. Mahmud, A. Gargoom, and E. M. Farahani, *Challenges to voltage and frequency stability of microgrids under renewable integration* (2020 Australasian Universities Power Engineering Conference). New York: IEEE (in English), 2020.

[4]   P. Kundur, N. J. Balu, and M. G. Lauby, *Power system stability and control.* McGraw-hill New York, 1994.

[5]   J. A. Neto, A. Z. De Souza, E. V. De Lorenci, T. P. Mendes, P. M. Dos Santos, and B. D. N. Nascimento, "Static voltage stability analysis of an islanded microgrid using energy function," *IEEE Access,* vol. 8, pp. 201005-201014, 2020.

[6]   N. Hosseinzadeh, A. Aziz, A. Mahmud, A. Gargoom, and M. Rabbani, "Voltage stability of power systems with renewable-energy inverter-based generators: A review," *Electronics,* vol. 10, no. 2, p. 115, 2021.

[7]   K. Alzaareer, M. Saad, H. Mehrjerdi, C. Z. El-Bayeh, D. Asber, and S. Lefebvre, "A new sensitivity approach for preventive control selection in real-time voltage stability assessment," *Int. J. Electr. Power Energy Syst.,* vol. 122, p. 106212, 2020.

[8]   Y. Song, D. J. Hill, and T. Liu, "Static voltage stability analysis of distribution systems based on network-load admittance ratio," *IEEE Trans. Power Syst.,* vol. 34, no. 3, pp. 2270-2280, 2018.

[9]   L. Y. Ren and P. Zhang, "Generalized Microgrid Power Flow," (in English), *IEEE Trans. Smart Grid,* Article vol. 9, no. 4, pp. 3911-3913, Jul 2018, doi: 10.1109/tsg.2018.2813080.

[10]   Z. Y. Chen, Q. Li, M. M. Wan, W. L. Li, and IEEE, "A simplified method for voltage stability analysis of wind power integration," in *2018 International Conference on Power System Technology,* (International Conference on Power System Technology. New York: IEEE, 2018, pp. 1646-1652.

[11]   K. E. Antoniadou-Plytaria, I. N. Kouveliotis-Lysikatos, P. S. Georgilakis, and N. D. Hatziargyriou, "Distributed and decentralized voltage control of smart distribution networks: Models, methods, and future research," *IEEE Trans. Smart Grid,* vol. 8, no. 6, pp. 2999-3008, 2017.

[12]   Q. Huang, R. Huang, W. Hao, J. Tan, R. Fan, and Z. Huang, "Adaptive power system emergency control using deep reinforcement learning," *IEEE Trans. Smart Grid,* vol. 11, no. 2, pp. 1171-1182, 2019.

[13]   D. E. Olivares *et al.,* "Trends in microgrid control," *IEEE Trans. Smart Grid,* vol. 5, no. 4, pp. 1905-1919, 2014.

[14]   B. B. Adetokun, C. M. Muriithi, and J. O. Ojo, "Voltage stability assessment and enhancement of power grid with increasing wind energy penetration," (in English), *Int. J. Electr. Power Energy Syst.,* Article vol. 120, p. 11, Sep 2020, Art no. 105988, doi: 10.1016/j.ijepes.2020.105988.

[15]   Y. Lee and H. Song, "A reactive power compensation strategy for voltage stability challenges in the Korean power system with dynamic loads," *Sustainability,* vol. 11, no. 2, p. 326, 2019.

[16]   X. Tang, D. Zhang, and H. Chai, "Synthetical Optimal Design for Passive-Damped LCL Filters in Islanded AC Microgrid," *Journal of Energy and Power Technology,* vol. 3, no. 3, pp. 1-1, 2021.

[17]   H. Chai, M. Priestley, X. Tang, and J. Ravishankar, "Implementation of microgrid virtual laboratory in a design course in electrical engineering," in *2020 IEEE International Conference on Teaching, Assessment, and Learning for Engineering (TALE)*, 2020: IEEE, pp. 509-515.

[18]   N. Hosseinzadeh, A. Aziz, A. Mahmud, A. Gargoom, and M. Rabbani, "Voltage Stability of Power Systems with Renewable-Energy Inverter-Based Generators: A Review," (in English), *Electronics,* Review vol. 10, no. 2, p. 27, Jan 2021, Art no. 115, doi: 10.3390/electronics10020115.

[19]   P. Kundur *et al.*, "Definition and classification of power system stability IEEE/CIGRE joint task force on stability terms and definitions," *IEEE Trans. Power Syst.,* vol. 19, no. 3, pp. 1387-1401, 2004.

[20]   M. Farrokhabadi *et al.*, "Microgrid stability definitions, analysis, and examples," *IEEE Trans. Power Syst.,* vol. 35, no. 1, pp. 13-29, 2019.

[21]   Y.-H. Moon, H.-S. Ryu, J.-G. Lee, and B. Kim, "Uniqueness of static voltage stability analysis in power systems," in *2001 Power Engineering Society Summer Meeting. Conference Proceedings (Cat. No. 01CH37262)*, 2001, vol. 3: IEEE, pp. 1536-1541.

[22]   G. Morison, B. Gao, and P. Kundur, "Voltage stability analysis using static and dynamic approaches," *IEEE Trans. Power Syst.,* vol. 8, no. 3, pp. 1159-1171, 1993.

[23]   B. Fan, S. Guo, J. Peng, Q. Yang, W. Liu, and L. Liu, "A consensus-based algorithm for power sharing and voltage regulation in DC microgrids," *IEEE Trans. Ind. Inform.,* vol. 16, no. 6, pp. 3987-3996, 2019.

[24]   M. Crow and J. Ayyagari, "The effect of excitation limits on voltage stability," *IEEE Transactions on Circuits and Systems I: Fundamental Theory and Applications,* vol. 42, no. 12, pp. 1022-1026, 1995.

[25]   S. Kabir, O. Krause, R. Bansal, and J. Ravishanker, "Dynamic voltage stability analysis of sub-transmission networks with large-scale photovoltaic systems," in *2014 IEEE PES general meeting| conference & exposition*, 2014: IEEE, pp. 1-5.

[26]   C. Xu, P. Li, X. Li, D. Chen, Y. Zhang, and B. Lei, "Small disturbance voltage stability considering thermostatically controlled load," in *2011 International Conference on Advanced Power System Automation and Protection*, 2011, vol. 2: IEEE, pp. 862-866.

[27]   M. W. Younas and S. A. Qureshi, "Voltage stability improvement of a reactive power constrained longitudinal network feeding predominantly agricultural loads in scattered remote areas," in *2008 Australasian Universities Power Engineering Conference*, 2008: IEEE, pp. 1-6.

[28]   X. Fu and X. Wang, "Determination of load shedding to provide voltage stability," *Int. J. Electr. Power Energy Syst.,* vol. 33, no. 3, pp. 515-521, 2011.

[29]   X. Wu, Y. Zhang, A. Arulampalam, and N. Jenkins, "Electrical stability of large scale integration of micro generation into low voltage grids," *International Journal of Electronics,* vol. 1, no. 4, pp. 1-23, 2005.

[30]   R. A. Rhia, H. Daghrour, and M. Alsamara, "Optimal Location of Distributed Generation and its Impacts on Voltage Stability," in *2021 12th International Renewable Engineering Conference (IREC)*, 2021: IEEE, pp. 1-6.

[31]   S. K. SUDABATTULA and K. MUNISWAMY, "Optimal Allocation of Different Types of Distributed Generators in Distribution System," *Gazi U. J. Sci.,* vol. 32, no. 1, pp. 186-203, 2019.

[32]   K. H. Truong, P. Nallagownden, I. Elamvazuthi, and D. N. Vo, "A quasi-oppositional-chaotic symbiotic organisms search algorithm for optimal allocation of DG in radial distribution networks," *Appl. Soft. Comput.,* vol. 88, p. 106067, 2020.

[33]   P. Niveditha and M. S. Sujatha, "Optimal Allocation and Sizing of DG in Radial Distribution System- A Review," (in English), *Int. J. Grid Distrib. Comput.,* Review vol. 11, no. 6, pp. 49-57, Jun 2018, doi: 10.14257/ijgdc.2018.11.6.05.

[34]   Y. Han, X. Ning, P. Yang, and L. Xu, "Review of power sharing, voltage restoration and stabilization techniques in hierarchical controlled DC microgrids," *IEEE Access,* vol. 7, pp. 149202-149223, 2019.

[35]   J. Zhang, C. Tse, K. Wang, and C. Chung, "Voltage stability analysis considering the uncertainties of dynamic load parameters," *IET generation, transmission & distribution,* vol. 3, no. 10, pp. 941-948, 2009.

[36]   G. Lammert, D. Premm, L. D. P. Ospina, J. C. Boemer, M. Braun, and T. Van Cutsem, "Control of photovoltaic systems for enhanced short-term voltage stability and recovery," *IEEE Trans. Energy Convers.,* vol. 34, no. 1, pp. 243-254, 2018.

[37]   M. Furukakoi, M. S. S. Danish, A. M. Howlader, and T. Senjyu, "Voltage stability improvement of transmission systems using a novel shunt capacitor control," *Int. J. Emerg. Electr. Power Syst.,* vol. 19, no. 1, 2018.

[38]   J. Liu, J. Li, H. Song, A. Nawaz, and Y. Qu, "Nonlinear secondary voltage control of islanded microgrid via distributed consistency," *IEEE Trans. Energy Convers.,* vol. 35, no. 4, pp. 1964-1972, 2020.

[39]   T. Qian, Y. Liu, W. Zhang, W. Tang, and M. Shahidehpour, "Event-triggered updating method in centralized and distributed secondary controls for islanded microgrid restoration," *IEEE Trans. Smart Grid,* vol. 11, no. 2, pp. 1387-1395, 2019.

[40]   N. Afrin, F. Yang, and J. Lu, "Optimized reactive power support strategy for photovoltaic inverter to intensify the dynamic voltage stability of islanded microgrid," *Int. Trans. Electr. Energy Syst.,* vol. 30, no. 6, p. e12356, 2020.

[41]   M. H. Hemmatpour, M. Mohammadian, and A. A. Gharaveisi, "Optimum islanded microgrid reconfiguration based on maximization of system loadability and minimization of power losses," *Int. J. Electr. Power Energy Syst.,* vol. 78, pp. 343-355, 2016.

[42]   S. Alzahrani, R. Shah, and N. Mithulananthan, "Examination of Effective VAr with Respect to Dynamic Voltage Stability in Renewable Rich Power Grids," *IEEE Access,* vol. 9, pp. 75494-75508, 2021.

[43]   R. R. Micky, R. Lakshmi, R. Sunitha, and S. Ashok, "Assessment of voltage stability in microgrid," in *2016 International Conference on Electrical, Electronics, and Optimization Techniques (ICEEOT)*, 2016: IEEE, pp. 1268-1273.

[44]   P. S. Kundur, "Power system stability," *Power System Stability and Control,* pp. 8-1, 2017.

[45]   L. Aththanayake, N. Hosseinzadeh, A. Mahmud, A. Gargoom, and E. M. Farahani, "Comparison of Different Techniques for Voltage Stability Analysis of Power Systems," in *Australasian Universities Power Engineering Conference (AUPEC)*, Hobart, AUSTRALIA, Nov 29-Dec 03 2020, NEW YORK: IEEE, in Australasian Universities Power Engineering Conference, 2020. [Online]. Available: <u><Go to ISI></u>://WOS:000657261900018. [Online]. Available: <u><Go to ISI></u>://WOS:000657261900018

[46]   J. Machowski, Z. Lubosny, J. W. Bialek, and J. R. Bumby, *Power system dynamics: stability and control*. John Wiley & Sons, 2020.

[47]   G. Li, T. Jiang, Q. Xu, H. Chen, and H. Jia, "Sensitivity analysis based on local voltage stability margin and its application," *Electric Power Automation Equipment,* vol. 32, no. 4, pp. 1-5, 2012.

[48]   J. Zeng, Q. Liu, J. Zhong, S. Jin, and W. Pan, "Influence on static voltage stability of system connected with wind power," in *2012 Asia-Pacific Power and Energy Engineering Conference*, 2012: IEEE, pp. 1-4.

[49]   Y. Chi, Y. Liu, W. Wang, and H. Dai, "Voltage stability analysis of wind farm integration into transmission network," in *2006 International Conference on Power System Technology*, 2006: IEEE, pp. 1-7.

[50]   R. Toma and M. Gavrilas, "The impact on voltage stability of the integration of renewable energy sources into the electricity grids," in *2014 International Conference and Exposition on Electrical and Power Engineering (EPE)*, 2014: IEEE, pp. 1051-1054.

[51]   A. Rabiee, M. Vanouni, and M. Parniani, "Optimal reactive power dispatch for improving voltage stability margin using a local voltage stability index," *Energy Conv. Manag.,* vol. 59, pp. 66-73, 2012.

[52]   M. You-jie, L. Xiao-shuang, Z. Xue-song, and L. Ji, "The comments on dynamic bifurcation of voltage stability in power system," in *2010 WASE International Conference on Information Engineering*, 2010, vol. 4: IEEE, pp. 272-275.

[53]   D. Yang, X. Wang, F. Liu, K. Xin, Y. Liu, and F. Blaabjerg, "Adaptive reactive power control of PV power plants for improved power transfer capability under ultra-weak grid conditions," *IEEE Trans. Smart Grid,* vol. 10, no. 2, pp. 1269-1279, 2017.

[54]   X. Guo *et al.*, "Analysis and enhancement of active power transfer capability for DFIG-based WTs in very weak grid," *IEEE Journal of Emerging and Selected Topics in Power Electronics,* 2021.

[55]   S. M. Burchett *et al.*, "An optimal Thevenin equivalent estimation method and its application to the voltage stability analysis of a wind hub," *IEEE Trans. Power Syst.,* vol. 33, no. 4, pp. 3644-3652, 2017.

[56]   X.-P. Zhang, C. Rehtanz, and B. Pal, *Flexible AC transmission systems: modelling and control*. Springer Science & Business Media, 2012.

[57]   P. Li *et al.*, "Time-domain simulation investigates short-term voltage stability with dynamic loads," in *2009 Asia-Pacific Power and Energy Engineering Conference*, 2009: IEEE, pp. 1-5.

[58] B. H. Lee and K. Y. Lee, "Dynamic and static voltage stability enhancement of power systems," *IEEE Trans. Power Syst.,* vol. 8, no. 1, pp. 231-238, 1993.

[59] S. Abe, Y. Fukunaga, A. Isono, and B. Kondo, "Power system voltage stability," *IEEE Transactions on Power Apparatus and Systems,* no. 10, pp. 3830-3840, 1982.

[60] L. Ren and P. Zhang, "Generalized microgrid power flow," *IEEE Trans. Smart Grid,* vol. 9, no. 4, pp. 3911-3913, 2018.

[61] Z. Chen, L. Qing, M. Wan, and W. Li, "A simplified method for voltage stability analysis of wind power integration," in *2018 International Conference on Power System Technology (POWERCON)*, 2018: IEEE, pp. 1646-1652.

[62] Y. Wang, Z. Lu, Y. Min, and Z. Wang, "Small signal analysis of microgrid with multiple micro sources based on reduced order model in islanding operation," in *2011 IEEE Power and Energy Society General Meeting*, 2011: IEEE, pp. 1-9.

[63] Z. Shuai, Y. Peng, X. Liu, Z. Li, J. M. Guerrero, and Z. J. Shen, "Parameter stability region analysis of islanded microgrid based on bifurcation theory," *IEEE Trans. Smart Grid,* vol. 10, no. 6, pp. 6580-6591, 2019.

[64] R. B. d. L. Guedes, F. H. J. R. d. Silva, L. F. C. Alberto, and N. G. Bretas, "Large disturbance voltage stability assessment using extended Lyapunov function and considering voltage dependent active loads," in *IEEE Power Engineering Society General Meeting, 2005*, 2005: IEEE, pp. 1760-1767.

[65] Y. J. Ma, S. F. Lv, X. S. Zhou, Z. Q. Gao, and IEEE, "Review Analysis of Voltage Stability in Power System," in *IEEE International Conference on Mechatronics and Automation (ICMA)*, Takamatsu, JAPAN, Aug 06-09 2017, NEW YORK: IEEE, 2017, pp. 7-12. [Online]. Available: <Go to ISI>://WOS:000426271700002. [Online]. Available: <Go to ISI>://WOS:000426271700002

[66] M. Polis, C. Wang, and F. Lin, "Voltage stability and robustness for microgrid systems," in *2013 European Control Conference (ECC)*, 2013: IEEE, pp. 2038-2043.

[67] E. V. De Lorenci, A. C. Z. de Souza, and B. I. L. Lopes, "Energy function applied to voltage stability studies - DiscussiOn on low voltage solutions with the help of tangent vector," (in English), *Electr. Power Syst. Res.,* Article vol. 141, pp. 290-299, Dec 2016, doi: 10.1016/j.epsr.2016.08.004.

[68] A. R. N. Rao, P. Vijaya, and M. Kowsalya, "Voltage stability indices for stability assessment: a review," (in English), *Int. J. Ambient Energy,* Review vol. 42, no. 7, pp. 829-845, May 2021, doi: 10.1080/01430750.2018.1525585.

[69] M. H. Roos, P. H. Nguyen, J. Morren, and J. G. Slootweg, "Modeling and Experimental Validation of Power Electronic Loads and DERs For Microgrid Islanding Simulations," (in English), *IEEE Trans. Power Syst.,* Article vol. 35, no. 3, pp. 2279-2288, May 2020, doi: 10.1109/tpwrs.2019.2953757.

[70] H. Zaheb *et al.*, "A contemporary novel classification of voltage stability indices," *Applied Sciences,* vol. 10, no. 5, p. 1639, 2020.

[71] N. Beg, A. Armstorfer, A. Rosin, H. Biechl, and IEEE, *Mathematical Modeling and Stability Analysis of a Microgrid in Island Operation* (2018 International Conference on Smart Energy Systems and Technologies). New York: IEEE (in English), 2018.

[72]   M. Sagara, M. Furukakoi, T. Senjyu, M. S. S. Danish, and T. Funabashi, "Voltage stability improvement to power systems with energy storage systems," in *2016 17th International Conference on Harmonics and Quality of Power (ICHQP)*, 2016: IEEE, pp. 7-10.

[73]   M. S. S. Danish, A. Yona, and T. Senjyu, "Voltage stability assessment index for recognition of proper bus for load shedding," in *2014 International Conference on Information Science, Electronics and Electrical Engineering*, 2014, vol. 1: IEEE, pp. 636-639.

[74]   M. S. S. Danish, *Voltage stability in electric power system: a practical introduction*. Logos Verlag Berlin GmbH, 2015.

[75]   A. Ekwue, H. Wan, D. Cheng, and Y. Song, "Singular value decomposition method for voltage stability analysis on the National Grid system (NGC)," *Int. J. Electr. Power Energy Syst.,* vol. 21, no. 6, pp. 425-432, 1999.

[76]   C. J. Xia, X. T. Zheng, L. Guan, and S. Baig, "Probability analysis of steady-state voltage stability considering correlated stochastic variables," (in English), *Int. J. Electr. Power Energy Syst.,* Article vol. 131, p. 10, Oct 2021, Art no. 107105, doi: 10.1016/j.ijepes.2021.107105.

[77]   S. Greene, I. Dobson, and F. L. Alvarado, "Sensitivity of the loading margin to voltage collapse with respect to arbitrary parameters," *IEEE Trans. Power Syst.,* vol. 12, no. 1, pp. 262-272, 1997.

[78]   H. Chen, J. Shao, T. Jiang, R. Zhang, X. Li, and G. Li, "Security Control Strategy for Integrated Energy System Using Parameter Sensitivity," *Zhongguo Dianji Gongcheng Xuebao/Proceedings of the Chinese Society of Electrical Engineering,* Article vol. 40, no. 15, pp. 4831-4842, 2020, doi: 10.13334/j.0258-8013.pcsee.191081.

[79]   S. E. Sadeghi and A. A. Foroud, "A new approach for static voltage stability assessment in distribution networks," (in English), *Int. Trans. Electr. Energy Syst.,* Article vol. 30, no. 3, p. 21, Mar 2020, Art no. e12203, doi: 10.1002/2050-7038.12203.

[80]   S. Kumar, A. Kumar, and N. K. Sharma, "A novel method to investigate voltage stability of IEEE-14 bus wind integrated system using PSAT," (in English), *Front. Energy,* Article vol. 14, no. 2, pp. 410-418, Jun 2020, doi: 10.1007/s11708-016-0440-8.

[81]   A. C. Xue *et al.*, "A New Quantitative Analysis Method for Overvoltage in Sending End Electric Power System With UHVDC," (in English), *IEEE Access,* Article vol. 8, pp. 145898-145908, 2020, doi: 10.1109/access.2020.3015267.

[82]   L. Rodriguez-Garcia, S. Perez-Londono, and J. Mora-Florez, "An optimization-based approach for load modelling dependent voltage stability analysis," (in English), *Electr. Power Syst. Res.,* Article vol. 177, p. 10, Dec 2019, Art no. 105960, doi: 10.1016/j.epsr.2019.105960.

[83]   P. Kessel and H. Glavitsch, "Estimating the voltage stability of a power system," *IEEE Trans. Power Deliv.,* vol. 1, no. 3, pp. 346-354, 1986.

[84]   Y. R. Li, L. Fu, K. Meng, and Z. Y. Dong, "Assessment and Enhancement of Static Voltage Stability With Inverter-Based Generators," (in English), *IEEE Trans. Power Syst.,* Article vol. 36, no. 3, pp. 2737-2740, May 2021, doi: 10.1109/tpwrs.2021.3062224.

[85]   S. Chu, D. Y. Yang, W. C. Ge, C. Liu, G. W. Cai, and L. Kou, "Global sensitivity analysis of voltage stability in the power system with correlated renewable energy," (in English), *Electr. Power Syst. Res.,* Article vol. 192, p. 10, Mar 2021. [Online]. Available: <Go to ISI>://WOS:000639409300012.

[86]   S. S. Parihar and N. Malik, "Optimal allocation of renewable DGs in a radial distribution system based on new voltage stability index," (in English), *Int. Trans. Electr. Energy Syst.,* Article vol. 30, no. 4, p. 19, Apr 2020, Art no. e12295, doi: 10.1002/2050-7038.12295.

[87]   M. H. Hemmatpour, M. Mohammadian, and A.-A. Gharaveisi, "Simple and efficient method for steady-state voltage stability analysis of islanded microgrids with considering wind turbine generation and frequency deviation," *IET Generation, Transmission & Distribution,* vol. 10, no. 7, pp. 1691-1702, 2016, doi: https://doi.org/10.1049/iet-gtd.2015.1047.

[88]   W. P. Qin, D. Dong, and X. D. Mi, "Voltage Stability Analysis of Islanded Microgrid," in *Advances in Mechatronics, Automation and Applied Information Technologies, Pts 1 and 2*, vol. 846-847, Q. Lu and C. G. Zhang Eds., (Advanced Materials Research. Durnten-Zurich: Trans Tech Publications Ltd, 2014, pp. 199-+.

[89]   X. Y. Xu, Z. Yan, M. Shahidehpour, H. Wang, and S. J. Chen, "Power System Voltage Stability Evaluation Considering Renewable Energy With Correlated Variabilities," (in English), *IEEE Trans. Power Syst.,* Article vol. 33, no. 3, pp. 3236-3245, May 2018, doi: 10.1109/tpwrs.2017.2784812.

[90]   M. B. Wafaa and L. A. Dessaint, "Approach to dynamic voltage stability analysis for DFIG wind parks integration," (in English), *IET Renew. Power Gener.,* Article vol. 12, no. 2, pp. 190-197, Feb 2018, doi: 10.1049/iet-rpg.2016.0482.

[91]   A. Petean-Pina, C. Opathella, B. Venkatesh, and IEEE, "Effect of Wind Generation Uncertainty on Voltage Stability - A Singular Value Analysis," in *2018 IEEE Electrical Power and Energy Conference*, (IEEE Electrical Power and Energy Conference. New York: IEEE, 2018.

[92]   N. Serem, L. K. Letting, and J. Munda, "Voltage Profile and Sensitivity Analysis for a Grid Connected Solar, Wind and Small Hydro Hybrid System," (in English), *Energies,* Article vol. 14, no. 12, p. 26, Jun 2021, Art no. 3555, doi: 10.3390/en14123555.

[93]   A. Selim, S. Kamel, and F. Jurado, "Voltage stability analysis based on optimal placement of multipleDGtypes using hybrid optimization technique," (in English), *Int. Trans. Electr. Energy Syst.,* Article vol. 30, no. 10, p. 20, Oct 2020, Art no. e12551, doi: 10.1002/2050-7038.12551.

[94]   S. Rahman *et al.*, "Analysis of Power Grid Voltage Stability With High Penetration of Solar PV Systems," (in English), *IEEE Trans. Ind. Appl.,* Article vol. 57, no. 3, pp. 2245-2257, May-Jun 2021, doi: 10.1109/tia.2021.3066326.

[95]   B. Y. Qin, H. Y. Li, X. M. Zhang, T. Ding, K. Ma, and S. W. Mei, "Quantitative short-term voltage stability analysis of power systems integrated with DFIG-based wind farms," (in English), *IET Gener. Transm. Distrib.,* Article vol. 14, no. 19, pp. 4264-4272, Oct 2020, doi: 10.1049/iet-gtd.2019.1701.

[96]   A. O. Muhammed and M. Rawa, "A Systematic PVQV-Curves Approach for Investigating the Impact of Solar Photovoltaic-Generator in Power System Using PowerWorld Simulator," (in English), *Energies,* Article vol. 13, no. 10, p. 21, May 2020, Art no. 2662, doi: 10.3390/en13102662.

[97]   W. J. Huang and D. J. Hill, "Network-based analysis of long-term voltage stability considering loads with recovery dynamics," (in English), *Int. J. Electr. Power Energy Syst.,* Article vol. 119, p. 9, Jul 2020, Art no. 105891, doi: 10.1016/j.ijepes.2020.105891.

[98]   L. Gumilar, M. Sholeh, S. N. Rumokoy, D. Monika, and IEEE, *Analysis Voltage Stability in the Interconnection of Battery Charging Station and Renewable Energy* (Proceedings of Icoris

2020: 2020 the 2nd International Conference on Cybernetics and Intelligent System). New York: IEEE (in English), 2020, pp. 57-62.

[99] F. A. Vieira and Ieee, *Voltage Stability Analysis for DP Mobile Offshore Drilling Units Using the Continuous Power Flow* (2019 IEEE Electric Ship Technologies Symposium). New York: IEEE (in English), 2019, pp. 165-171.

[100] S. Kazmi, A. W. Khawaja, Z. M. Haider, R. Tauheed ur, S. Kazmi, and IEEE, *Voltage Stability of Wind Turbine based Micro Grid Using Simulation Platforms* (2019 5th International Conference on Power Generation Systems and Renewable Energy Technologies). New York: IEEE (in English), 2019, pp. 303-308.

[101] K. Singh, S. Bhuyan, M. N. Kumar, and S. Mishra, "Analysis of Voltage Stability in Radial Distribution System for Hybrid Microgrid," in *Advances in Smart Grid and Renewable Energy*, vol. 435, S. SenGupta, A. F. Zobaa, K. S. Sherpa, and A. K. Bhoi Eds., (Lecture Notes in Electrical Engineering. New York: Springer, 2018, pp. 49-55.

[102] S. Nikkhah and A. Rabiee, "Optimal wind power generation investment, considering voltage stability of power systems," (in English), *Renew. Energy,* Article vol. 115, pp. 308-325, Jan 2018, doi: 10.1016/j.renene.2017.08.056.

[103] M. Hammad, A. Harb, and IEEE, "Static Analysis for Voltage Stability of the Northern Jordanian Power System," in *2018 9th International Renewable Energy Congress*, (International Renewable Energy Congress. New York: IEEE, 2018.

[104] M. Ghaffarianfar and A. Hajizadeh, "Voltage Stability of Low-Voltage Distribution Grid with High Penetration of Photovoltaic Power Units," (in English), *Energies,* Article vol. 11, no. 8, p. 13, Aug 2018, Art no. 1960, doi: 10.3390/en11081960.

[105] R. R. Micky, R. Lakshmi, R. Sunitha, S. Ashok, and IEEE, *Assessment of Voltage Stability in Microgrid* (2016 International Conference on Electrical, Electronics, and Optimization Techniques). New York: IEEE (in English), 2016, pp. 1268-1273.

[106] M. Barbaro and R. Castro, "Design optimisation for a hybrid renewable microgrid: Application to the case of Faial island, Azores archipelago," *Renew. Energy,* vol. 151, pp. 434-445, 2020.

[107] A. Woyte, V. Van Thong, R. Belmans, and J. Nijs, "Voltage fluctuations on distribution level introduced by photovoltaic systems," *IEEE Trans. Energy Convers.,* vol. 21, no. 1, pp. 202-209, 2006.

[108] J. Petinrin and M. Shaabanb, "Impact of renewable generation on voltage control in distribution systems," *Renewable and Sustainable Energy Reviews,* vol. 65, pp. 770-783, 2016.

[109] Shivam and R. Dahiya, "Stability analysis of islanded DC microgrid for the proposed distributed control strategy with constant power loads," (in English), *Comput. Electr. Eng.,* Article vol. 70, pp. 151-162, Aug 2018, doi: 10.1016/j.compeleceng.2018.02.020.

[110] S. Alzahrani, R. Shah, and N. Mithulananthan, "Exploring the Dynamic Voltage Signature of Renewable Rich Weak Power System," (in English), *IEEE Access,* Article vol. 8, pp. 216529-216542, 2020, doi: 10.1109/access.2020.3041410.

[111] R. L. Sinder, T. M. L. Assis, and G. N. Taranto, "Impact of photovoltaic systems on voltage stability in islanded distribution networks," (in English), *J. Eng.-JOE,* Article no. 18, pp. 5023-5027, Jul 2019, doi: 10.1049/joe.2018.9369.

[112]   F. Katiraei, M. R. Iravani, and P. W. Lehn, "Micro-grid autonomous operation during and subsequent to islanding process," *IEEE Trans. Power Deliv.,* vol. 20, no. 1, pp. 248-257, 2005.

[113]   A. K. Sinha, Amita, and IEEE, *Transient Stability Improvement of Grid Using Photo-Voltaic Solar Farm* (2nd International Conference on Intelligent Circuits and Systems). New York: IEEE (in English), 2018, pp. 366-371.

[114]   J. A. S. Neto, A. C. Z. De Souza, E. V. De Lorenci, T. P. Mendes, P. M. D. Dos Santos, and B. D. Nascimento, "Static Voltage Stability Analysis of an Islanded Microgrid Using Energy Function," (in English), *IEEE Access,* Article vol. 8, pp. 201005-201014, 2020, doi: 10.1109/access.2020.3036107.

[115]   B. B. Adetokun, C. M. Muriithi, and J. O. Ojo, "Voltage stability assessment and enhancement of power grid with increasing wind energy penetration," *Int. J. Electr. Power Energy Syst.,* vol. 120, p. 105988, 2020.

[116]   S. D. Lu, M. H. Wang, C. Y. Tai, M. C. Tsou, F. C. Gu, and IEEE, "Formulation of Low Voltage Ride-Through Curve Considering Offshore Wind Farms Integrated into an Islanding Power System-A Case Study in Taiwan," in *2018 International Symposium on Computer, Consumer and Control*, (International Symposium on Computer Consumer and Control. New York: IEEE, 2018, pp. 117-120.

[117]   G. R. Lekhema, W. A. Cronje, I. Korir, and Asme, "HIGH RELIABILITY MICRO-GRID FOR A NUCLEAR FACILITY EMERGENCY POWER SUPPLY," in *26th International Conference on Nuclear Engineering (ICONE-26)*, London, ENGLAND, Jul 22-26 2018, NEW YORK: Amer Soc Mechanical Engineers, 2018. [Online]. Available: <Go to ISI>://WOS:000461265200060. [Online]. Available: <Go to ISI>://WOS:000461265200060

[118]   S. Mokeke and L. Z. Thamae, "The impact of intermittent renewable energy generators on Lesotho national electricity grid," (in English), *Electr. Power Syst. Res.,* Article vol. 196, p. 12, Jul 2021, Art no. 107196, doi: 10.1016/j.epsr.2021.107196.

[119]   P. Liu and C. E. Yang, "LMI-based robust voltage tracking control for a class of renewable energy systems," (in English), *J. Chin. Inst. Eng.,* Article vol. 42, no. 2, pp. 107-118, Feb 2019, doi: 10.1080/02533839.2018.1552840.

[120]   S. Kang, J. Kim, J. W. Park, and S. M. Baek, "Reactive Power Management Based on Voltage Sensitivity Analysis of Distribution System with High Penetration of Renewable Energies," (in English), *Energies,* Article vol. 12, no. 8, p. 20, Apr 2019, Art no. 1493, doi: 10.3390/en12081493.

[121]   X. Y. Lu, X. Z. Wang, D. Rimorov, H. Sheng, G. Joos, and IEEE, "Synchrophasor-Based State Estimation for Voltage Stability Monitoring in Power Systems," in *2018 North American Power Symposium*, (North American Power Symposium. New York: IEEE, 2018.

[122]   B. Y. Qi, K. N. Hasan, and J. V. Milanovic, "Identification of Critical Parameters Affecting Voltage and Angular Stability Considering Load-Renewable Generation Correlations," (in English), *IEEE Trans. Power Syst.,* Article vol. 34, no. 4, pp. 2859-2869, Jul 2019, doi: 10.1109/tpwrs.2019.2891840.

[123]   A. A. Eajal, A. H. Yazdavar, E. F. El-Saadany, and K. Ponnambalam, "On the Loadability and Voltage Stability of Islanded AC-DC Hybrid Microgrids During Contingencies," (in English), *IEEE Syst. J.,* Article vol. 13, no. 4, pp. 4248-4259, Dec 2019, doi: 10.1109/jsyst.2019.2910734.

[124]   M. Coumont, F. Bennewitz, J. Hanson, I. Power, and S. Energy, "Influence of Different Fault Ride-Through Strategies of Converter-Interfaced Distributed Generation on Short-Term Voltage Stability," in *Proceedings of 2019 Ieee Pes Innovative Smart Grid Technologies Europe*, (IEEE PES Innovative Smart Grid Technologies Conference Europe. New York: IEEE, 2019.

[125]   J. Moirangthem, K. R. Krishnanand, S. K. Panda, G. Amaratunga, and IEEE, *Voltage Stability Assessment by Holomorphically Estimating the Bifurcation Point of Electric Grids* (2018 Ieee International Conference on Environment and Electrical Engineering and 2018 Ieee Industrial and Commercial Power Systems Europe). New York: IEEE (in English), 2018.

[126]   W. P. Qin, D. Dong, and X. D. Mi, "Voltage Stability Analysis of Islanded Microgrid," in *International Conference on Mechatronics and Semiconductor Materials (ICMSCM 2013)*, Xian, PEOPLES R CHINA, Sep 28-29 2013, vol. 846-847, DURNTEN-ZURICH: Trans Tech Publications Ltd, in Advanced Materials Research, 2014, pp. 199-+, doi: 10.4028/www.scientific.net/AMR.846-847.199.   [Online].   Available: <Go   to   ISI>://WOS:000339412900043

[127]   S. Banerjee, D. Das, and C. K. Chanda, "Voltage stability of radial distribution networks for different types of loads," *International Journal of Power and Energy Conversion,* vol. 5, no. 1, pp. 70-87, 2014.

[128]   X.-y. Qiu, J. Wang, H.-c. Liu, and X.-y. LI, "Voltage stability analysis of radial distribution networks," *JOURNAL-SICHUAN UNIVERSITY ENGINEERING SCIENCE EDITION,* vol. 34, no. 4, pp. 100-103, 2002.

[129]   J. P. Ramírez and J. H. T. Hernández, "Review of methodologies for the analysis of voltage stability in power systems," in *2013 IEEE International Autumn Meeting on Power Electronics and Computing (ROPEC)*, 2013: IEEE, pp. 1-7.

[130]   M. Hasani and M. Parniani, "Method of combined static and dynamic analysis of voltage collapse in voltage stability assessment," in *2005 IEEE/PES Transmission & Distribution Conference & Exposition: Asia and Pacific*, 2005: IEEE, pp. 1-6.

[131]   "IEEE   14-bus   power   system   network." https://wenku.baidu.com/view/a5eda49a51e79b896802269b?aggId=a5eda49a51e79b896 802269b (accessed 12 Aug, 2022).

[132]   Z. Cheng, H. Zhou, and H. Yang, "Research on MPPT control of PV system based on PSO algorithm," in *2010 Chinese Control and Decision Conference*, 2010: IEEE, pp. 887-892.

[133]   A.   Llario.   "Solar   irradiation   and   wattage   of   solar   panels." https://thesolarhub.org/forum/solar-irradiation-and-wattage-of-solar-panels/   (accessed 12/08, 2022).

[134]   O. Tremblay, L.-A. Dessaint, and A.-I. Dekkiche, "A generic battery model for the dynamic simulation of hybrid electric vehicles," in *2007 IEEE Vehicle Power and Propulsion Conference*, 2007: Ieee, pp. 284-289.

[135]   U. Eminoglu and M. Hocaoglu, "A voltage stability index for radial distribution networks," in *2007 42nd International Universities Power Engineering Conference*, 2007: IEEE, pp. 408-413.

[136]   R. Ranjan and D. Das, "Voltage stability analysis of radial distribution networks," *Electr. Power Compon. Syst.,* vol. 31, no. 5, pp. 501-511, 2003.

[137] D. Das, D. Kothari, and A. Kalam, "Simple and efficient method for load flow solution of radial distribution networks," *Int. J. Electr. Power Energy Syst.,* vol. 17, no. 5, pp. 335-346, 1995.

[138] D. Thukaram, H. W. Banda, and J. Jerome, "A robust three phase power flow algorithm for radial distribution systems," *Electr. Power Syst. Res.,* vol. 50, no. 3, pp. 227-236, 1999.